

UNIVERSITÀ
DEGLI STUDI
DI PADOVA

Sede Amministrativa: Università degli Studi di Padova

Dipartimento di Scienze Cardiache, Toraciche e Vascolari

SCUOLA DI DOTTORATO DI RICERCA IN : Scienze Mediche, Cliniche e Sperimentali

INDIRIZZO: Scienze Cardiovascolari

CICLO XXVIII

Advanced Echocardiographic Evaluation of Right Ventricular Function in Patients with Pulmonary Hypertension

Direttore della Scuola : Ch.mo Prof. Gaetano Thiene

Coordinatore d'indirizzo: Ch.mo Prof. Gaetano Thiene

Supervisore :Ch.mo Prof. Sabino Iliceto

Dottoranda: Diletta Peluso

A Gennaro ed al piccolo Antonio

Index

▪ Abbreviations	pag 1
▪ Riassunto	pag 3
▪ Summary	pag 6
▪ Introduction	pag 9
▪ Pulmonary hypertension	
○ Definition	pag 10
○ Classification	pag 10
○ Epidemiology	pag 14
○ Pathology	pag 18
○ Pathobiology.	pag 22
○ Genetic	pag 25
○ Genomics	pag 27
○ Physiopathology	pag 28
○ Diagnosis	pag 32
○ Clinical presentation	pag 33
○ Follow-up	pag 42
○ Therapy	pag 46
▪ The right ventricle	pag 51
▪ The right ventricular failure	pag 54
▪ Echocardiographic evaluation of the right ventricular function	pag 57
○ Two-dimensional speckle tracking	pag 58
○ Three-dimensional echocardiography	pag 61
▪ Aim of the study	pag 64

- Material and Methods
 - Study population pag 65
 - Echocardiographic acquisition pag 66
 - Echocardiographic analysis pag 67
 - Statistical analysis pag 73
- Results
 - Healthy subjects pag 74
 - Systemic sclerosis patients pag 76
 - Pulmonary hypertension patients..... pag 77
 - Characterization of right ventricular function and mechanics in
Healthy Subjects - Systemic Sclerosis – Pulmonary Hypertension ... pag 78
 - Characterization of right ventricular function and mechanics in Healthy
subjects, Pulmonary Hypertension at risk of RV dysfunction and Pulmonary
Hypertension with RV dysfunction..... pag 80
 - Different patterns of interventricular septum transversal displacement in
Pulmonary Hypertension patients pag 83
 - Determinants of right ventricular global pump function in Pulmonary
Hypertension patients pag 85
- Discussion pag 87
 - RV mechanics in healthy subjects pag 87
 - RV mechanics in Systemic Sclerosis patients without Pulmonary
Hypertension pag 89
 - RV mechanics in Pulmonary Hypertension patisnts pag 90
- Limitations pag 93
- Conclusions pag 94

- References pag 95
- Acknowledgments pag 131
- Curriculum Vitae pag 132
- PhD activities pag 139

Abbreviations

2DE = two-dimensional echocardiography

2D-STE = two-dimensional speckle tracking

3DE = three-dimensional echocardiography

ALK1 = activin receptor-like kinase-1

BMP2 = bone morphogenetic protein type II receptor

CCB = calcium channel blockers

CHD = congenital heart disease

CMR = cardiac magnetic resonance

COPD = chronic obstructive pulmonary disease

CT = computed tomography

CTD = connective tissue disease

CTEPH = chronic thromboembolic pulmonary hypertension

DLCO = lung diffusion capacity for carbon monoxide

DPG = diastolic pressure gradient

FC = functional class

IVS = interventricular septum

LongEF = longitudinal ejection fraction

LS = longitudinal strain

LV = left ventricle/ventricular

miRNA = microRNA

mPAP = mean pulmonary artery pressure

PAECs = pulmonary artery endothelial cells

PAH = pulmonary arterial hypertension

PAP = pulmonary artery pressure

PASMs = pulmonary artery smooth muscle cells

PAWP = pulmonary artery wedge pressure

PCH = pulmonary capillary haemangiomas

PEA = pulmonary endarterectomy

PH = pulmonary hypertension

PVOD = pulmonary veno-occlusive disease

PVR = pulmonary vascular resistance

RadEF = radial ejection fraction

RHC = right heart catheterization

RV = right ventricle/ventricular

RVEF = right ventricular ejection fraction

RVF = right ventricular failure

RVFW = right ventricular free wall

RVFWLS = right ventricular free wall longitudinal strain

RVGLS = right ventricular global longitudinal strain

SSc = systemic sclerosis

TD = transversal displacement

TR = tricuspid regurgitation

RIASSUNTO

Presupposti: il ventricolo destro (VDx) è una cavità cardiaca di forma complessa la cui funzione di pompa in condizioni di normalità sembra essere determinata prevalentemente dall'accorciamento longitudinale. Tale affermazione deriva da studi anatomici che hanno mostrato come nella parete ventricolare destra, lo strato di fibre miocardiche longitudinali sia il più rappresentato. L'ecocardiografia convenzionale dimostra numerosi limiti nello studio delle dimensioni e della funzione del VDx, legati principalmente alla complessità della sua forma e meccanica. Tuttavia, la funzione ventricolare destra ha dimostrato essere un importante fattore prognostico in alcune condizioni patologiche, tra cui l'ipertensione polmonare (PH). E' tuttora sconosciuta la sequenza di eventi che conducono alla disfunzione di pompa globale del VDx nei soggetti affetti da PH. Due metodiche ecocardiografiche di recente introduzione, lo speckle-tracking bidimensionale e l'ecocardiografia tridimensionale, permettono una più accurata valutazione delle dimensioni e funzione della cavità ventricolare destra. In particolare, consentono di valutare i volumi e la forma del VDx, la funzione di pompa globale e la sua meccanica miocardica, in termini di deformazione longitudinale e trasversale.

Scopo dello studio: valutare la meccanica del ventricolo destro in condizioni di normalità ed in presenza di PH, definendo le alterazioni meccaniche che determinano la progressiva disfunzione di pompa globale del VDx che caratterizza la storia clinica dei pazienti affetti da PH.

Materiali e metodi: sono stati arruolati 270 soggetti sani, 75 pazienti affetti da sclerosi sistemica (in quanto popolazione ad alto rischio di sviluppare PH) senza PH e 59 pazienti affetti da PH (esclusa PH tipo 2). In quest'ultimo gruppo alcuni soggetti sono stati sottoposti a più di un esame ecocardiografico, a distanza di tempo, per un totale di 81

ecocardiogrammi. Dalla popolazione di soggetti sani è stato scelto un campione di 57 soggetti sovrapponibile per età e sesso alle due popolazioni patologiche. Tutti i pazienti sono stati sottoposti ad almeno un ecocardiogramma completo, comprensivo di acquisizioni tridimensionali del VDx. Mediante un software dedicato da un'immagine bidimensionale dedicata per il VDx è stata eseguita l'analisi speckle tracking che ha permesso di valutare lo strain longitudinale e la deformazione trasversale della parete libera e del setto interventricolare. Il data set tridimensionale è stato analizzato mediante un software dedicato che ha permesso di misurare i volumi e la frazione di eiezione del VDx. Il beutel tridimensionale così ottenuto è stato successivamente analizzato con un software ad hoc che ha permesso di stimare separatamente il contributo longitudinale e radiale alla genesi della frazione di eiezione del VDx.

Risultati: dall'analisi del gruppo di soggetti sani sono stati ottenuti i valori di normalità di volume telediastolico e telesistolico, frazione di eiezione, strain longitudinale e displacement trasversale del VDx. Dall'analisi del beutel tridimensionale del VDx è emerso che la deformazione longitudinale e radiale contribuiscono in eguale misura alla funzione di pompa globale del VDx. I soggetti affetti da sclerosi sistemica hanno dimostrato valori leggermente superiori di pressione sistolica in arteria polmonare e resistenze vascolari polmonari totali rispetto ai soggetti sani, seppure senza raggiungere i criteri patologici. Invece, i valori di dimensione e funzione del VDx sono risultati sovrapponibili rispetto ai controlli sani. I pazienti affetti da PH hanno dimostrato volumi del VDx sensibilmente superiori con una ridotta frazione di eiezione. Le componenti longitudinale e radiale della frazione di eiezione sono risultate entrambe ridotte, ma in particolare il contributo relativo radiale ha dimostrato essere quello maggiormente alterato. Per quanto riguarda la meccanica miocardica, lo strain longitudinale della parete libera e del setto interventricolare è risultato ridotto ed anche la deformazione trasversale globale è

risultata alterata. In particolare nei soggetti con PH, soprattutto la meccanica del setto interventricolare ha dimostrato di essere alterata, con una minore entità di spostamento sistolico dello stesso verso il centro della cavità ventricolare sinistra. Dividendo i pazienti con PH in due gruppi (con frazione di eiezione conservata e frazione di eiezione ridotta), è stato possibile dimostrare che tutti i parametri di funzione e deformazione del VDX sono maggiormente alterati nel secondo gruppo. Tuttavia, mentre il contributo longitudinale alla frazione di eiezione è risultato preservato, il contributo radiale ha dimostrato di essere significativamente ridotto.

Conclusioni: in condizioni di normalità la funzione ventricolare destra sembra essere determinata in egual misura dalla deformazione longitudinale e radiale. In presenza di ipertensione polmonare, il progressivo deterioramento della funzione di pompa del VDX è veicolata prevalentemente da una riduzione del contributo radiale.

Summary

Background: the right ventricle (RV) is a complex shaped cardiac chamber, whose pump function is mainly driven by a longitudinal deformation, as showed by anatomical studies. Conventional echocardiography showed several limitations in the analysis of RV size and function. RV systolic dysfunction is an important prognostic factor in several pathological condition, among which pulmonary hypertension (PH). However, the progression of RV mechanical changes that lead to the RV pump function impairment remains to be clarified. The new echocardiographic techniques, two dimensional-speckle tracking (2D-STE) and three-dimensional echocardiography (3DE), allow to investigate volumes, ejection fraction and myocardial mechanics of the RV. Moreover, we developed a custom-made software package that applied to the 3DE beutel of the RV allows to discriminate between the relative contribution of the longitudinal and radial displacement to the global RV pump function.

Purpose: to value the mechanics of RV in healthy condition, in presence of systemic sclerosis (SSc), a condition predisposing to PH, and in presence of PH.

Methods: we enrolled 270 healthy subjects, 75 patients affected by SSc (a pathological condition at high risk of PH), without PH, and 59 patients affected by PH (excluded PH type 2). Some of PH patients underwent to more than one echocardiograms, for a total of 81 exams. 57 age- and gender-matched healthy volunteers have been selected. All subjects underwent a complete echocardiogram, including dedicated 3DE acquisition of the RV. A dedicated software has been applied on apical 2D image of the RV in order to measure the longitudinal strain (LS) and the transversal displacement (TD) of both the free-wall (RVFW) and the interventricular septum (IVS). 3DE data sets of the RV have been analyzed by RV function 2.0 (TomTec) in order to obtain volumes and ejection fraction

(RVEF). Then PH have been divided according to RV-EF: preserved ($\geq 45\%$) or impaired ($< 45\%$). Finally, the 3DE RV beutels were analyzed by our custom made software package obtaining the longitudinal EF (LongEF) and radial EF (RadEF) and their relative contribution to RVEF by calculating the ratios LongEF/RVEF and RadEF/RVEF.

Results: the analysis of the healthy volunteers provided reference values of RV volumes, ejection fraction, LS and TD. The 3DE RV beutel analysis showed that in healthy subjects the relative contribution of longitudinal and radial motion is equal. In SSc patients no significant differences about RV size and function have been demonstrated. PH patients showed significantly larger 3DE RV end-diastolic and end-systolic volumes (106 ± 39 ml vs 67 ± 14 ml and 65 ± 33 vs 28 ± 7 ml, respectively; $p < 0.0001$), lower 3D RVEF ($41 \pm 11\%$ vs $58 \pm 4\%$; $p < 0.0001$), lower LS values and impaired TD values than controls. Similarly, both LongEF and RadEF were lower ($18 \pm 7\%$ vs $27 \pm 4\%$ and $15 \pm 7\%$ vs $27 \pm 5\%$, respectively; $p < 0.0001$) in PH patients. However, only the RadEF/RVEF appeared impaired (36 ± 11 vs 47 ± 6 , $p < 0.0001$), whereas LongEF/RVEF (47 ± 9 vs 47 ± 6 , $p = \text{NS}$) was similar between pts and controls. Looking at the subgroup of patients with reduced RVEF, RV pump dysfunction was mainly driven by progressive reduction of the radial component of RV wall displacement.

Conclusions: in healthy condition, the radial component of RV wall displacement is as important as the longitudinal one to determine global RV pump function. In patients with PH, the impairment of RV pump function seems to be mainly driven by the progressive reduction of RV radial displacement.

Introduction

Pulmonary hypertension (PH) is a pathological process involving pulmonary circulation. It may appear in multiple clinical conditions, in which its development is associated with increased morbidity and mortality. The natural history of this pathological condition is characterized by the appearance of progressive right ventricular (RV) dysfunction, with RV failure being the main cause of patients' mortality. Then, accurate evaluation of RV function appears to be critical in PH patients follow-up. Accordingly, echocardiography plays a major role during initial assessment and follow-up of patients with PH. However, conventional two-dimensional (2DE) and Doppler echocardiography has several limitations to evaluate the RV, which are mainly related to its complex three-dimensional geometry and peculiar function.

The development of novel echocardiographic techniques, such as three-dimensional echocardiography (3DE) and two-dimensional speckle-tracking echocardiography (2D-STE) has provided new ways to obtain a more accurate and reproducible assessment of the RV morphology and function by echocardiography.

Pulmonary Hypertension

Definition

PH is diagnosed when mean pulmonary artery pressure (mPAP) measured invasively by right heart catheterization (RHC) at rest is higher than 25 mmHg [1]. Insufficient data are available about the normal behaviour of mPAP and pulmonary vascular resistance (PVR) during exercise. Moreover, no diagnostic threshold of exercise-induced changes in mPAP has been identified because of the lack of prognostic data. Then, according to the current guidelines, the entity of “PH on exercise” has not been accepted [2].

Classification

To be properly managed, patients with PH should be classified using hemodynamic and clinical parameters.

The first distinction to be made is between pre-capillary and post-capillary PH (Table 1), a haemodynamic classification. Pre-capillary PH is defined by the presence of low pulmonary artery wedge pressure (PAWP; ≤ 15 mmHg). It includes pulmonary arterial hypertension (PAH), PH due to lung diseases/ipoxia, chronic thromboembolic PH (CTEPH) and PH due to multifactorial and unclear mechanisms. Finally, PAH is a pre-capillary PH (with PAWP ≤ 15 mmHg and PVR > 3 WU) in the absence of other causes of pre-capillary PH. Conversely, post-capillary PH is defined by values of PAWP higher than 15 mmHg. It includes PH due to left heart diseases or multifactorial and unclear mechanisms. The latter entity can be divided in isolated or combined post-capillary PH. Differentiation is based on the values of the diastolic pressure gradient (DPG; lower or higher than 7 mmHg), a

haemodynamic parameter defined as the difference between diastolic PAP and PAWP (Table 1).

Table 1. Haemodynamic definitions of pulmonary hypertension

Definition	Characteristics
PH	mPAP \geq 25 mmHg
Pre-capillary PH	mPAP \geq 25 mmHg PAWP \leq 15 mmHg
Post-capillary PH	mPAP \geq 25 mmHg PAWP $>$ 15 mmHg
Isolated post-capillary PH	DPG $<$ 7 mmHg and/or PVR \leq 3 WU
Combined post-capillary PH	DPG \geq 7 mmGf and/or PVR $>$ 3 WU

DPG=diastolic pressure gradient; mPAP=mean pulmonary artery pressure; PH=pulmonary hypertension; PVR=pulmonary vascular resistance. From: Galiè N. et al 2015 ESC/ERS Guidelines for the diagnosis and treatment of pulmonary hypertension. Eur Heart J 2016;37(1):67-119 [2].

The clinical classification divides PH into five groups (Table 2) [3]. It is based on pathophysiological, clinical, and therapeutic considerations.

Table 2. Clinical classification of pulmonary hypertension

<p>1. Pulmonary arterial hypertension</p> <p>1.1 Idiopathic</p> <p>1.2 Heritable (BMP2 mutation; other mutations)</p> <p>1.3 Drugs and toxins induced</p> <p>1.4 Associated with:</p> <p> 1.4.1 Connective tissue disease</p> <p> 1.4.2 HIV infection</p> <p> 1.4.3 Portal hypertension</p> <p> 1.4.4 Congenital heart disease</p> <p> 1.4.5 Schistosomiasis</p> <p>1'. Pulmonary veno-occlusive disease and/or pulmonary capillary haemangiomatosis</p> <p>1''. Persistent pulmonary hypertension of the newborn</p>
<p>2. Pulmonary hypertension due to left heart disease</p> <p>2.1 Left ventricular systolic dysfunction</p> <p>2.2 Left ventricular diastolic dysfunction</p> <p>2.3 Valvular disease</p> <p>2.4 Congenital/acquired left heart inflow/outflow tract obstruction and congenital cardiomyopathies</p> <p>2.5 Other</p>
<p>3. Pulmonary hypertension due to lung diseases and/or hypoxia</p> <p>3.1 Chronic obstructive pulmonary disease</p> <p>3.2 Interstitial lung disease</p> <p>3.3 Other pulmonary diseases with mixed restrictive and obstructive pattern</p> <p>3.4 Sleep-disordered breathing</p> <p>3.5 Alveolar hypoventilation disorders</p> <p>3.6 Chronic exposure to high altitude</p> <p>3.7 Developmental lung diseases</p>
<p>4. Chronic thromboembolic pulmonary hypertension and other pulmonary artery obstructions</p> <p>4.1 Chronic thromboembolic pulmonary hypertension</p> <p>4.2 Other pulmonary artery obstructions</p>
<p>5. Pulmonary hypertension with unclear and/or multifactorial mechanisms</p> <p>5.1 Haematological disorders</p> <p>5.2 Systemic disorders</p> <p>5.3 Metabolic disorders</p> <p>5.4 Others</p>

From: Galiè N. et al 2015 ESC/ERS Guidelines for the diagnosis and treatment of pulmonary hypertension. Eur Heart J 2016;37(1):67-119 [2].

The first edition of the clinical classification dates back to 1973 [4]. It simply divided PH in primary and secondary, according to the presence/absence of identifiable causes. In 1998 in Evian (France) during the Second World Symposium on Pulmonary Hypertension, the first classification was replaced by the first version of the current classification. The aim of the “Evian classification” was to distinguish categories sharing similar pathophysiological mechanisms, clinical presentation and treatment strategies. A first update of the “Evian classification” was performed in 2003 in Venice [3]. At that time the introduction of a genetic classification was proposed, because of the recognition of bone morphogenetic protein type II receptor (BMP2) gene mutations as the possible cause of a sizable number of familial and sporadic case of PAH, but not only. However, it remained only a proposal, because the evidences about the role of genes in various forms of PH were still at an early stage [3]. The term “primary” and “secondary” PH were abandoned due to the evidence that the idiopathic form of PH share similar pathological findings with other forms of PH secondary to drug/toxins, connective tissue disease or HIV infection. Then, the terms of “pulmonary arterial hypertension” and “idiopathic arterial hypertension” were introduced. Pulmonary veno-occlusive disease (PVOD) and pulmonary capillary haemangiomatosis (PCH) were reclassified and included in the PAH group, because they have similar pathological and clinical features. Particularly they share: the possibility of pulmonary edema occurrence during epoprostenol therapy [5,6]; similar pathological conditions associated with PAH, such as scleroderma disease [7] or HIV infection [8,9]; and likely familial occurrence in both PVOD [10] and PCH [11], as well as in PAH. In 2008, during the fourth World Symposium on PH held in Dana Point (California), the “Evian-Venice classification” was maintained, with modifications of some specific points [12]. The term “familial” PAH was replaced by “heritable”, for the evidence of specific gene mutations identified not only in familial but in sporadic cases too [13,14]. A clinical and anatomical-

pathophysiological version of the classification of PAH related to congenital heart disease [15] was also introduced. The group of “associated PAH” was updated, with the introduction of schistosomiasis as an associated condition, because of the demonstration that schistosomiasis has similar specific clinical and pathological features [16]. PVOD and PCH were reclassified as group 1’, because they share some features with idiopathic PAH but also demonstrate some differences. Finally, in 2015 the current version of the clinical guidelines on PH [2] was published. In this document some other modifications of the clinical classification have been made. Pre-capillary PH associated with chronic haemolytic anaemia has been moved from group 1 to 5, because it appears significantly different regard to pathological and haemodynamic characteristics, as well as to response to specific therapies. The group 1’ has been expanded with the inclusion of idiopathic, heritable, drug/toxin/radiation-induced and associated forms of PVOD/PCH. Persistent PH of the newborn has been subcategorized alone as group 1”, because it demonstrated to be a heterogeneous group of conditions [17-19]. Finally, some paediatric heart diseases have been included in group 2.

Epidemiology

Literature reports about the incidence of PH are limited. About 80% of patients with PH live in the developing world, where heart disease and lung disease have become the most frequent causes of pulmonary hypertension [20]. Particularly, in industrialised countries, pulmonary hypertension affects mainly elderly people whereas the majority of young people with PH are diagnosed in the developing world.

An overview of the global distribution of the most prevalent forms of PH is shown in Figure 1.

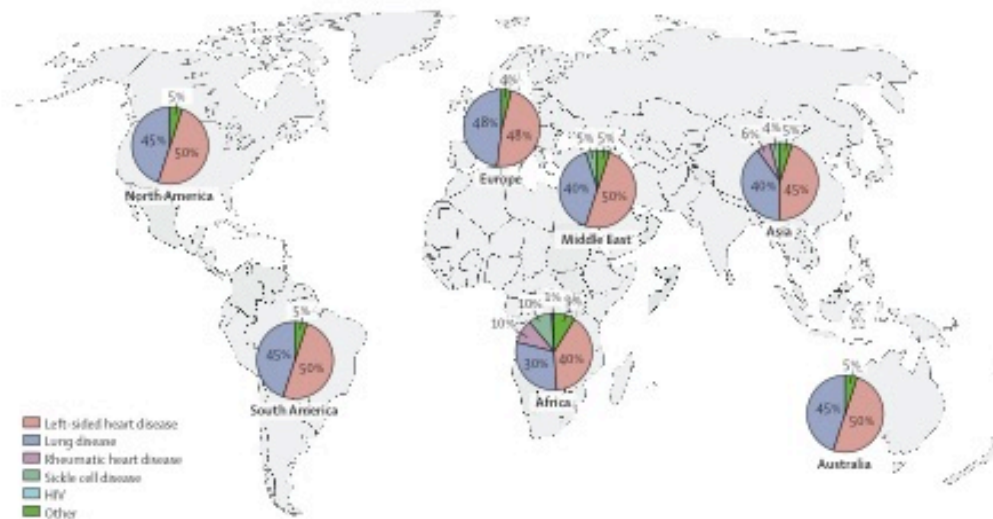


Figure 1. Estimated global distribution of the most prevalent form of pulmonary hypertension. From: Hoepfer MM et al. Lancet Respir Med 2016;4:306-22 [20].

Figure 2 provides an overview of the global distribution of the most prevalent forms of PAH.

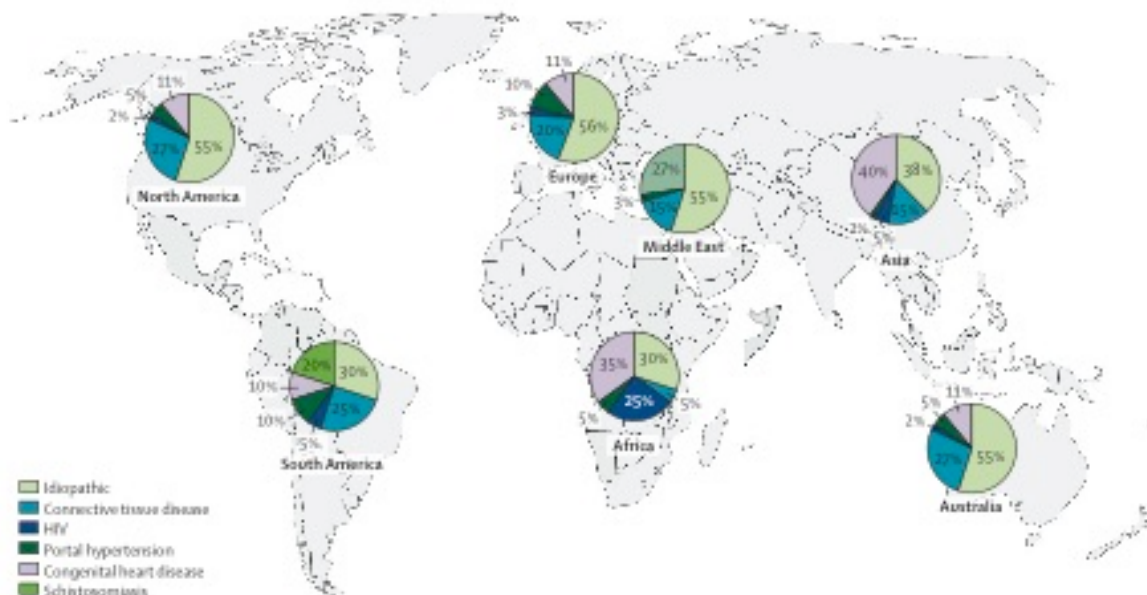


Figure 2. Estimated global distribution of the most prevalent form of pulmonary arterial hypertension. From: Hoepfer MM et al. Lancet Respir Med 2016;4:306-22 [20].

The data presented in Figure 1 and 2 should be presented with caution as most of the underlying evidence has been derived from populations at risk for PH and are based on echocardiographic data rather than from population-based studies with patients undergoing RHC.

Group 1. In Europe, PAH prevalence and incidence are in the range of 15–60 subjects per million population and 5–10 cases per million per year, respectively [21]. In registries, around 50% of PAH patients have idiopathic, heritable or drug-induced PAH. In the subgroup of associated conditions, the leading cause is connective tissue disease (CTD), mainly systemic sclerosis (SSc) [22]. Indeed, SSc accounts for more than 70% of cases of CTD-related PH [23].

PAH affects predominantly females of childbearing age [24]. The estimated time between symptom onset and diagnosis is about 2 years and the mean survival of untreated PAH patients is 2.8 years [25]. Several factors for the development of PAH have been identified. They are defined as any factor or condition that is suspected to play a predisposing or facilitating role in disease development. Risk factors were classified as definite, likely or possible, based on the strength of their association with PH and their probable causal role [26]. Definite risk factors for PAH are listed in the clinical classification table (Table 2) among associated PAH conditions. Different drug and toxins with the corresponding risk level are listed in Table 3.

Table 3. Updated risk level of drugs and toxins known to induce pulmonary arterial hypertension

Definite	Likely	Possible
<ul style="list-style-type: none"> • Aminorex • Fenfluramine • Dexfenfluramine • Toxic rapeseed oil • Benfluorex • Selective serotonin reuptake inhibitors 	<ul style="list-style-type: none"> • Amphetamines • Dasatinib • L-tryptophan • Methamphetamines 	<ul style="list-style-type: none"> • Cocaine • Phenylpropanolamine • St. John's wort • Amphetamine-like drugs • Interferon α and β • Some chemotherapeutic agents such as alkylating agents.

From: Galiè N. et al 2015 ESC/ERS Guidelines for the diagnosis and treatment of pulmonary hypertension. Eur Heart J 2016;37(1):67-119 [2].

Group 2. The prevalence of PH in patients with chronic heart failure increases with the progression of functional class (FC) impairment. Up to 60% of patients with severe left ventricular (LV) systolic dysfunction and up to 70% of patients with heart failure with preserved ejection fraction may present with PH. In left-sided valvular diseases, the prevalence of PH increases with the severity of the condition and related symptoms. When present, left heart disease related-PH results in more severe symptoms and worse exercise tolerance and exerts a negative impact on outcome [27-29]. Compared with PAH, this group of patients are often older, female, with a higher prevalence of cardiovascular comorbidities [30].

Group 3. The most common lung diseases associated with PH are chronic obstructive pulmonary disease (COPD), interstitial lung disease and combined pulmonary fibrosis and emphysema. Mild PH is common in both severe interstitial lung disease and severe chronic obstructive lung disease [31], while severe PH is uncommon [32]. Severe PH can be seen in the combined emphysema/fibrosis syndrome, where the prevalence of PH is high [33]. The

severity of PH is usually poorly associated with the severity of the underlying lung disease [34-35]. In any lung disease the appearance of PH is accompanied by a deterioration of exercise capacity and shorter survival [36-37].

Group 4. In the Spanish PH Registry, CTEPH prevalence and incidence were 3.2 cases per million and 0.9 cases per million per year, respectively [38]. Even though a prevalence of CTEPH of 3.8% has been reported in survivors of acute pulmonary embolism (PE), the true incidence of CTEPH after acute PE is lower, in the range of 0.5–2% [39]. A history of acute PE was reported for 74.8% of patients from the International CTEPH Registry [40]. Associated conditions included thrombophilic disorders (lupus anticoagulant/antiphospholipid antibodies, protein S and C deficiency, activated protein C resistance including factor V Leiden mutation, prothrombin gene mutation, antithrombin III deficiency and elevated factor VIII) in 31.9% of patients and splenectomy in 3.4%.

Pathology

The various PH groups are characterized by different pathological features [41-42]. They present with either a predominance of pulmonary arterial remodeling or vein remodeling or a variable contribution of both. Paradigmatic of the former is idiopathic PAH, whereas pure PVOD and PH due to left heart dysfunction are characterized predominantly by venous remodeling [43].

Group 1 (PAH): pathological lesions affect the distal pulmonary arteries (<500 μm of diameter) in particular. They are characterized by medial hypertrophy, intimal proliferative and fibrotic changes (concentric, eccentric), adventitial thickening with perivascular inflammatory infiltrates, complex lesions (plexiform, dilated lesions), and thrombotic lesions (Figure 3). Pulmonary veins are classically unaffected. The first

pathological classification is attributable to Heath and Edwards [44-45] (Table 4).

Table 4. Heath and Edwards grading scheme for vascular pathology in pulmonary arterial hypertension

Grade	Vascular pathology
1.	Distal extension of muscle and medial thickening of distal arterioles
2.	Medial hypertrophy with neointima in small muscular arteries
3.	Progressive fibrotic vascular occlusion, concentric intimal fibrosis
4.	Progressive arterial dilation with plexiform lesions
5.	Chronic dilatation with medial and intimal fibrosis, angiomatoid lesions and hemosiderosis
6.	Necrotizing arteritis

From: de Jesus Perez VA. Molecular pathogenesis and current pathology of pulmonary hypertension. Heart Fail Rev 2016; 21(3): 239-57 [47].

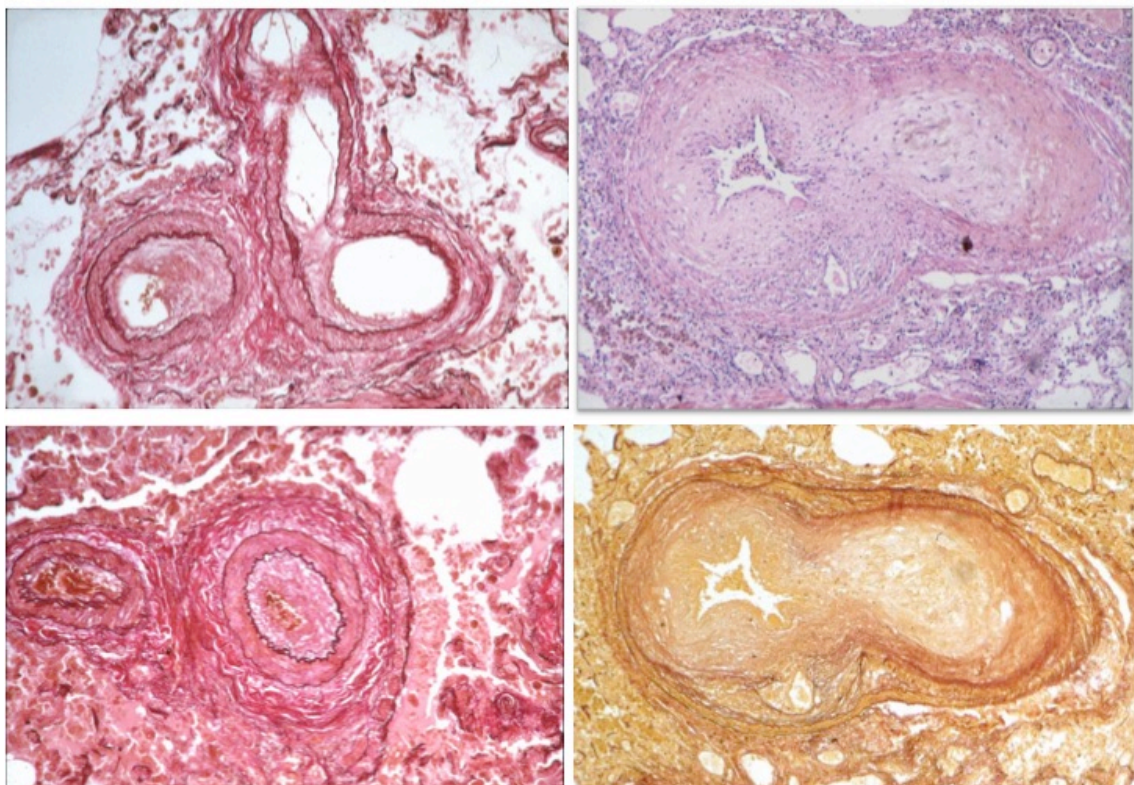


Figure 3. Pathological lesions of pulmonary arterial hypertension lungs characterized by intima and media remodeling with obstruction of arterioles, perivascular inflammation and aneurismatic lesions. Courtesy of Prof G. Thiene, Cardiovascular Pathology, Padua University.

These pathological lesions are distributed through the entire lung. The exact sequence of histological occurring in PAH remains to be clarified. The extent of intima and media remodeling appears to progress independently because we could not find a close correlation between both forms of remodeling. However, media remodeling could antedate intima remodeling as suggested by the few human studies with sequential lung biopsies. Intima remodeling could be linked to alterations of pulmonary artery flow, imparted by media remodeling and vasoconstriction or, alternatively, develop as an independent event [46].

It has been speculated that higher grade lesions are associated with worse hemodynamic parameters and right heart failure. However, lung tissue sections from PAH patients demonstrate a wide spectrum of lesion severity [47]. Moreover, number, distribution and severity of the lung lesions have been demonstrated to be similar among PAH patients receiving or not long-term specific therapies [48]. Anyway, authors admit that random sampling could serve as a source of bias that needs to be considered prior to reaching a definite conclusion [48].

Group 1': includes mainly PVOD which involves septal veins and pre-septal venules (constant involvement) with occlusive fibrotic lesions, venous muscularization, frequent capillary proliferation (patchy), pulmonary oedema, occult alveolar haemorrhage, lymphatic dilatation and lymphnode enlargement (vascular transformation of the sinus), and inflammatory infiltrates. Distal pulmonary arteries are affected by medial hypertrophy, intimal fibrosis, and uncommon complex lesions.

Group 2 (PH due to left heart disease): pathological changes in this group are characterized by enlarged and thickened pulmonary veins, pulmonary capillary dilatation, interstitial oedema, alveolar haemorrhage, and lymphatic vessel and lymph node enlargement. Distal

pulmonary arteries may be affected by medial hypertrophy and intimal fibrosis.

Group 3 (PH due to lung diseases and/or hypoxia): pathological changes in these cases include medial hypertrophy and intimal obstructive proliferation of the distal pulmonary arteries. A variable degree of destruction of the vascular bed in emphysematous or fibrotic areas may also be present.

Group 4 (CTEPH): pathological lesions are characterized by organized thrombi tightly attached to the pulmonary arterial medial layer in the elastic pulmonary arteries, replacing the normal intima (Figure 4). These may completely occlude the lumen or form different grades of stenosis, webs, and bands [49]. Interestingly, in the non-occluded areas, a pulmonary arteriopathy indistinguishable from that of PAH (including plexiform lesions) can develop [50]. Collateral vessels from the systemic circulation (from bronchial, costal, diaphragmatic and coronary arteries) can grow to reperfuse at least partially the areas distal to complete obstructions.

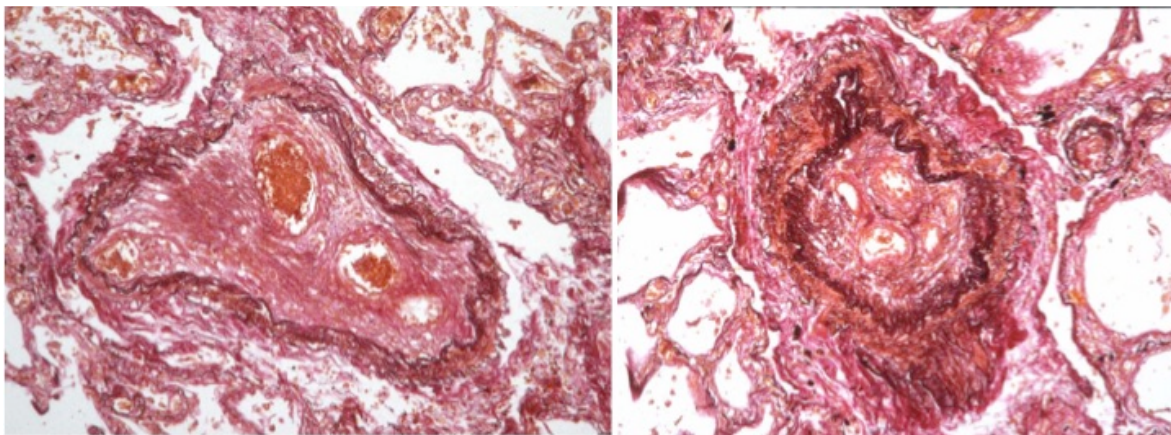


Figure 4. Pathological lesions of chronic thromboembolic pulmonary hypertension characterized by organized and recanalized endovascular thrombi. Courtesy of Prof G. Thiene, Cardiovascular Pathology, Padua University.

Group 5 (PH with unclear and/or multifactorial mechanisms): this group includes heterogeneous conditions with different pathological pictures for which the aetiology is unclear or multifactorial.

Pathobiology

Different pathobiological features [51-53] characterize the different clinical PH groups.

Group 1: The exact process responsible for the initiation, aggravation or acceleration of PH remains to be defined. Mechanisms underlying PAH disease are vasoconstriction, proliferative and obstructive remodeling of the pulmonary vessel, inflammation and thrombosis. Then, the pathogenesis appeared to be multifactorial (Figure 5).

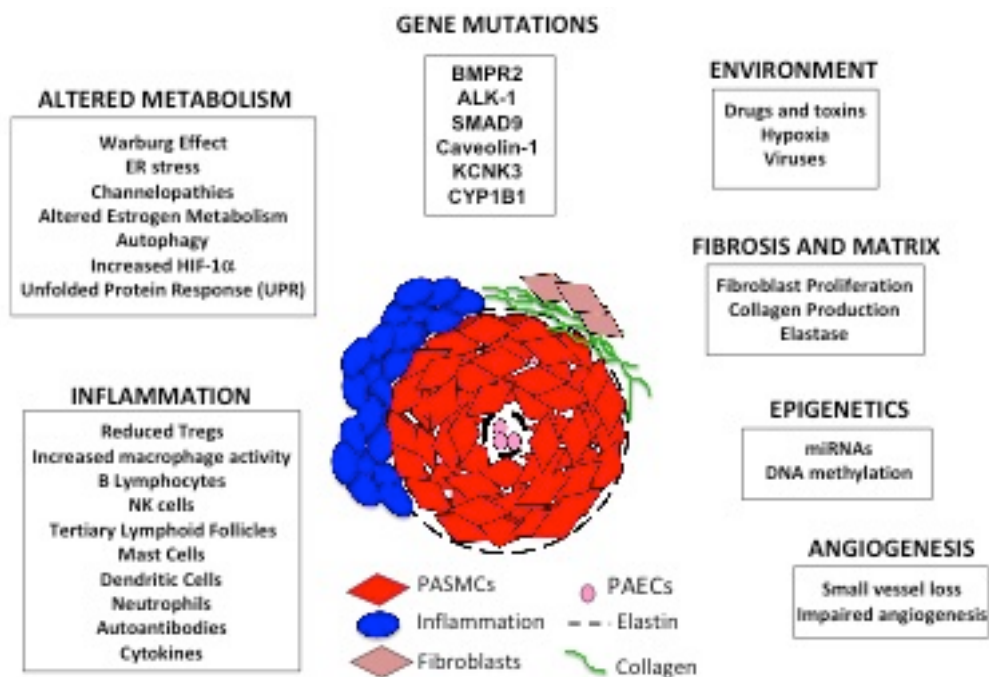


Figure 5. Summary of mechanisms involved in pathogenesis of PAH. From: de Jesus Perez VA. Molecular pathogenesis and current pathology of pulmonary hypertension. Heart Fail Rev 2016; 21(3): 239-57 [47].

The proposed theory is based on the action of multiple contributing factors on a background of genetic predisposition [43] (Figure 6).

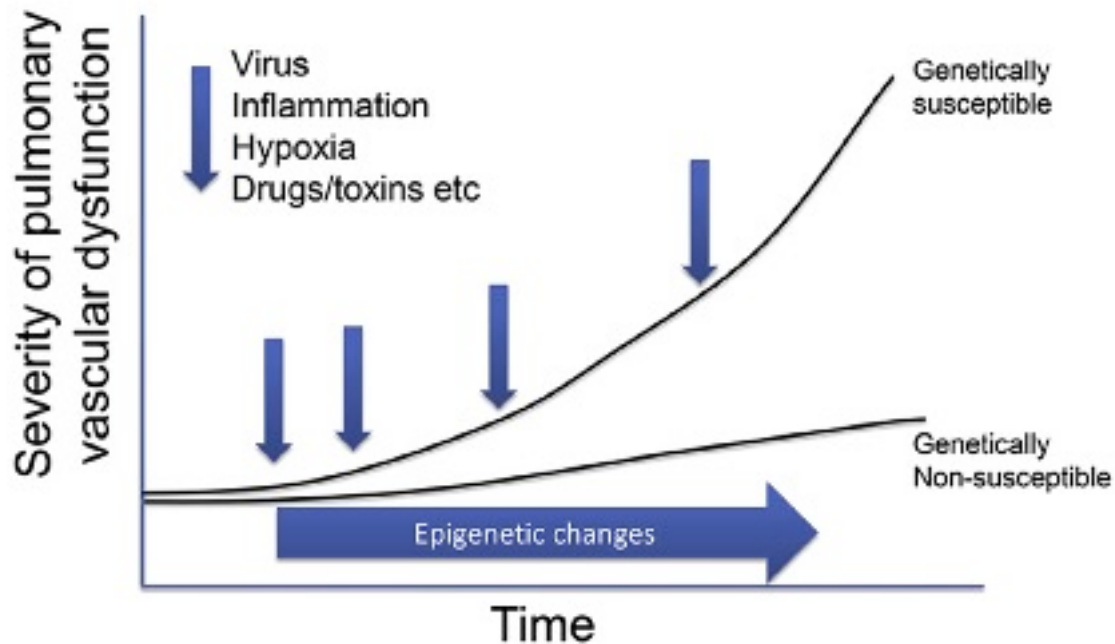


Figure 6. Proposed multifactorial factors influencing progression of pulmonary hypertension. From: Tudor RM et al. JACC 2013;62(25 Suppl):D4-12 [43].

Vasoconstriction has been related to abnormal function of the smooth muscle cell and to endothelial dysfunction, with impaired production of vasodilator and anti-proliferative agents and overexpression of vasoconstrictor and proliferative substances. Many of these abnormalities promote vascular remodeling, too. In addition, an increased production of extracellular matrix occurs in the adventitia layer. Prothrombotic abnormalities have been demonstrated, with presence of thrombi in both the small distal and proximal pulmonary arteries [12].

→ Inflammation has been long recognized as an important pathogenetic element in PH [54]. In addition to the oblitative changes caused by the anomalous growth of vascular cells, there is also evidence that perivascular infiltration with inflammatory cells is a

common finding in PAH vascular lesions. These infiltrates are predominantly composed of macrophages, dendritic cells, mast cells and lymphocytes that can appear as disorganized cell clusters or form highly organized pulmonary tertiary lymphoid tissues [48]. Beyond these pathological findings, there is also evidence that circulating levels of certain autoantibodies and inflammatory cytokines are elevated, which reflect activation of innate and adaptive immunity pathways [55-56]. While it is unclear whether inflammation is a trigger or a complication of the vascular pathology, available evidence supports its role as a major modifier of disease progression and has opened exciting opportunities for drug development [47]. Major unanswered questions still remain: i) the etiology of the abnormal host response to inflammation that leads to the initiation and progression of PH; ii) if the inflammatory response in PAH is caused by autoimmunity or infection; iii) which specific features of the inflammatory response can be enhanced (if protective) or blocked (if detrimental) for therapeutic intervention [43].

Group 2. Mechanisms involved in PH etiology are multiple and included the passive backward transmission of the pressure elevation. This is the case of the so-called “isolated post-capillary PH”. Sometimes, the increase in pulmonary artery pressure (PAP) is oversized respect to the increase of the PAWP, demonstrated by a DPG higher than 7 mmHg. This is the “combined form” of post-capillary PH. In this situation the elevation of PVR is due to an increase in the vasomotor tone of the pulmonary arteries, which is usually reversible under acute pharmacological testing, and/or to fixed structural obstructive remodelling of the pulmonary artery resistance vessels, not responding to acute pharmacological challenge [57]. Which factors lead to one or the other form is poorly understood.

Group 3. Pathobiological and pathophysiological mechanisms involved in this setting are multiple and include hypoxic vasoconstriction, mechanical stress of hyperinflated lungs,

loss of capillaries, inflammation, and toxic effects of cigarette smoke [12].

Group 4. Non-resolution of acute embolic masses which later undergo fibrosis leading to mechanical obstruction of pulmonary arteries is the most important pathobiological process in CTEPH. Another mechanism is recurrent pulmonary thromboembolism or in situ thrombosis. They may be initiated or aggravated by abnormalities in either the clotting cascade, endothelial cells, or platelets [58]. Platelet abnormalities and biochemical features of a procoagulant environment within the pulmonary vasculature support a potential role for local thrombosis in initiating the disease in some patients. In most cases, it remains unclear whether thrombosis and platelet dysfunction are the cause or the consequence of the disease. Inflammatory infiltrates are commonly detected in the pulmonary endarterectomy (PEA) specimens. Thrombophilia studies have shown that lupus anticoagulant may be found in about 10% of such patients, and 20% carry anti-phospholipid antibodies, lupus anticoagulant, or both. A recent study has demonstrated that the plasma level of factor VIII, a protein associated with both primary and recurrent venous thromboembolism, is elevated in 39% of patients with CTEPH.

Genetic

Group 1. The first gene discovered to be linked to PAH has been BMPR2. This gene is involved in the regulation of the bone morphogenetic protein signaling pathway, that plays a major role in regulating normal bone development and deposition of calcium in tissues [59-61]. Mutations in BMPR2 have been reported in approximately 75% of subjects with 1 or more affected relatives (heritable PAH) and approximately 20% of those with idiopathic PAH [62-64]. Mutations in several other genes have been found, including mutations in the activin receptor-like kinase-1 (ALK1) gene (65), the endoglin (66), the SMAD9 e (67), the

Caveolin-1 (68), and recently, the KCNK3 (69) genes. Mutations in BMPR2 or ALK-1 are emerging as determinants of severity of PAH. Patients with BMPR2 or ALK-1 mutations present with higher pulmonary vascular resistance (70). There is also evidence that these patients present with more severe disease and die at a younger age compared with PAH patients without mutations [71]. Moreover, they are less likely to respond acutely to vasodilators (72). Recent evidence suggests that the degree of pulmonary vascular remodeling is greater in patients with BMPR2 mutations compared with non-BMPR2-related disease at the time of transplantation (73). Clinical studies have shown that not all carriers of BMPR2 mutations actually develop the disease as the estimated penetrance is about 20%, leading to the consideration of other genetic factors that could be acting as modifiers [47].

Apart from major effects of rare sequence variants in heritable forms of PAH, interindividual differences in response to the same stimulus are well documented in subjects exposed to environmental hypoxia at high altitude or in the context of high pulmonary blood flow or pulmonary venous hypertension. This variable expressivity most certainly involves the impact of unknown genetic influences regulating the pulmonary vascular response. Elegant studies demonstrated that this response is inherited (74), though the identification of the genetic basis of PAH is the subject of ongoing research (75).

Group 1: Heritable PVOD/PCH has been recognized in consanguineous families, suggesting recessive transmission. Whole genome sequencing demonstrated that bi-allelic mutations in eukaryotic translation initiation factor 2 alpha kinase 4 were present in all familial PVOD/PCH and in 25% of histologically confirmed sporadic PVOD/PCH [76]. This gene encodes a serine-threonine kinase present in all eukaryotes that can induce changes in gene expression in response to amino acid deprivation.

Group 2. No specific genetic linkage has been identified [77].

Group 3. Gene polymorphism might contribute towards determining the severity of PH in hypoxaemic patients with COPD [78].

Group 4. No specific genetic mutations have been linked to the development of CTEPH.

Group 5. The heterogeneity of this group prevents an appropriate description of genetics, epidemiology and risk factors in these guidelines.

Genomics

Besides investigation of genetic mutations, molecular investigation of lung tissues or specific cell types can provide important information about the mechanisms of the disease.

Somatic genetic changes. Many evidences in the last decade permit to advance the hypothesis that the pathogenesis of PAH is a neoplastic-like process [79-81]. Microdissection of plexiform lesions from the lungs of idiopathic and anorexigen-induced PAH cases showed that endothelial cells have a monoclonal pattern of X-inactivation (80, 82). Many of the abnormal properties observed in pulmonary artery endothelial cells (PAECs) and pulmonary artery smooth muscle cells (PASMCS) are analogous to cancer, including increased proliferation, decreased apoptosis, activation of hypoxia-inducible factor- 1-alpha, mitochondrial abnormalities, and a shift from oxidative to glycolytic metabolism (83-89).

Epigenetic. Regulation of gene expression is a finely tuned event that is coordinated by various mechanisms that work in tandem to ensure that a given gene product is expressed

at target levels. Among these mechanisms, microRNAs (miRNAs) are responsible for regulating the size of the pool of mRNA transcripts available for translation both temporally and in a context-dependent manner [90]. Dysregulation in specific miRNAs has been observed in PAH and appears to contribute to the abnormal expression of candidate genes associated with increased smooth muscle cell proliferation and survival, active inflammation and development of PAH in various animal models [90-91].

Another epigenetic mechanism involved in gene regulation is DNA methylation, which can target promoter and enhancer regions to reduce their access to transcription factors [92]. Epigenetic traits are stably heritable phenotypes resulting from changes in a chromosome without alterations in deoxyribonucleic acid sequence (93). Epigenetic changes are thought to lead to cellular reprogramming, the process by which a differentiated cell type can be induced to adopt an alternate cell fate. This idea seems to be consistent with observations in pulmonary hypertension, in which PAECs, PSMCs, and adventitial fibroblasts have all been demonstrated to acquire significantly altered characteristics, including stable increases in proliferation, resistance to apoptosis, metabolic switching, and pro-inflammatory gene expression. A candidate for epigenetic study is *BMP2*, with significantly down-regulated expression in many PAH lungs, even in the absence of a germline mutation [94-95].

Physiopathology

Right ventricular remodeling

Patients suffering from severe forms of PAH frequently die of RV failure (RVF) [96]. However, patients affected by PH differ substantially in tendency to develop RVF. This leads to a variable natural history with some subjects living a surprisingly long time and

others dying more rapidly [97]. RV remodeling in PAH represents a continuum. Experimental studies often differentiate 2 patterns of RV remodeling on the basis of morphometric and molecular characteristics: adaptive and maladaptive remodeling. Adaptive remodeling is characterized by more concentric remodeling (Figure 7) and preserved systolic and diastolic function, whereas maladaptive remodeling is associated with more eccentric hypertrophy and worse systolic and diastolic function [98].

A clinical definition of RVF remains a work in progress; it could be defined as a state that is morphologically and functionally distinct from compensated RV hypertrophy [96].



Figure 7. long-axis section of the right ventricle of a patient affected by pulmonary arterial hypertension; it has to be noticed the remarkable hypertrophy of the free wall. Courtesy of Prof G. Thiene, Cardiovascular Pathology, Padua University.

Urashima et al. studied the transcriptional differences between the RV and the LV subjected to pressure overload in rodents and demonstrated a differential expression of genes between the pressure-overloaded RVs compared with the LV counterparts, suggesting that the RV and the LV do not respond to pressure overload identically [99]. Some features have been recognized to characterize the myocardium in RVF patients. Alterations of metabolism pathways have been demonstrated: decreased fatty acid and glucose oxidation, increased glucose uptake and glycolysis, abnormal mitochondrial ultrastructure and oxidative capacity [100]. Another salient feature is the impaired angiogenesis [101], driven by a reduction in vascular endothelial growth factor signaling inhibition [102]. However, whether decreased expression of the vascular endothelial growth factor and the accompanying reduction in capillaries are causes or consequences of RVF remain to be tested. Perhaps a direct consequence of capillary rarefaction in RVF tissue would be cell death and replacement interstitial fibrosis, which have been documented in RVF tissue [103-104]. Moreover, cardiomyocyte apoptosis plays a role in the development of RV dysfunction [105].

The exact mechanism underlying the appearance of RV failure is not clearly understood. Some hypothesis have been proposed [96]:

- one contemplates the autophagy as a model explaining transition from RV adaptive hypertrophy to RVF. Authors postulate that RV remains compensated by inducing adaptive autophagy with an adequate turnover of damaged proteins and damaged organelles. Transitions to RVF happens when autophagy becomes maladaptive, the damaged proteins and organelles that are not removed accumulate, and the “congested” cells die. In short, they hypothesize that maladaptive autophagy causes RVF.
- another hypothesis is based on the possibility that individuals who present earlier

with RVF symptoms are genetically prone to express the RVF program.

- the last hypothesis contemplate that phenotypically altered lung vascular cells from the sick lung circulation contribute to the progression from adaptive to maladaptive RV hypertrophy. In an intricate model of cardiopulmonary interaction, circulating cells and cell fragment, free-DNA and miRNAs from the sick lung circulation come into contact with the myocardial microcirculation. It has been demonstrated that circulating free DNA can be cytotoxic [106], and miRNA can reprogram endothelial cell genes.

Diagnosis

The diagnosis of PH is based on clinical suspicion, driven by symptoms and physical examination, followed by serial instrumental exams carried out to confirm the suspicion and to define aetiology and severity of the disease [2]. The approved diagnostic algorithm, taken from the current guidelines [2], has shown in 8.

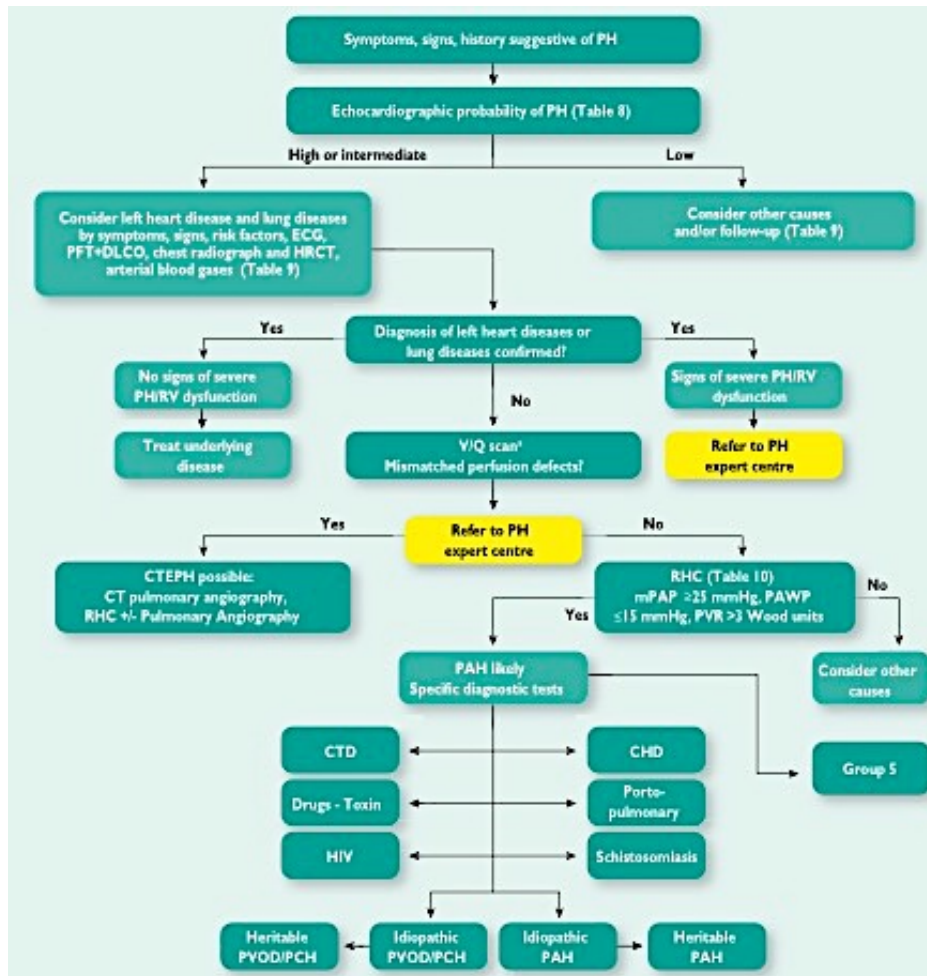


Figure 8. Diagnostic algorithm. From: Galiè N. et al 2015 ESC/ERS Guidelines for the diagnosis and treatment of pulmonary hypertension. Eur Heart J 2016;37(1):67-119 [2].

CHD = congenital heart diseases; CT = computed tomography; CTD = connective tissue disease; CTEPH = chronic thromboembolic pulmonary hypertension; DLCO= carbon monoxide diffusing capacity; ECG=electrocardiogram; HIV=human immunodeficiency virus; HR_CT=high resolution CT; mPAP=mean pulmonary artery pressure; PA = pulmonary angiography; PAH = pulmonary arterial hypertension; PAWP = pulmonary artery wedge pressure; PFT = pulmonary function tests; PH = pulmonary hypertension; PVOD/PCH = pulmonary veno-occlusive disease or pulmonary capillary hemangiomatosis; PVR = pulmonary vascular resistance; RHC = right heart catheterisation; RV = right ventricular; V/Q = ventilation/perfusion. ^aCT pulmonary angiography alone may miss diagnosis of chronic thromboembolic pulmonary hypertension.

Clinical presentation

Symptoms are non specific and mainly related to RV dysfunction and/or related to the disease that causes or is associated with PH. Typical symptoms include shortness of breath, fatigue, weakness, angina and syncope. At the beginning they are typically triggered by exertion; while in advanced cases they occur at rest, too. Other rare symptoms could be related to mechanical complications or abnormal distribution of blood flow in pulmonary vascular bed: haemoptysis; hoarseness or angina caused by a dilated pulmonary artery compressing the left recurrent laryngeal nerve or the left main coronary artery, respectively; cardiac tamponade due to rupture or dissection of a dilated pulmonary artery.

Typical signs include: left parasternal lift, an accentuated pulmonary component of the second heart sound, an RV third heart sound, a pansystolic murmur of tricuspid regurgitation (TR) and a diastolic murmur of pulmonary regurgitation. Elevated jugular venous pressure, hepatomegaly, ascites, peripheral oedema and cool extremities characterize patients with advanced disease.

Electrocardiogram. An electrocardiogram may provide supportive evidence of PH, but if normal it does not exclude the diagnosis. It is more likely abnormal in severe rather than in mild PH. Abnormalities may include P pulmonale, right axis deviation, RV hypertrophy, RV strain, right bundle branch block, and QTc prolongation. While RV hypertrophy has insufficient sensitivity (55%) and specificity (70%) to be a screening tool, RV strain is more sensitive [107].

Chest radiograph. It is abnormal in 90% of patients with idiopathic PAH at the time of diagnosis. It may assist in differential diagnosis by showing signs suggesting lung or left heart diseases. However, the severity of PH does not correlate with abnormalities at chest Rx and a normal one does not exclude PH.

Echocardiogram. As shown in Figure 8, in presence of a clinical suspicion of PH the echocardiogram is the first exam to be performed. It allows to estimate systolic PAP and to confirm or reject the suspicion of PH. Echocardiographic estimation of sPAP has been validated by Berger et al and Currie et al in 1985 [108-109].

Then, several studies have shown modest to good correlations between estimated RV systolic pressure and invasively measured pressures ($R = 0.57-0.93$), suggesting that technical and biological variability are not negligible [110]. A few aspects must be kept in mind to ensure accurate estimates of systolic PAP. Because velocity measurements are angle dependent, TR Doppler velocity should be taken from multiple views (and off axis if necessary), searching for the best envelope and maximal velocity. In case of a suboptimal continuous-wave Doppler spectrum, the injection of contrast agents (agitated saline, sonicated albumin, air-blood-saline mixture) may be required to achieve clear delineation of the jet envelope [111-112]. Potential overestimation of Doppler velocities should be taken into account because of contrast artifacts. Furthermore, in severe TR with a large color flow regurgitant jet, the peak velocity may not reflect the true RV-right atrial pressure gradient because of early equalization of RV pressure and RAP.

Other echocardiographic features, aside systolic PAP, might raise and support the suspicion of PH. These parameters describe the RV size and pressure overload, the pattern of blood flow velocity out of the RV, the diameter of the pulmonary artery and an estimate of right atrial pressure [113-115] (Table 5).

Table 5. Echocardiographic signs suggesting pulmonary hypertension.

A. The ventricles	B: Pulmonary artery	C. Inferior vena cava and right atrium
Right ventricle/left ventricle basal diameter ratio > 1.0	Right ventricular outflow Doppler acceleration time < 105 msec and/or midsystolic notching	Inferior cava diameter > 21 mm with decreased inspiratory collapse (<50% with a sniff or <20% with quiet inspiration)
Flattening of the interventricular septum (left ventricular eccentricity index > 1.1 in systole and/or diastole)	Early diastolic pulmonary regurgitation velocity > 2.2 m/sec	Right atrial area /end-systole) > 18 cm ²
	PA diameter > 25 mm	

From: Galiè N. et al 2015 ESC/ERS Guidelines for the diagnosis and treatment of pulmonary hypertension. Eur Heart J 2016;37(1):67-119. PA= pulmonary artery [2].

Taking together, all these informations permit to assign a level of probability of PH (Table 6): high, intermediate and low. When interpreted in a clinical context, the echocardiographic result is required to decide the need for right cardiac catheterization in individual patients.

Table 6. Echocardiographic probability of pulmonary hypertension

Peak tricuspid regurgitation velocity (m/s)	Presence of other echo "PH sign"	Echocardiographic probability of pulmonary hypertension
≤ 2.8 or not measurable	No	Low
≤ 2.8 or not measurable	Yes	Intermediate
2.9-3.4	No	
2.9-3.4	Yes	High
> 3.4	Not required	

From: Galiè N. et al 2015 ESC/ERS Guidelines for the diagnosis and treatment of pulmonary hypertension. Eur Heart J 2016;37(1):67-119. PH=pulmonary hypertension [2].

The recommended plan for further patient investigation based on echocardiographic probability of PH is shown in Table 7 for symptomatic patients.

Table 7. Diagnostic management suggested according to echocardiographic probability of pulmonary hypertension in patients with symptoms compatible with pulmonary hypertension.

Echocardiographic probability of PH	W/o risk factors or associated condition for PAH or CTEPH	Class/ Level	With risk factors or associated conditions for PAH or CTEPH	Class/ Level
Low	Alternative diagnosis should be considered	Ia/C	Echo f-up should be considered	Ia/C
Intermediate	Alternative diagnosis, echo f-up should be considered	Ia/C	Further assessment of PH including RHC should be considered	Ia/B
	Further investigation of PH may be considered	Ib/C		
High	Further investigation of PH (including RHC) is recommended	I/C	Further investigation of PH including RHC is recommended	I/C

From: Galiè N. et al 2015 ESC/ERS Guidelines for the diagnosis and treatment of pulmonary hypertension. Eur Heart J 2016;37(1):67-119 [2].

CTEPH=chronic thromboembolic pulmonary hypertension; PAH=pulmonary arterial hypertension; PH=pulmonary hypertension; RHC=right heart catheterization

Table 8 shows the recommended investigation plan based on PH probability by echocardiogram, for asymptomatic patients.

Table 8. Diagnostic management suggested according to echocardiographic probability of pulmonary hypertension in asymptomatic patients.

Echocardiographic probability of PH	W/o risk factors or associated condition for PAH or CTEPH	Class/Level	With risk factors or associated conditions for PAH or CTEPH	Class/Level
Low	No work up for PAH required	III/C	Echo f-up may be considered	IIb/C
Intermediate	Echo f-up should be considered	IIa/C	Echo f-up is recommended	I/B
			Is associated scleroderma, RHC should be considered	IIa/B
High	RHC should be considered	IIa/C	RHC is recommended	I/C

From: Galiè N. et al 2015 ESC/ERS Guidelines for the diagnosis and treatment of pulmonary hypertension. Eur Heart J 2016;37(1):67-119 [2].

CTEPH=chronic thromboembolic pulmonary hypertension; PAH=pulmonary arterial hypertension; PH=pulmonary hypertension; RHC=right heart catheterization

Moreover, echocardiography can be helpful in detecting the cause of suspected or confirmed PH, such as congenital heart disease (CHD) or LV heart disease.

If the echocardiographic probability of PH appears to be high or intermediate, the diagnostic algorithm contemplates tests targeted to the identification of the more common clinical groups of PH (2 and 3).

Pulmonary function tests and arterial blood gases. Pulmonary function tests and arterial blood gases identify the contribution of underlying airway or parenchymal lung disease. Patients with PAH have usually mild to moderate reduction of lung volumes related to disease severity. Although diffusion capacity can be normal in PAH, most patients have decreased lung diffusion capacity for carbon monoxide (DLCO). An abnormal low DLCO, defined as <45% of predicted, is associated with a poor outcome [116-117]. The

differential diagnosis of a low DLCO in PAH includes PVOD, PAH associated with scleroderma and parenchymal lung disease. COPD as a cause of hypoxic PH is diagnosed on the evidence of irreversible airflow obstruction together with increased residual volumes and reduced DLCO [118]. Arterial blood gases of COPD patients show a decreased PaO₂ with normal or increased PaCO₂ [119]. A decrease in lung volume combined with decreased diffusion capacity for carbon monoxide may indicate interstitial lung disease. The prevalence of nocturnal hypoxaemia and central sleep apnoeas are high in PAH (70–80%) [120-121]. Overnight oximetry or polysomnography should be performed where obstructive sleep apnoea syndrome or hypoventilation are considered.

High-resolution computed tomography. Computed tomography (CT) imaging can provide important information on vascular, cardiac, parenchymal and mediastinal abnormalities. It may raise the suspicion of PH by showing an increased pulmonary artery diameter and pulmonary:ascending aorta diameter ratio ≥ 1 . Moreover, CT contribute to identify causes of PH such as CTEPH or lung disease, or provide clues as to the form of PAH (e.g. oesophageal dilation in SSc or congenital cardiac defects). Finally, CT may provide prognostic information [122]. High-resolution CT provides detailed views of the lung parenchyma and facilitates the diagnosis of interstitial lung disease and emphysema. High-resolution CT may also be very helpful where there is a clinical suspicion of PVOD [123].

If Group 2 or 3 PH have been excluded, presence of group 4-PH has to be investigated.

Ventilation/perfusion lung scan. The ventilation/perfusion scan is the screening method of choice for CTEPH because of its higher sensitivity compared with CT pulmonary angiogram, especially in inexperienced centres [124]. A normal- or low-probability ventilation/perfusion scan effectively excludes CTEPH with a sensitivity of 90–100% and a specificity of 94–100%. However, many ventilation/perfusion scans are not diagnostic.

While a perfusion scan is still recommended as the screening test of choice, ventilation scans are often replaced with either a recent chest radiograph or a recent high-resolution CT of the lungs, but such practices are not really evidence-based. If the ventilation/perfusion scan shows multiple segmental perfusion defects, a diagnosis of group 4 (CTEPH) PH should be suspected [125]. The final diagnosis of CTEPH (and the assessment of suitability for pulmonary endarterectomy (PEA)) will require CT pulmonary angiography, RHC and/or selective pulmonary angiography (Figure 9).

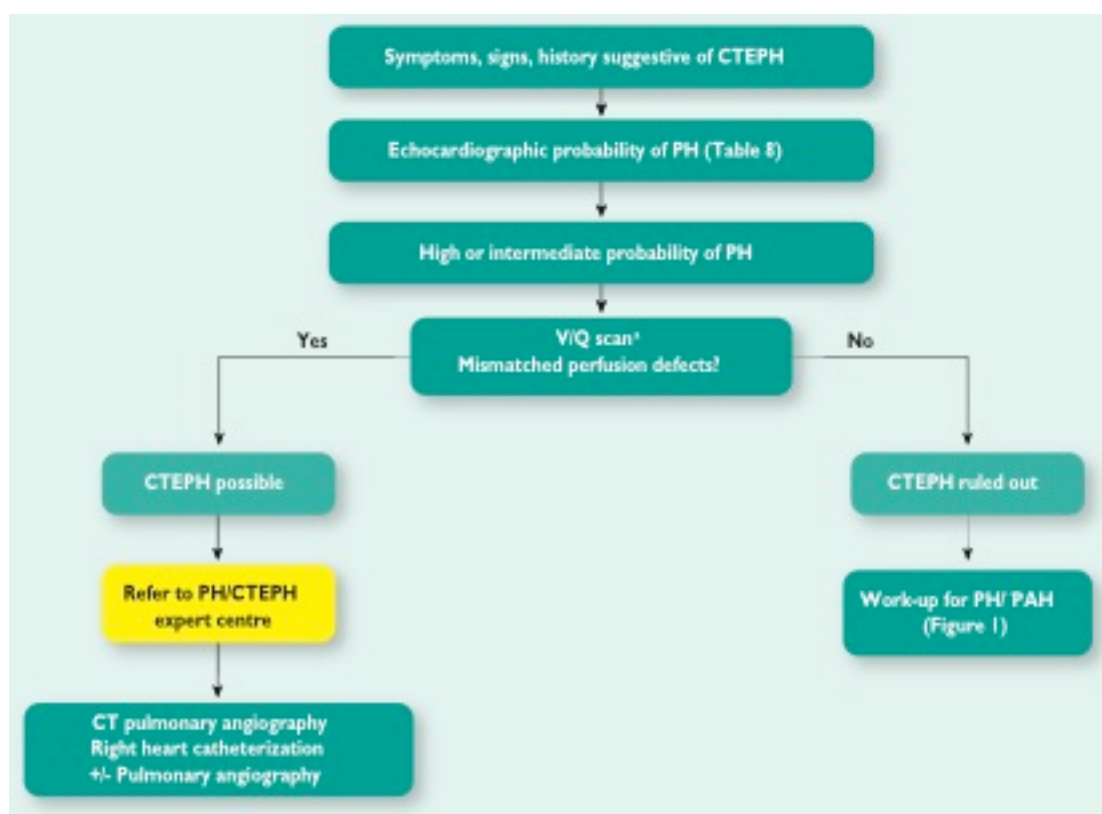


Figure 9. Diagnostic algorithm for chronic thromboembolic pulmonary hypertension. From: Galiè N. et al 2015 ESC/ERS Guidelines for the diagnosis and treatment of pulmonary hypertension. Eur Heart J 2016;37(1):67-119 [2].

CT = computed tomography; CTEPH = chronic thromboembolic pulmonary hypertension; PAH = pulmonary arterial hypertension; PH = pulmonary hypertension; V/Q = ventilation/perfusion.

^aCT pulmonary angiography alone may miss diagnosis of chronic thromboembolic pulmonary hypertension.

Contrast-enhanced computed tomography. Contrast CT angiography of the PA is helpful in determining whether there is evidence of surgically accessible CTEPH. It can delineate the typical angiographic findings in CTEPH, such as complete obstruction, bands and webs and intimal irregularities, as accurately and reliably as digital subtraction angiography [126-127]. It has become an established imaging modality for confirming CTEPH [128]; however, this investigation alone cannot exclude the disease [129].

Pulmonary angiography. Traditional pulmonary angiography is required in most patients for the workup of CTEPH to confirm diagnosis and identify those who may benefit from PEA or balloon pulmonary angioplasty [130-131]. The final step in the diagnostic pathway is selective pulmonary angiography in the anterior-posterior and lateral projections illustrating ring-like stenosis, webs ('slits'), pouches, wall irregularities, complete vascular obstructions as well as bronchial collaterals, and supports the technical assessment of operability.

Angiography can be performed safely by experienced staff in patients with severe PH using modern contrast media and selective injections.

Once excluded PH from group 2, 3 and 4; the attention has to be focused on make the diagnosis of group 1 and 5.

Right heart catheterization and vasoreactivity. RHC should be performed after the completion of other investigations so that it can answer specific questions that may arise from these investigations and avoid an unnecessary procedure where an alternative diagnosis is revealed. RHC is required to confirm the diagnosis of PAH and CTEPH, to assess the severity of haemodynamic impairment and to undertake vasoreactivity testing

of the pulmonary circulation in selected patients. When performed at expert centres, these procedures have low morbidity (1.1%) and mortality (0.055%) rates [132]. Left heart catheterization has to be performed in patients with clinical risk factors for coronary artery disease or heart failure with preserved ejection fraction, as well as in patients with echocardiographic signs of systolic and/or diastolic LV dysfunction. Measurement of LV end-diastolic pressure is also important to avoid misclassification of patients with an elevated PAWP when this is unexpected and may be inaccurate. Pulmonary vasoreactivity testing for identification of patients suitable for high-dose calcium channel blocker (CCB) treatment is recommended only for patients with idiopathic-PAH, heritable-PAH or drug-induced PAH. Inhaled nitric oxide (NO) at 10–20 parts per million (ppm) is the standard of care for vasoreactivity testing, but i.v. epoprostenol, i.v. adenosine or inhaled iloprost can be used as alternatives. A positive acute response is defined as a reduction of the mean PAP ≥ 10 mmHg to reach an absolute value of mean PAP ≤ 40 mmHg, with an increased or unchanged cardiac output. Only about 10% of patients with idiopathic-PAH will meet these criteria. Interpretation of the PAWP at a single point in time needs to be performed in a clinical context. In many patients with left heart disease, PAWP may be reduced to < 15 mmHg with diuretics [133-135]. For this reason, the effect of an acute volume challenge on left heart filling pressures has been considered [136].

Cardiac magnetic resonance. Cardiac magnetic resonance (CMR) imaging could have high predictive value for the identification of PH; however, it cannot exclude PH [137-139]. It is accurate and reproducible in the assessment of RV size, morphology and function and allows non-invasive assessment of blood flow, including stroke volume, cardiac output, pulmonary arterial distensibility and RV mass. In patients with PH, CMR may also be useful in cases of suspected CHD if echocardiography is not conclusive. CMR provides useful prognostic information in patients with PAH both at baseline and at follow-up [140-142].

Blood test and immunology. Blood tests are required to identify the aetiology of some forms of PH, as well as end-organ damage. Serological testing are required to detect underlying CTD, hepatitis and HIV. Liver function may be abnormal because of high hepatic venous pressure, liver disease and/or endothelin receptor antagonist therapy. Patients with CTEPH should undergo thrombophilia screening. N-terminal pro-brain natriuretic peptide may be elevated in patients with PH and is an independent prognostic factor.

Abdominal ultrasound scan. Similar to blood tests, abdominal ultrasound may be useful for identification of some of the clinical entities associated with PAH. Abdominal ultrasound may confirm but not formally exclude portal hypertension.

Genetic testing. Patients with sporadic or familial PAH or PVOD/PCH should be advised about the availability of genetic testing and counselling because of the strong possibility that they carry a disease-causing mutation. Trained professionals should offer counselling.

Follow-up

The attention will be focused mainly on PAH patients. Their regular assessment in expert PH centres is recommended, with a follow-up visit every 3-6 months for stable patients. There is no single variable that provides sufficient prognostic informations. Then, a multidimensional approach is needed, as shown in Table 9.

Table 9. Risk assessment in pulmonary arterial hypertension.

Determinants of prognosis	Low risk < 5%	Intermediate risk 5-10%	High risk > 10%
Clinical signs of right heart failure	Absent	Absent	Present
Progression of symptoms	No	Slow	Rapid
Syncope	No	Occasional syncope	Repeated syncope
WHO functional class	I, II	III	IV
6 MWD	> 440 m	165-440 m	< 165 m
Cardiopulmonary exercise testing	Peak VO ₂ > 15 ml/min/Kg (>65% pred) VE/VCO ₂ slope < 36	Peak VO ₂ 11-15 ml/min/kg (35-65% pred) VE/VCO ₂ slope 36-44.9	Peak VO ₂ < 11 ml/min/kg (<35% pred) VE/VCO ₂ slope ≥ 45
NT-proBNP plasma levels	BNP < 50 ng/l NT-proBNP < 300 ng/ml	BNP 50-300 ng/l NT-proBNP 300-1400 ng/ml	BNP > 300 ng/l NT-proBNP > 1400 ng/ml
Imaging (echo, CMR)	RA area < 18 cm ² No pericardial effusion	RA area 18-26 cm ² No or minimal pericardial effusion	RA area > 26 cm ² pericardial effusion
Haemodynamics	RAP < 8 mmHg CI ≥ 2.5 l/min/m ² SvO ₂ > 65%	RAP 8-14 mmHg CI 2-2.4 l/min/m ² SvO ₂ 60-65%	RAP > 14 mmHg CI < 2 l/min/m ² SvO ₂ < 60%

From: Galiè N. et al 2015 ESC/ERS Guidelines for the diagnosis and treatment of pulmonary hypertension. Eur Heart J 2016;37(1):67-119 [2].

BNP=brain natriuretic peptide; CI=cardiac index; CMR=cardiac magnetic resonance; MWD=minute walking distance; RA=right atrium; RAP=right atrial pressure; SvO₂=mixed venous oxygen saturation; VE/VCO₂=minute ventilation – carbon dioxide production relationship; WHO=world health organization

Not all these parameters must be assessed at each visit, but at least functional class plus one measurement of exercise capacity and RV function have to be re-checked. Not all variables may be in the same risk group; the comprehensive assessment of individual patients guide treatment decisions. An adequate treatment response is considered in presence of the achievement and/or maintenance of a low-risk profile.

The most important questions to be addressed at each visit are:

- is there any evidence of clinical deterioration since the last assessment?
- if so, is clinical deterioration caused by progression of PH or by a concomitant illness?
- is RV function stable and sufficient?
- is the current status compatible with a good long-term prognosis (does the patient meet the low-risk criteria)?

Clinical assessment remains a key part of the evaluation of patients with PH. WHO FC remains one of the most powerful predictors of survival [143-145].

The 6-minute walking test, a submaximal exercise test, remains the most widely used exercise test. The test is easy to perform, inexpensive and familiar to patients and centres. However, it is influenced by several factors (sex, age, height, weight, comorbidities, need for O₂, learning curve and motivation) that must be taken into account for the interpretation of the result. Test results are usually given in absolute numbers because only absolute values, but not changes in 6-minute walking distance, provide prognostic information. Anyway, there is no single threshold that is applicable for all patients [143, 146-148]. It is recommended to use the Borg score at the end of the 6-minute walking test to determine the level of effort. In addition, some studies suggest that adding peripheral O₂ measurements and heart rate response may improve the prognostic relevance, but these findings await independent confirmation [149-150]. Cardiopulmonary exercise testing is usually performed as a maximal exercise test and provides important information on exercise capacity as well as on gas exchange, ventilator efficacy and cardiac function during exercise. Several variables determined by cardiopulmonary exercise test provide prognostic information, although peak VO₂ is most widely used for therapeutic decision

making [151-152].

A wide variety of biomarkers have been explored as prognostic tools, but so far brain natriuretic peptide and NT-pro brain natriuretic peptide remain the only biomarkers that are widely used in the routine practice of PH centres as well as in clinical trials [153].

RV function is a key determinant of outcome in patients with PH [140, 154-160]. In this scenario non-invasive imaging techniques, such as echocardiography and CMR, cover a major role [161]. A number of CMR prognostic markers have been identified, including increased RV volume, reduced LV volume, reduced RV ejection fraction and reduced stroke volume. There is some evidence that follow-up CMR studies may have utility in the long-term management of PAH by identifying RVF prior to the development of clinical features [140, 142, 162-163].

Echocardiographic evaluation of the RV will be discussed more extensively further in the text.

Haemodynamics assessed by RHC provide important prognostic information: RA pressure, cardiac index and mixed venous oxygen saturation are the most robust indicators of RV function and prognosis. There are still uncertainties around the optimal timing of follow-up RHC. Strategies vary between centres, from regular invasive haemodynamic assessments to a predominantly non-invasive follow-up strategy. There is no evidence that an approach involving regular RHC is associated with better outcomes than a predominantly non-invasive follow-up strategy. However, there is consensus among experts that RHC should be performed whenever therapeutic decisions can be expected from the results, which may include changes in medications and/or decisions regarding listing for transplantation.

Therapy

Similar to what we did about the follow-up chapter, the therapy section will mainly focus the attention on PAH patient with a little part on CTEPH patients.

The current treatment strategy for PAH patients include: general measures, supportive therapy, specific drug therapy [164].

General measures include avoidance of pregnancy. Although outcome of pregnancies in PAH has improved [165], it is still associated with a significant mortality rate. Immunization of patients against influenza and pneumococcal infection is recommended. Pneumonia has been reported to be cause of death in 7% of cases of PAH patients [25]. In addition, a psychosocial support is recommended because PH is a disease with a significant psychological, social and emotional impact on patients and their families [166]. A supervised exercise training for physically deconditioned patients is recommended. However, before starting physical activity, patients should be optimally pharmacologically treated and in stable condition. More than one randomized trials demonstrated the efficacy of exercise training in improving functional capacity and quality of life [167-171]. Nevertheless, the optimal method of exercise and the intensity and duration of the training remain to be defined. In case of elective surgery, epidural rather than general anaesthesia has to be preferred, because probably better tolerated [172-174].

Supportive therapy include administration of diuretics, in patients with signs of RVF and fluid retention, and continuous long-term O₂ therapy, when arterial blood O₂ pressure is less than 60 mmHg. Routine oral anticoagulant treatment is not recommended, since data from registry and randomized clinical trials appear heterogeneous and inconclusive [175-177].

Specific drug therapy must be administered according to the therapeutic algorithm showed

in the current guidelines (Figure 10).

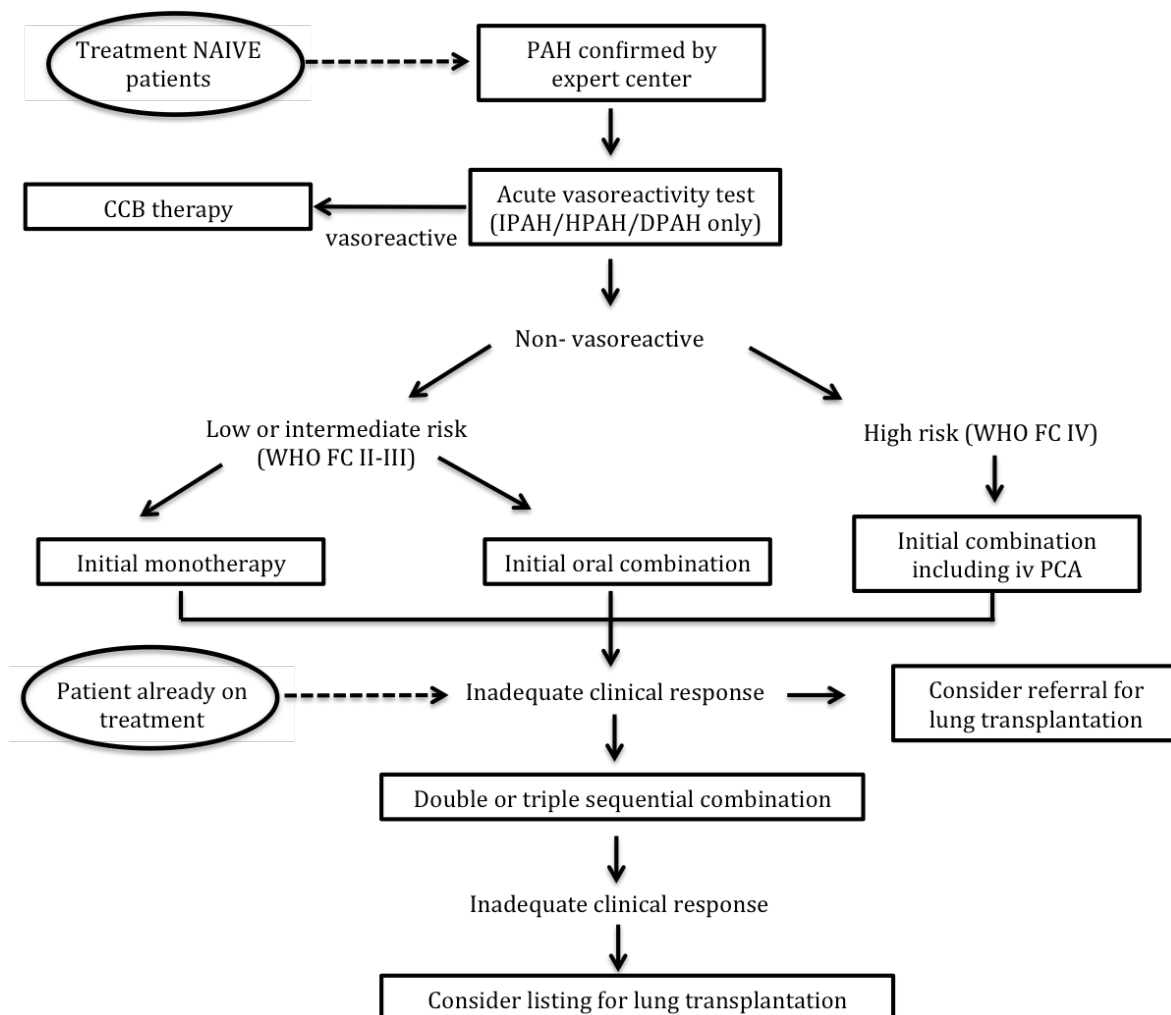


Figure 10. Therapeutic algorithm for pulmonary hypertension patients.

From: Galiè N. et al 2015 ESC/ERS Guidelines for the diagnosis and treatment of pulmonary hypertension. Eur Heart J 2016;37(1):67-119 [2].

CCB=calcium channel blockers; DPAH=drug-induced PAH; FC=functional class; HPAH=heritable PAH; IPAH=idiopathic PAH; PAH=pulmonary arterial hypertension; PCA= prostacyclin analogues; WHO=world health organization

Disease specific treatment includes the administration of high doses of calcium channel blockers (CCBs), only in patients affected by idiopathic-PAH, heritable-PAH and drug-induced PAH with a positive response at vasodilator test. However, it has been

demonstrated that only a small number of patients with a positive vasodilator test do well with CCBs [178-179]. The CCBs predominantly used are nifedipine, diltiazem and amlodipine, with particular emphasis on nifedipine and diltiazem [178-179]. Patients who are treated with CCBs should be followed closely to check both safety and efficacy, with a complete reassessment, including RHC, after 3-4 months of therapy. Continuation of the CCBs therapy is recommended in presence of an adequate clinical and haemodynamic response, defined by a functional WHO class I or II and a marked haemodynamic improvement (see Table 9). If patients do not respond to CCBs therapy, specific PAH therapy is required. Vasodilator responsiveness does not appear to predict a favourable long-term response to CCB therapy in patients with PAH in the setting of CTD, HIV, portopulmonary hypertension and PVOD [180-181].

Specific therapy includes three classes of drugs: endothelin receptor antagonists; phosphodiesterase type 5 inhibitors and guanylate cyclase stimulators; prostanoid (prostacyclin analogues and prostacyclin receptor agonists). The administration of the first class is driven by the demonstration of the endothelin system activation in both plasma and lung tissue of PAH patients [182], along with the prominent role of the endothelin system activation in the pathogenesis of PAH [183]. This class of drugs includes ambrisentan, bosentan and the recently introduced macitentan. The administration of phosphodiesterase type 5 inhibitors and guanylate cyclase stimulators is based on the evidence that the pulmonary vasculature contains a substantial amount of phosphodiesterase type 5. This class of drugs acts through a vasodilator effect, obtained by the NO/cGMP pathway modulation, and an anti-proliferative effect [184-185]. Prostacyclins are endogeneously produced predominantly by endothelial cells. They induce vasodilation of all vascular bed and inhibition of platelet aggregation; moreover they have both cytoprotective and antiproliferative activities [186]. The administration of

prostanoid is driven by the evidence that in PAH patients a dysregulation of the prostacyclin pathways is present [187].

Both endothelin receptor antagonists and phosphodiesterase type 5 inhibitors are administered either to patients responders to vasodilator tests but without an adequate response to CCBs therapy or to patients non-responders to vasoreactive test. This latter category of patients can be treated with either initial monotherapy or initial combination therapy. If the non-vasoreactive patient is at high risk, initial combination therapy (including intravenous prostanoid) should be considered. An adequate treatment response is defined by the achievement or maintenance of a low-risk profile (see section on Follow-up). In case of inadequate response to initial mono- or combination therapy, sequential double or triple therapy is recommended.

It seems reasonable to consider eligibility for lung transplantation after an inadequate clinical response to the initial monotherapy or initial combination therapy and to refer the patient for lung transplantation soon after the inadequate clinical response is confirmed on maximal combination therapy.

Patients included in other PAH groups can benefit of specific management therapies, tailored on the single case. In patients with PAH associated with congenital heart disease the possibility of undergo to the defect correction has to be considered. It is feasible only in patient with prevalent systemic-to-pulmonary shunt with low PVR, while is contraindicated in patients with high PVR values, in patients with Eisenmenger syndrome and is useless in patients with small/coincidental defects. In patients with CTEPH the treatment of choice is pulmonary endarterectomy. The majority of patients experience relief of symptoms and near normalization of haemodynamics [188-190]. Operability of patients with CTEPH is determined by multiple factors: patient acceptance, expertise of the

surgical team and available resources. General criteria include preoperative WHO-FC II-IV and surgical accessibility of thrombi in the main, lobar or segmental pulmonary arteries. Advanced age, per se, is not a contraindication for surgery. There is no PVR threshold or measure of RV dysfunction that can be considered to preclude pulmonary endarterectomy. Riociguat is recommended in symptomatic patients who have been classified as having persistent/recurrent CTEPH after surgical treatment or inoperable.

The right ventricle

A proper knowledge of RV anatomy and physiology is mandatory before trying to understand the pathological aspects of RV function.

The RV shows a complex shape. In contrast to the ellipsoidal shape of the LV, the RV appears triangular when viewed from the side and crescent shaped when viewed in cross section [191]. It can be divided in three main parts: the inlet, the outlet, and the apical, trabeculated part (Figure 11). The RV free wall myocardium is composed mainly by circumferential fibers in the superficial layer and longitudinal fibers in the subendocardial layer [192]. Usually, the circumferential fiber layer is less developed than the longitudinal one. This myocardial fiber architecture explains why, in healthy subjects, RV pump function is determined mainly by longitudinal shortening, rather than by transversal displacement (TD) [193-194].

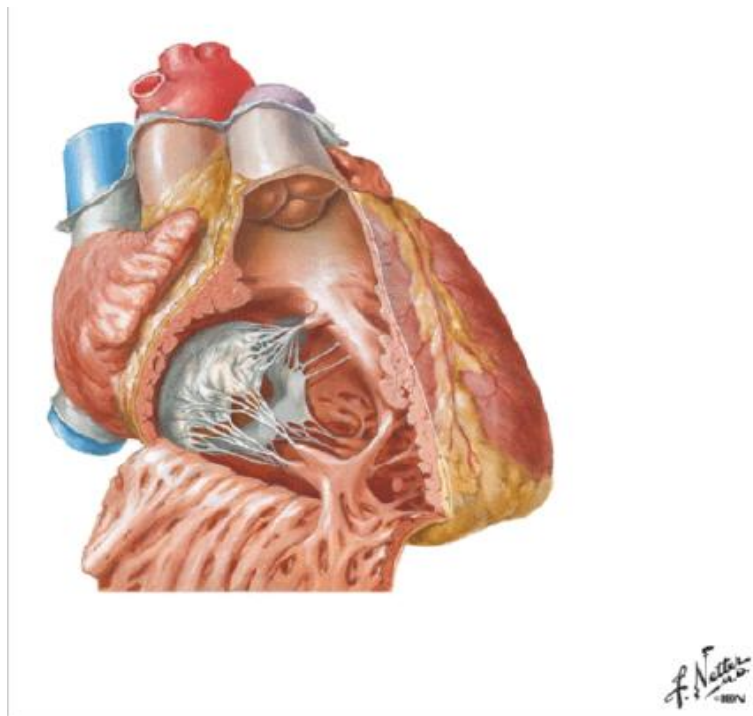


Figure 11. Opened right ventricle: anterior view. From: Netter FH. Atlas of Human Anatomy, 6th edition.

The physiological RV contraction follows a peristaltic pattern that starts from the inlet part and ends to the outlet one 25–50 msec later [195-196]. Several distinct events contribute to overall RV pump function: (i) inward movement of the RV free wall, which produces a bellows effect; (ii) contraction of the longitudinal fibers, which draws the tricuspid annulus toward the RV apex; (iii) infundibular contraction; and (iv) contraction of the LV, which assists RV contraction via mechanical transduction across the shared interventricular septum, as well as via circumferentially oriented superficial myofibers that are contiguous between the two ventricles. Therefore, the RV presents regional contraction differences that contribute in distinct magnitude and timing to its global systolic function [197-198].

In patients with RV pressure overload, with consequent RV hypertrophy, the hypertrophied fibers change their spatial orientation and become more circumferential. As a consequence, in PH patients, circumferential and radial shortening increase their contribution to the RV pump function compared to normal subjects [199-200].

Under normal conditions, the RV is coupled with a low-impedance and highly distensible pulmonary vascular system with a right-sided pressures that are significantly lower than comparable left-sided pressures [201]. As for the LV, determinants of RV systolic function are pre-load, contractility and afterload. The latter represents the load that RV has to overcome during ejection. It has been demonstrated that, compared to the LV, the RV demonstrates an increased sensitivity to afterload change [202-203].

Right and LV filling and emptying are tightly coupled. This phenomenon named “ventricular interdependence” refers to the fact that the size, the shape and the compliance of one ventricle affects the size, the shape and the pressure-volume relationship of the other ventricle through direct mechanical interactions [204]. Ventricular interdependence is more apparent with changes in loading conditions and plays an important role in the

pathophysiology of RV dysfunction. We can distinguish diastolic and systolic interdependence. The first depends mainly from the pericardium, while the latter is mediated mainly through the interventricular septum. Experimental animal studies showed that 20% to 40% of RV systolic pressure and volume outflow results from LV contraction [204]. Moreover, in presence of scarring of the RV the septum is able to maintain circulatory stability as long as the RV is not dilated [205].

The right ventricular failure

RVF is a complex clinical syndrome that can result from any structural or functional cardiovascular disorder that impairs the ability of the RV to fill or to eject blood [206].

In the past the predominant view was that, in presence of PH, the RV fails because of the afterload mismatch, and although patients died of RVF, the treatment of PH should be directed towards the pulmonary vasculature rather than the RV. A number of papers have suggested that this may not be the whole story. First of all, a Dutch group [142] showed that RV dysfunction can progress even in patients who appear to have responded to vasodilator therapy by reducing pulmonary vascular resistance. Moreover, RV failure impacts on survival in any type of PH but with variable burden, depending on causal disease and comorbidities [207]. Indeed, patients with Eisenmenger syndrome show a better survival and develop RV failure only at a late stage of the disease [208]. This makes the point that RV function is more complex than simply a function of pulmonary vascular narrowing. The most important factors appear to be the type and severity of myocardial injury or stress, the time course of the disease (acute or chronic), and the time of onset of the disease process (newborn, pediatric, or adult years) [206]. The mechanisms underlying the occurrence of RVF are still not well understood; current hypotheses have been previously described in the pathophysiology section. Ruiters *et al* [209] recently demonstrated that the cellular alterations characterizing the failing RV in PH are represented in the free-wall but not in the interventricular septum.

Few data are available in literature about the progression of the RV function decline in PH patients. Mauritz *et al*. [210] showed, using CMR, that the progression of RV dysfunction is mainly related to the loss of RV TD, showing also a good correlation between prognosis and

extent of residual TD. Moreover, they showed that the decline in TD is mostly due to a progressive leftward displacement of interventricular septum (IVS) rather than to a further decrease of RV free wall (RVFW) TD [210]. They hypothesized that RV dysfunction in PH patients may start with a reduction of tricuspid anulus plane systolic excursion (TAPSE), that continues to decrease until a lower limit is reached. Progression of the disease induces a further deterioration of the RV function through a loss of transversal shortening. As for longitudinal shortening, a lower limit also is reached for the RVFW TD; thus, increased leftward septal bowing is the main explanation for a further decline in RV transverse shortening in progressive PH [210]. Differently from the pattern showed in presence of acute pulmonary embolism, RV apex involvement is a constant feature of RV dysfunction in chronic PH [211], as demonstrated by 2D-STE [212-213]. Particularly, Unlu S et al [214] showed that the visually assessed RV apical traction, a motion pattern caused by the traction of the RV apex from the LV, occur in a sizable number of PH patients with reduced EF and represents a prognostic factor in this group of patients.

Consequences of RVF are summarized in the following Figure 12.

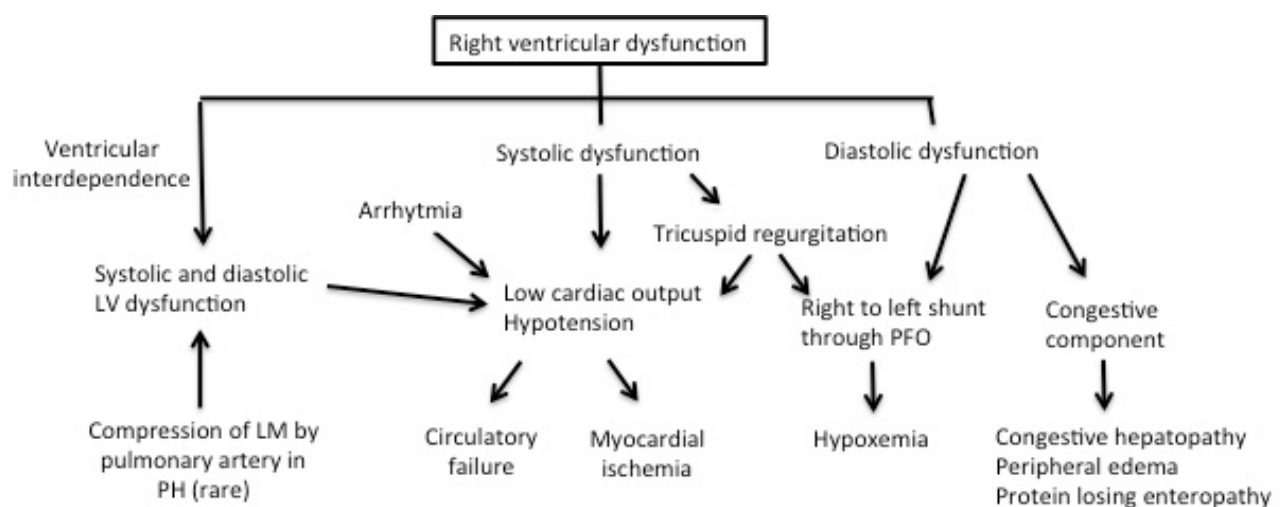


Figure 12. Pathophysiology of right ventricular failure.
From: Haddad F et al. Circulation 2008; 117: 1717-31 [206].

RVF is mainly characterized by a low cardiac output state. As stated before, ventricular interdependence plays an important role in the pathophysiology of RVF, especially in the acute setting. RV dilatation and/or pressure overload cause a leftward shift of the septum, changing LV geometry; RV dilatation also may increase the constraining effect of the pericardium. These changes contribute to the low cardiac output state by decreasing LV distensibility and preload. RV diastolic dysfunction impairs RV filling and increases diastolic RV pressures and right atrial pressures. This may lead to fluid retention and congestive hepatopathy, as well as cardiac cirrhosis in more advanced cases. RVF may also lead to significant TR

, which may further aggravate RV volume overload and decrease cardiac output [206].

Then, the cardinal clinical manifestations are: fluid retention; decreased systolic reserve or low cardiac output; atrial or ventricular arrhythmias.

Echocardiographic evaluation of the right ventricular function

Many factors contribute to the challenges posed by the echocardiographic RV assessment. These include: the complex geometry of the RV; the limited definition of RV endocardial surface caused by heavily trabeculated myocardium; the retrosternal position, which can limit echocardiographic windows; respiratory variability RV filling and the marked load dependence of indices of RV function [192]. Multiple standardized 2DE views should be obtained for a comprehensive assessment of the different segments of the RV, including the apical four-chamber, RV-focused apical four-chamber and modified apical four-chamber views, left parasternal long- and short-axis, left parasternal RV inflow, and subcostal views [114]. Additional non-standard views may be required for an accurate evaluation of specific regions of interest.

Conventional echocardiography provides several parameters to measure RV function, such as RV fractional area change, TAPSE, lateral wall S wave velocity by Tissue Doppler and myocardial performance index (Figure 13). Among them only TAPSE has shown to be a strong predictor of survival in PH patients [215]. However, all of them value the RV function only in one section, without taking into account neither the three-dimensional shape of the chamber nor its whole spatial motion. Then, conventional echocardiographic measurements of RV function do not always reflect true RV pump function due to the complex geometry of the RV and its extreme dependence on loading conditions [216]. New echocardiographic techniques, such as 2D speckle tracking echocardiography (STE) and 3D echocardiography (3DE), have been employed to provide a more comprehensive assessment of RV function. Indeed, these new echocardiographic techniques overcome the

main limitations of both two-dimensional echo (geometric assumptions about RV geometry) and M-mode and Doppler related techniques (external reference, angle-dependency) and provide a more comprehensive assessment of RV function, which is not limited to the assessment of the longitudinal excursion anymore [161].

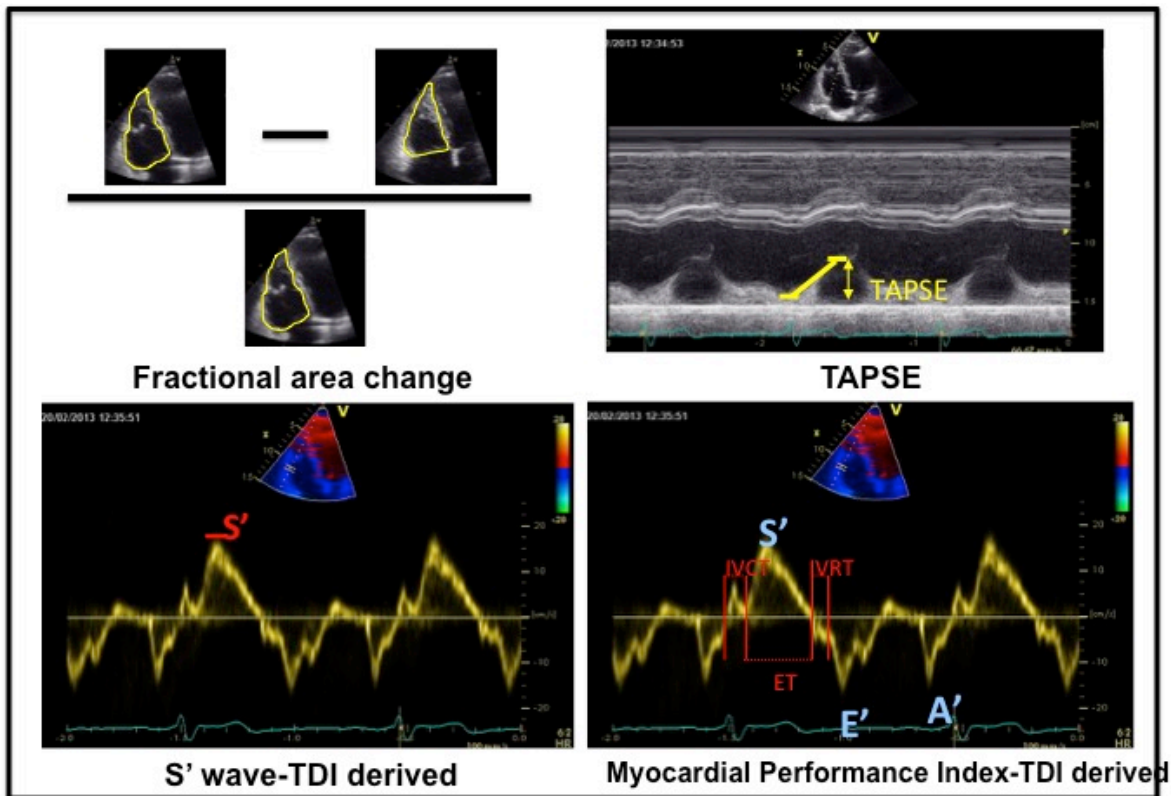


Figure 13. Echocardiographic conventional parameters for right ventricular function evaluation. TAPSE=tricuspid annulus plane systolic excursion; TDI=tissue doppler imaging

Two-dimensional Speckle Tracking Echocardiography

Deformation imaging by 2D-STE has been introduced to assess LV myocardial function and recently applied to detect RV myocardial function in several pathological conditions [217-225]. Compared to Tissue Doppler Imaging, 2D-STE is an angle-independent technique based on internal reference, thus, avoiding limitations related to translational cardiac motion. Preliminary researches showed good correlations with the

other standard echo parameters of RV function, in particular with TAPSE [226]. Among non-volumetric echo parameters, RV free-wall strain by STE demonstrated the closest correlation with RV-ejection fraction (RVEF) measured by CMR [227].

A recent, by date the largest study of healthy subjects showed different methods to measure RV longitudinal strain (LS), both global (RVGLS) and free-wall (RVFWLS) [228]. Authors provided reference values (lower limits of normality) for 2D-STE derived RV LS: for 6-segment RVGLS $-24.7 \pm 2.6\%$ (-20.0%) for men and $-26.7 \pm 3.1\%$ (-20.3%) and for 3-segment RVFWLS $-29.3 \pm 3.4\%$ (-22.5%) for men and $-31.6 \pm 4.0\%$ (-23.3%) for women [229]. In the most up-to-date version of the chamber quantification guidelines an abnormality threshold for the RVFWLS was set at -20% [114].

To date there is no agreement on what is the correct method to evaluate the RV function by 2D-STE, if including or not the IVS. While some research groups analyze only the RV FWLS [222, 229] others include the IVS in the assessment of RV function [226, 230]. Recently, Focardi et al [231] demonstrated that both RVGLS and RVFWLS strongly correlated with CMR-derived RVEF in a heterogeneous group of cardiac patients. However, among them, RVFWLS demonstrated the strongest correlation [231].

Despite clear rules on RV Ls measurements have not yet been defined, several studies applying RV LS are available. RV LS was reported to be significantly impaired in patients with PH and inversely correlated with systolic PAP and RV dimensions [216,221,226,232,233]. RVGLS correlated strongly with RVEF assessed by CMR (Pearson's $r = 0.69$) [234-235]. RVFWLS $\geq -18\%$ detected hemodynamic signs of RVF (Right atrial pressure >15 mmHg, cardiac index <2 L/min per m^2) as well as 3DE derived RVEF $< 39\%$ (AUC 0.88 vs AUC 0.89) [211].

RV Ls values demonstrated a significant prognostic role in PH which was incremental to

clinical status, overcoming the other echocardiographic parameters [225,236,237]. RV LS has been reported to be a predictor of cardiovascular events [211,236], all-cause mortality and complications [237]. Moreover, Fine et al. [237] demonstrated that abnormal RV LS is predictive of reduced survival, stratifying patients prognosis.

RV function is heavily load dependent and myocardial deformation is influenced by loading conditions, too. Accordingly, it has been demonstrated that in patients with RV pressure overload, both with and without loss of myocardial contractility, RV LS was significantly lower than in normal subjects [238]. These data show that RV LS can be decreased in presence of both increased afterload and normal contractility, and in presence of increased afterload and myocardial damage with decreased contractility [238], underlying the fact that the diagnostic significance of RV LS values must always be related to RV loading conditions [239-240]. However, the main determinant of RV LS impairment seems to be myocardial contractility. Indeed PH patients with RV dysfunction showed lower RV LS values in comparison to PH patients with preserved RV function [238]. Not only the absolute value of RV LS is predictive of prognosis in PH patients, but also its variation during follow-up demonstrated a prognostic role. Patients with an improvement >5% of RV LS during follow-up demonstrated better survival respect to patients without [241].

Another 2D-STE RV LS parameter is RV intraventricular dyssynchrony index (RV IVDI), recently described [242-245]. It is calculated as the standard deviation of the time to peak-systolic strain for RVFW and IVS segments, adjusted to heart rate. Impairment of RV IVDI derives mainly from delayed contraction of RVFW [243]. It occurs frequently in PAH patients [246] and demonstrated to be an independent predictor of clinical worsening, with possibility of normalization during effective treatments accompanied by a large reduction of PVR [246]. Determinants of RV RVDI have to be defined. Badagliacca et al showed the presence of a correlation among RV IVDI and RV dilation and eccentric

hypertrophy pattern, suggesting a role of segmental wall stress heterogeneity as the major determinant of mechanical delay [247]. To date, larger studies are required to determine its clinical significance and its role in clinical routine.

Three-dimensional echocardiography

3DE is a recently introduced echocardiographic technique. It demonstrated to be feasible, accurate and reproducible in measuring RV volumes and ejection fraction in adults [248-256], as well as in children [257-258]. Nevertheless, the feasibility of obtaining a good quality full volume 3D data set acquisition which includes the RV anterior and apical lateral segments as well as the RV outflow tract, in patients with poor imaging windows and/or dilated RV, remains the main limitation of the technique. Accuracy tends to decrease with increasing RV size, limiting its application in patients with more dilated RV [259].

Recent studies showed a close correlation between 3DE and CMR in measuring RV volumes and ejection fraction [256,260-261] (Table 10).

Table 10. Differences between right ventricular volumes assessed by three-dimensional echocardiography and cardiac magnetic resonance

Author	Three-dimensional echocardiography		
	End-Diastolic Volume (ml)	End-systolic Volume (ml)	Ejection Fraction (%)
Grapsa et al	-4 (-11, 4)	0 (-6, 6)	-1 (-3, 0)
Sugeng et al [269]	-14 (-28, 0)	-9 (-19, 1)	-2 (-4, 0)
Van der Zwaan et al	-34 (-43, -25)	-11 (-19, 3)	-4 (-6, -2)
Leibundgut et al [260]	-10 (-15, -6)	-5 (-8, -1)	0 (-2, 1)
Shimada et al [261]	-14 (-18, -10)	-6 (-8, -3)	-1 (-2, 0)

Modified from: Badano et al. J Cardiovasc Ultras 2012; 20(1): 1-22 [256].

Although 3DE appeared to underestimate RV volumes in comparison to CMR [261], this underestimation showed to be systematic [253], confirming the good agreement between the two techniques and the accuracy of 3DE. As well as in healthy subjects, Li et al [262] demonstrated a close correlation among RVEF measured by 3DE and CMR in PH patients.

Normative data for 3DE RV volumes including age-, body size-, and sex-specific reference values based on large cohort studies of healthy volunteers has recently become available [253,263]. The current guidelines on echocardiographic chamber quantification for the first time included recommendations for 3DE RV analysis specifying upper limits of RV end-diastolic volume (87 ml/m² in men and 74 ml/m² in women) and RV end-systolic volume (44 ml/m² in men and 36 ml/m² in women) [114].

Applying 3DE, Maffesanti et al [253] was able to confirm the correlation between RV volumes and anthropometric variables (such as gender, age, and body size), previously demonstrated by CMR [264].

Using 3DE, it has been confirmed that in normal people the three compartments of the RV provides a different contribution in RV systolic contraction, both in timing as in strength [265-266]. Inflow and outflow tracts are the most active RV compartments contributing to its pump function, whereas the apex contributes less, following a chronological order in contraction, that reflects the peristaltic pump function of the RV [265]. In pts with PH, the relative contribution of the three compartments to RV pump function seems to remain unchanged, with the loss of the timing differences. The three compartments contract simultaneously losing the peristaltic function and making the RV behave as a single chamber. This change is coupled by changes of the RV shape, from a triangular to a cylindrical one [265]. In particular, a new methodology which allows to assess 3DE-derived global and regional RV shape indices based on analysis of the RV curvature has been

recently developed and tested in normal subjects and in patients with pulmonary arterial hypertension [267]. It allows to demonstrate that in patients with pressure overload the RVOT is more round, both body and apical portions of the septum are more convex bulging into the LV at both end-diastole and end-systole, with a more flattened apical free wall. The curvature of the RV inflow tract was a more robust predictor of death than RVEF, RV volumes, or other regional curvature indices [267].

3DE allows to calculate RVEF from end-diastolic and end-systolic volume measurements, providing an adequate assessment of true global RV pump function. Recent studies confirmed that 3DE measurement of the RVEF is accurate, reproducible and correlate well with CMR both in adults and children [255,257,268,269]. In the most recent meta-analysis aimed to explore the accuracy of different imaging modalities (2DE, 3DE, radionuclide ventriculography, CT, gated single-photon emission CT, and invasive cardiac cineventriculography) for RVEF, using CMR as reference method, 3DE has proven to be the most reliable technique, overestimating the RVEF only by 1.16% with the lowest limits of agreement (from -0.59 to 2.92%) [270]. The reference values of 3DE RVEF have been recently obtained on a large cohorts of healthy volunteers [253,263]. According to the current guidelines on echocardiographic chamber quantification, 3DE-derived RVEF should be considered a method of choice for quantifying RV systolic function, with the abnormality threshold <45% [114].

In PH, RVEF measured by CMR [142] demonstrated prognostic power. 3DE demonstrated to be superior in comparison to conventional echocardiography in identifying RV dysfunction in patients with PH [271]. Recently, Vitarelli et al [211] demonstrated that 3DE RVEF is accurate in predicting RVF, defined by haemodynamic parameters, and is an independent predictor of mortality at multivariate analysis.

Aim of the study

The aim of the study was the characterization of RV mechanics, in term of relative contribution of longitudinal and radial motion, in patients with PH. In order to better understand the RV mechanics in patients with PH, we first assessed the normal RV mechanics in healthy subjects and in its changes in a population at risk of PH, such as systemic sclerosis patients. Then, we investigated the RV anatomical and functional remodeling that occurs in the determination of the progressive RV dysfunction characterizing the clinical hystory of PH.

Material and Methods

Study population

Three populations have been enrolled: healthy subjects; patients affected by SSc, as a group at risk of PH; and patients affected by PH.

Healthy subjects were prospectively recruited from October 2011 to July 2013 among hospital employees, fellows in training, their relatives, and people screened for driving or working licenses. Criteria of recruitment included: age ≥ 18 years, no history or symptoms of cardiovascular or lung disease, normal physical examination, and ECG. Exclusion criteria were as follows: smoking, systolic blood pressure >140 mmHg, diastolic blood pressure >80 mmHg, history of drug-treated hypertension, diagnosis of diabetes mellitus, impaired fasting glucose >100 mg/dL, body mass index >30 kg/m², creatinine >1.3 mg/dL, estimated glomerular filtration rate < 60 mL/min per 1.73 m², history of dyslipidemia (total cholesterol >240 mg/dL, low-density lipoprotein cholesterol >130 mg/dL, and total triglycerides >150 mg/dL), poor apical acoustic window, unknown silent pathology detected by echocardiography (wall motion abnormalities; valvular stenoses of any degree; more than mild valvular regurgitation by multiparametric quantitative assessment), professional sport activity, pregnancy, frequent extrasystoles precluding echocardiographic protocol acquisitions. Among the healthy subjects a subgroup was selected in order to be age and gender-matched with the SSc and PH populations. Written informed consent was obtained from all volunteers, and the study was approved by the local Ethics Committee (protocol 2380P approved on 06/10/2011).

Patients with SSc have been randomly enrolled between October 2012 and May 2014. Diagnosis of SSc was in agreement with the ACR/EULAR classification criteria [272].

Exclusion criteria were the presence of known cardiovascular disease and the confirmed or suspected PH, measured by echocardiography according to the current PH guidelines [2]. Particularly, patients with maximum velocity of TR > 2.8 m/sec have been considered with possible or probable PH and then have been excluded. Written informed consent was obtained from all patients, and the study was approved by the local Ethics Committee.

Between October 2010 and January 2016, patients affected by PH have been enrolled. Inclusion criteria was the definite diagnosis of PH obtained at RHC. Exclusion criteria was PH secondary to left heart disease, group 2 of the current PH classification [2].

Echocardiographic acquisition

A complete standard M-mode, 2D, and Doppler examination was performed, and additional dedicated 2DE and 3DE acquisitions were obtained according to the study protocol. All echocardiographic studies were performed by experienced researchers using a Vivid E9 scanner (GE Vingmed, Horten, Norway) equipped with M5S and 4V probes. The 2DE acquisition protocol included dedicated apical 4-chamber RV-focused views. Image depth and sector size were adjusted to ensure an adequate temporal resolution (50–80 fps) for 2D-STE-derived strain quantitation. Three consecutive cardiac cycles were recorded. For 3DE analysis, 4- and 6-beat full-volume RV data sets were acquired during breath-hold from the apical approach, taking care to avoid any artifacts and include the entire structure in the acquisition.

Echocardiographic analysis

Systolic PAP was estimated based on the TR peak velocity and mean right atrial pressure (estimated from inferior vena cava size and respiratory excursion) [113]. PVR was calculated with the equation: $\text{TR Velocity}/\text{TVI-RVOT} \times 10 + 0.16$, demonstrated to provide a good noninvasive estimation of invasive PVR by Abbas et al [273].

Analysis of RV 3DE datasets allowed the evaluation of RV volumes and RVEF. Particularly, they have been assessed offline using 4D RV Function 2.0 software package (TomTec Imaging Systems, Unterschleissheim, Germany), applied on dedicated 3D data sets, and a software platform for data management (Research Arena. TomTec Imaging Systems). RV volumes were indexed for body surface area according to DuBois and DuBois formula [274]. The work flow of the RV analysis software is as follows: Step 1, view adjustment: within the 3DE data set 2 orthogonal cut planes of LV, showing apical 4-chamber and 2-chamber, are automatically selected and have to be correctly aligned; then 2 orthogonal cut planes of RV have to be adjusted. From these adjustments an orthogonal LV plane passing through the aortic valve will be obtained; landmarks have to be positioned at the hinge points of the aortic valve cusps. Then a transversal plane of the RV will be obtained, in which a transversal line has to be positioned joining the endocardial surface of the septum to the RV free-wall one (Figure 14). Step 2, tracking revision: on the basis of the initial view adjustment and the landmarks, the program automatically provides 4-chamber and three coronal views of the right ventricle at end-diastole. The contours are automatically identified. Before to start with the contours adjustment, the hinge point of tricuspid leaflets and pulmonary valve cusps can be checked and eventually replaced in order to ameliorate the definition of the inlet and outlet RV regions. Then, the observer can modify the contours using dedicated tools. The same process will be performed at the end-systolic

frame (Figure 15 A and B). End-diastolic and end-systolic frames are automatically selected by the software. Step 3, RV analysis: finally, the RV analysis display offers the dynamic model, a time-volume curve and values of RV volumes and function (Figure 16).

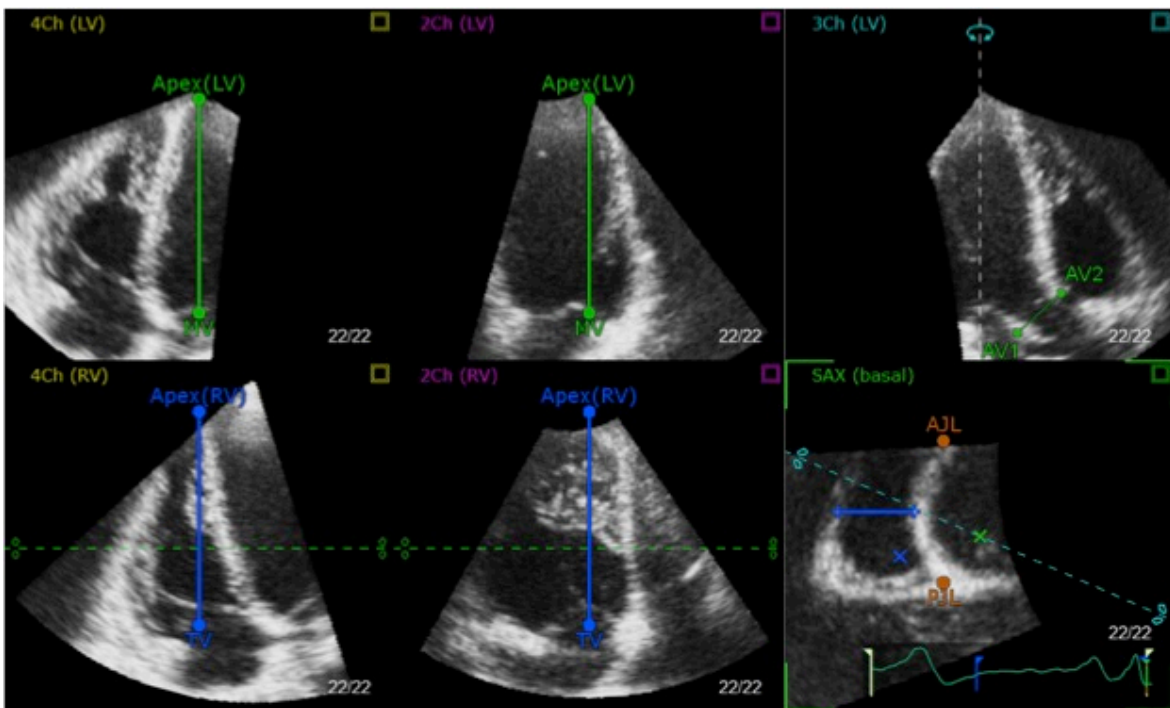


Figure 14. Step 1 of the work-flow of 3DE RV volumes measurement. View adjustment.

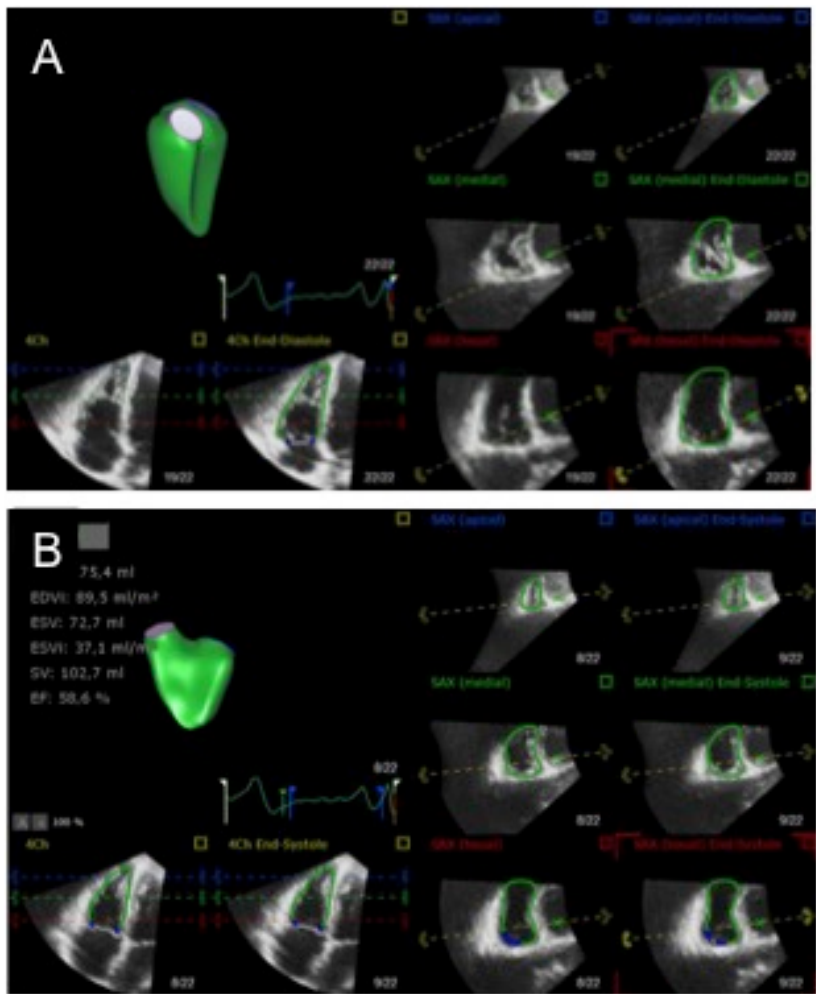


Figure 15. Step 2 of the work-flow of 3DE RV volumes measurement. Tracking revision of the end-diastolic (A) and end-systolic RV contours

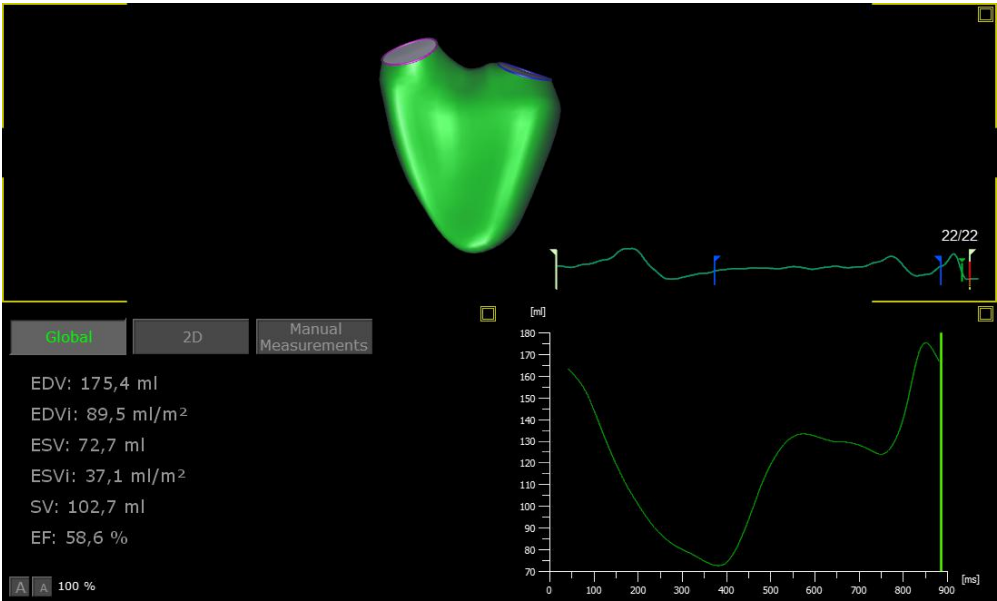


Figure 16. Step 3 of the work-flow of 3DE RV volumes measurement. RV analysis with final results.

From the 3D analysis we obtained the RV beutel, on which a custom-made software has been applied. It is able to investigate separately longitudinal and radial displacement, deny one of them. It permits to quantitate separately longitudinal and radial contribution to RVEF (Figure 17). From the ratio among radial or longitudinal EF and total RVEF, obtained from the 3D analysis, it was possible to estimate the relative contribution of longitudinal and radial displacement to the global RV pump function, respectively the Radial EF/RVEF (RadEF/RVFE) and Longitudinal EF/RVEF (LongEF/RVEF).

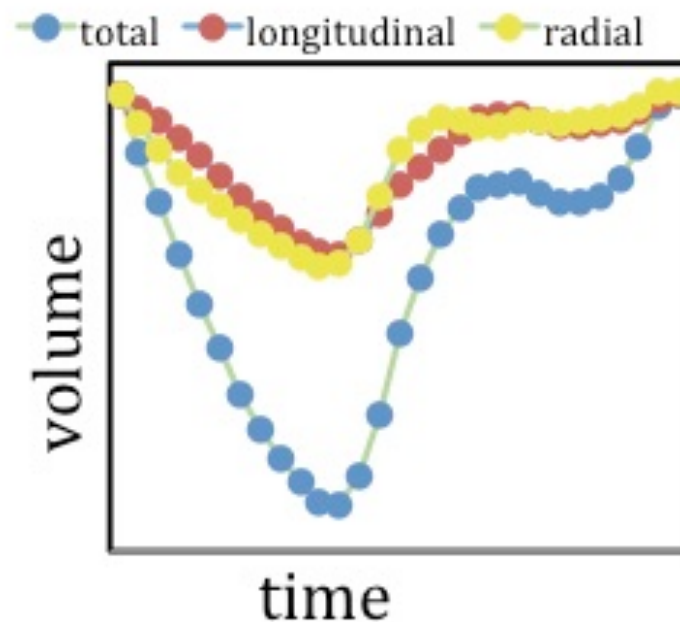


Figure 17. Time-volume curves of right ventricular total (blue dotted curve), longitudinal (red dotted curve) and radial (yellow dotted curve) deformation in a healthy subject, evaluated by a custom-made software, showing a similar contribution of longitudinal and radial to right ventricular global pump function. Courtesy of Dr A Kovacs, Semmelweis University Heart and Vascular Center, Budapest.

Conversely, RV 2D-STE analysis allowed the evaluation of RV myocardial deformation. This analysis was done using Q-analysis software package (EchoPAC BT 13; GE Vingmed). After manual tracing the end-systolic RV endocardial border, a region of interest (ROI) was

automatically generated; its width and position were manually adjusted to include the entire myocardial wall and to exclude the pericardium. Pulmonary valve closure was identified on the pulse-wave Doppler tracing of the RV outflow tract. The software automatically divides the RVFW and the IVS in 3 segments (basal, mid, and apical), resulting in a 6-segment model. The quality of the tracking was automatically validated by software and confirmed visually from the 2D images. Subjects in whom >2 segments per RV showed persistent inadequate tracking despite attempts to readjust the ROI position and width were excluded from analysis. The global RVLS was automatically calculated by the software and corresponded to the average of the 6 segments systolic peak strain values (Figure 18). The RVFWLS was calculated averaging the systolic peak strain values of the 3 free-wall segments, as described elsewhere [228]. A dedicated tool available in the Q-analysis software package EchoPAC BT 12 permits to obtain the TD of the RV myocardium. Particularly, 6 curves will be obtained: 3 positive curves (corresponding to the displacement of RV free wall (RVFW) segments) and 3 negative ones (corresponding to the displacement of the IVS segments) (Figure 19). The RVFW global TD was obtained as the arithmetic mean of the systolic peak values of the 3 lateral segments; IVS TD was obtained as the arithmetic mean of the systolic peak of the 3 IVS segments. Global TD was obtained averaging the absolute values of RV FW and IVS TD.

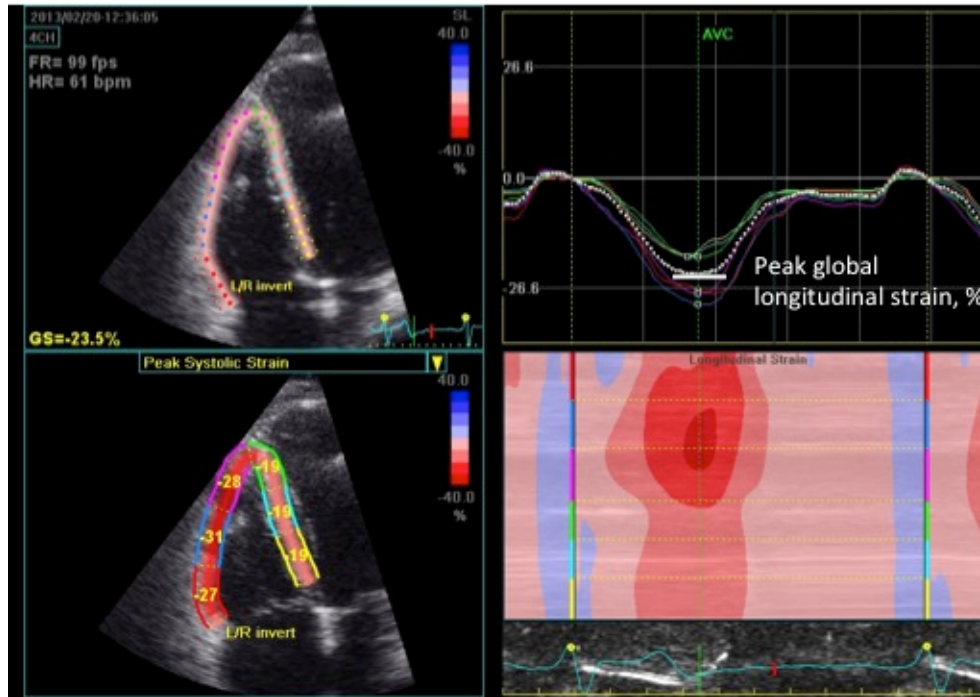


Figure 18. Longitudinal strain evaluation of the right ventricle by two-dimensional speckle tracking echocardiography.

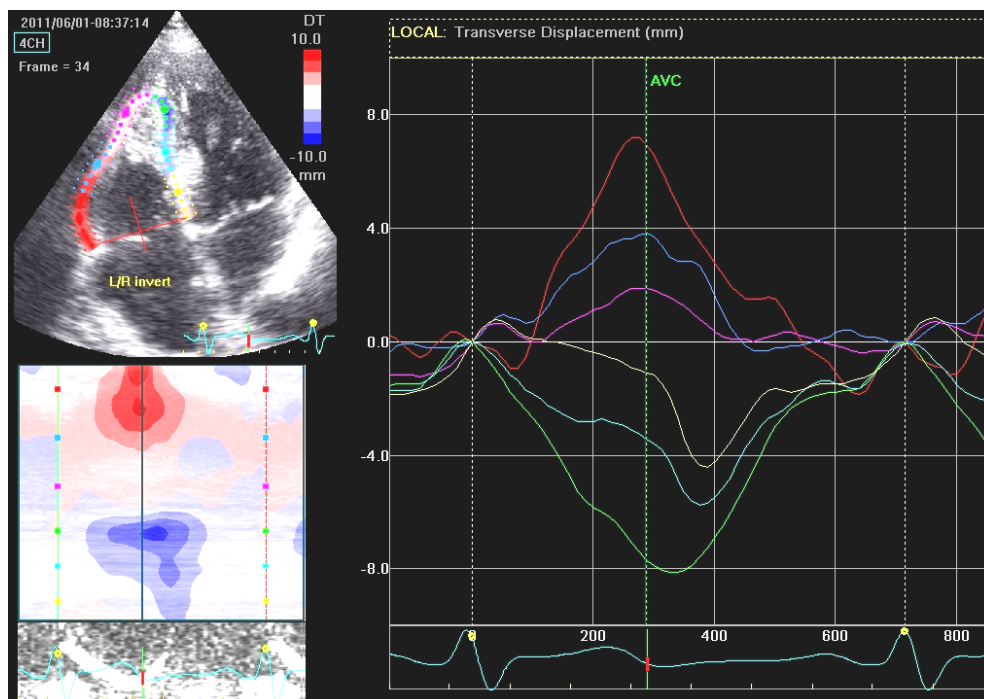


Figure 19. Transversal displacement evaluation of the right ventricle by two-dimensional speckle tracking echocardiography. Positive curves display RV Free Wall displacement, the negative ones display the interventricular septum displacement.

Statistical analysis

Normal distribution of variables was assessed by Kolmogorov–Smirnov test. Accordingly, continuous variables are summarized as mean±SD, if normally distributed, and as median (25th and 75th percentiles) otherwise. Categorical variables were reported as percentages. In all analyses, RVLS parameters and RV IVS TD were considered negative (lower values indicating better deformation). Lower/upper limits of normality were identified as the mean minus/plus 2 SD. In order to investigate differences among normal, patients at risk of PH and patients with PH, the selected healthy population, SSc and PH populations were compared. In order to investigate the modifications of RV mechanics in PH pathology, PH population has been divided in two groups: patients at risk of RV dysfunction and patients with definite RV dysfunction. The parameter chosen to define the absence or presence of RV dysfunction was the 3DE RVEF. Particularly, the RVEF 45% value has been used as cut-off value, according to the current chamber quantification guidelines [114]. Differences among mean±SD were tested with T-test and ANOVA test, in case of normal distribution. Otherwise, non parametric test (U-Mann Whitney) was performed.

Regression analysis was performed to investigate correlations among RVEF and longitudinal EF, radial EF, PVR and systolic PAP (Pearson and Spearman tests). All these variables, statistically significant at univariate analysis, were included in the multivariate analysis, performed by binary logistic regression analysis.

All analyses were performed using SPSS 13.0 (SPSS Inc, Chicago, IL). $P < 0.05$ were considered significant.

Results

Healthy subjects

A total of 270 subjects fulfilled the inclusion criteria. Anthropometric and echocardiographic characteristics are summarized in Table 11. The age ranged from 18 to 76 years and distribution per decade is quite homogeneous. Women were more prevalent than men (56%). Men showed larger body size and higher values of systolic and diastolic artery pressure. Moreover, men showed larger LV and right atrial size. Systolic PAP appeared higher in women, while PVR were similar in men and women. Men showed larger RV size, even after indexation for BSA, and lower RV pump function. TAPSE and S' appeared similar between men and women. 2D-STE LS demonstrated that RVGLS and RVFWLS were significantly different, with higher values for RVFWLS; moreover, their values differ among gender with values significantly higher in women. Lower limits of normality were -20% and -22% for RVGLS and RVFWLS respectively. RVFW TD showed positive values, while IVS TD showed negative values. Global TD showed positive values. No differences among gender has been shown. Lower limits of normality for RVFW and global TD were 1.4 and 2.1, respectively. Upper limit of normality for IVS TD was -1.9.

Table 11. Healthy subjects. Clinical and echocardiographic characteristics

	All (270)	Men (119)	Women (151)	p
<i>Anthropometric variables</i>				
Age, ys	44 ± 14	44 ± 14	44 ± 14	0.91
Height, cm	170 ± 9	177 ± 7	165 ± 7	<0.0001
Weight, Kg	67 ± 11	76 ± 9	61 ± 8	<0.0001
BSA, m ²	1.78 ± 0.2	1.9 ± 0.12	1.7 ± 0.1	<0.0001
Heart rate, bpm	67 ± 10	66 ± 10	67 ± 10	0.31
SAP, mmHg	122 ± 14	128 ± 13	117 ± 14	<0.0001
DAP, mmHg	74 ± 8	77 ± 8	71 ± 8	<0.0001
<i>Echocardiographic characteristics</i>				
LV EDV, ml/m ²	54 ± 10	59 ± 10	50 ± 8	<0.0001
LV EF, %	64 ± 4	63 ± 4	66 ± 4	<0.0001
2D RA MaxVol, ml/m ²	22 (18-27)	25 (21-30)	20 (16-24)	<0.0001
sPAP, mmHg	21 ± 6	20 ± 7	22 ± 6	0.02
PVR, WU	1.4 (1.1-1.6)	1.3 (1-1.6)	1.4 (1.2-1.6)	0.24
RV EDA, cm ² /m ²	10.3 ± 1.9	11 ± 1.8	9.8 ± 1.7	<0.0001
RV ESA, cm ² /m ²	5.2 ± 1.1	5.7 ± 1.2	4.8 ± 1	<0.0001
RV FAC, %	50 ± 6	48 ± 7	51 ± 6	0.003
3D RV EDV, ml/m ²	56 ± 12	61 ± 12	52 ± 10	<0.0001
3D RV ESV, ml/m ²	23 ± 6	26 ± 6	21 ± 5	<0.0001
3D RV EF, %	59 ± 6	58 ± 6	60 ± 6	0.007
TAPSE, mm	25 (23-27)	24 (23-27)	25 (24-27)	0.3
S', cm/sec	14 (13-16)	15 (14-16)	14 (13-16)	0.98
RVGLS, %	-26 ± 3 ^s	-25 ± 3	-27 ± 3	<0.0001
RVFWLS, %	-31 ± 4 ^s	-29 ± 4	-32 ± 4	<0.0001
RV FW TD, mm	4.4 ± 1.5	4.4 ± 1.1	4.4 ± 1.5	0.67
IVS TD, mm	-4.5 ± 1.3	-4.6 ± 1.2	-4.5 ± 1.1	0.31
Global RV TD, mm	4.5 ± 1.2	4.5 ± 1.2	4.5 ± 1.1	0.82

BSA=body surface area; DAP=diastolic artery pressure; EDA=end-diastolic area; EDV=end-diastolic volume; EF=ejection fraction; ESA=end-systolic area; ESV=end-systolic volume; FAC=fractional area change; IVS=interventricular septum; LV=left ventricular; PVR=pulmonary vascular resistance; RA=right atrial; RV=right ventricular; RVFWLS=RV free wall longitudinal strain; RVGLS=RV global longitudinal strain; SAP=systolic artery pressure; sPAP=systolic pulmonary artery pressure; TAPSE=tricuspid annulus plane systolic excursion; TD=transversal displacement; WU=Wood Unit.

We obtained normal values of longitudinal and radial RVEF, and their relative contribution to global RVEF only in the cohort of healthy subjects who were age and gender matched with SSc and PH ones (Table 12). Both longitudinal and radial components equally contributed to global RVEF. In addition, the extent of longitudinal and radial components to global RVEF were similar between men and women. Lower limits of normality for longitudinal and radial components of RVEF were 19% and 17%, respectively; while the ratios LongEF/RVEF and RadEF/RVEF were similar (35% for both). In healthy subjects both longitudinal and radial motion showed a moderate linear correlation with 3DE RVEF ($r=0.51$, $p<0.0001$; $r=0.61$, $p<0.0001$, respectively).

Table 12. Subgroup of healthy subjects. Echocardiographic longitudinal and radial parameters

	All (57)	Men (12)	Women (45)	P*
3D LongEF, %	27 ± 4 [°]	27 ± 4	27 ± 4	0.7
3D RadEF, %	27 ± 5 [°]	27 ± 4	27 ± 6	0.6
3D LongEF/RVEF	47 ± 6 ^ç	48 ± 5	47 ± 6	0.93
3D RadEF/RVEF	47 ± 6 ^ç	47 ± 7	47 ± 6	0.87

*=men vs women; [°]p=NS; ^çp=NS

LongEF=longitudinal ejection fraction; RadEF=radial ejection fraction ; RVEF= right ventricular ejection fraction

Systemic sclerosis patients

75 patients fulfilled the inclusion criteria for SSc. Mean age was 56 ± 13 years. Women were more prevalent than men (87%). Mean disease duration were 14 ± 9 years. The cutaneous form was diffuse in 41% and limited in 59% of patients. All of them showed positivity for antinucleus antibody with the following distribution: anti-centromere in 39%, scl-70 in 40% and aspecific in 21%.

Pulmonary hypertension patients

59 patients fulfilled the inclusion criteria for PH. Some of them underwent more than one echocardiogram during their clinical follow-up, at different timing. Then, we collected a total of 81 complete echocardiographic studies. The mean age was 59 ± 14 years. Women were prevalent (79%). Patients were affected from different form of PH, with the following distribution: 64% of type 1; 7% of type 3; 16% of type 4; 2% of type 5 and the remaining were undefined. According to protocol, no patients with type 2 (secondary to left heart disease) was included. LV 2DE end-diastolic volume was 85 ± 26 ml and LV 2DE EF was $66 \pm 6\%$. The majority of patients (82 % of them) showed a normal \dot{V} diastolic function or an abnormal relaxation pattern, while 15% showed a pseudonormal pattern and 3% a restrictive pattern.

At the time of the echocardiographic study, 48% patients were symptomatic (NYHA class \geq II); 15% of them showed right bundle branch block at electrocardiogram; 55% of them were in specific therapy for PH (4 patients with calcium channel blockers; 27 patients with endothelin inhibitors; 20 patients with phosphodiesterase inhibitors; 2 patients with prostanoid; 3 patients with riociguat), of whom 83% single therapy and 17% combined therapy.

Characterization of right ventricular function and mechanics in

Healthy Subjects - Systemic Sclerosis – Pulmonary Hypertension

Comparative data among healthy subjects, systemic sclerosis patients and PH patients are reported in Table 13.

The three groups were similar for age and gender. SSc patients showed to have a lower BSA and higher heart rate and systolic artery pressure values. Right atrial maximal volume was similar among normals and SSc patients, but consistently larger in PH patients. Systolic PAP and PVR were significantly higher in PH patients, but near normal in SSc patients. RV appeared to be larger in PH patients with no differences between healthy subjects and SSc patients. RV pump function was significantly impaired in PH patients, but in SSc patients was similar to that of healthy subjects. The analysis of RV mechanics demonstrated preserved values of longitudinal and radial function in SSc patients, both as absolute than relative values. Conversely, in PH patients longitudinal and radial function absolute values were reduced, while the relative contribution of longitudinal motion was preserved, whereas the radial contribution demonstrated to be impaired, near the lower limit of normality (Figure 20). TAPSE and S' wave were lower in SSc and mainly in PH, but without reaching pathological values. Myocardial deformation analysis by 2D-STE showed that both RVGLS and RVFWLS were preserved in SSc patients, and impaired in PH patients. TD analysis demonstrated normal values in SSc patients; while PH patients demonstrated a slight decrease of RVFW TD, a significant reduction of the leftward septal motion and a decreased global RV TD.

Table 13. Comparative analysis between healthy subjects, systemic sclerosis patients and pulmonary hypertension patients.

	Healthy (57)	SSc pts (75)	PH pts (81)	p
<i>Anthropometric variables</i>				
Age, ys	56 ± 10	56 ± 13	59 ± 14	0.15
Female, %	81	87	79	0.43
Height, cm	165 ± 8	164 ± 8	163 ± 9	0.30
Weight, Kg	66 ± 10	62 ± 10	66 ± 11	0.03
BSA, m ²	1.72 ± 0.15	1.67 ± 0.16	1.72 ± 0.17	0.05
Heart rate, bpm	66 ± 7	77 ± 11	73 ± 13	<0.0001
SAP, mmHg	126 ± 17	133 ± 22	124 ± 20	0.05
DAP, mmHg	74 ± 8	77 ± 8	73 ± 11	0.10
<i>Echocardiographic characteristics</i>				
2D RA MaxVol, ml/m ²	22 (18-26)	25 (21-33)	44 (32-57)	<0.0001
sPAP, mmHg	23 ± 5	27 ± 5	59 ± 22	<0.0001
PVR, WU	1.4 (1.3-1.6)	1.6 (1.5-1.9)	3 (2.3-4)	<0.0001
RV EDA, cm ² /m ²	10 ± 2*	11.6 ± 2.4*	18 ± 5.5*	<0.0001
RV FAC, %	52 ± 5*	47 ± 7*	31 ± 10*	<0.0001
3D RV EDV, ml/m ²	67 ± 14	64 ± 16	106 ± 39*	<0.0001
3D RV ESV, ml/m ²	28 ± 7	27 ± 10	65 ± 33*	<0.0001
3D RVEF, %	58 ± 4	58 ± 6	41 ± 11*	<0.0001
3D LongEF, %	27 ± 4	28 ± 6	18 ± 7* _‡	<0.0001
3D RadEF, %	27 ± 5	25 ± 6	15 ± 7* _‡	<0.0001
3D LongEF/RVEF	47 ± 6	49 ± 9	47 ± 9	0.10
3D RadEF/RVEF	47 ± 6	44 ± 8	36 ± 11*	<0.0001
TAPSE, mm	26 ± 2	22 ± 4	18 ± 5	<0.0001
S', cm/sec	15 ± 3	13 ± 2	11 ± 3	<0.0001
RVGLS, %	-25 ± 3	-24 ± 3	-17 ± 6*	<0.0001
RVFW LS, %	-31 ± 4	-29 ± 5	-20 ± 7*	<0.0001
RVFW TD, mm	5.3 ± 2	4.9 ± 2	4 ± 2.4*	0.011
IVS TD, mm	-4.8 ± 1.3	-4 ± 1.7*	-1.9 ± 3*	<0.0001
Global RV TD, mm	5 ± 1.4	4.5 ± 1.6	2.9 ± 2.3*	<0.0001

+p=significant. BSA=body surface area; DAP=diastolic artery pressure; EDA=end-diastolic area; EDV=end-diastolic volume; ESA=end-systolic area; ESV=end-systolic volume; FAC=fractional area change; IVS=interventricular septum; LongEF=longitudinal ejection fraction; LV=left ventricular; PVR=pulmonary vascular resistance; RA=right atrial; RadEF=radial ejection fraction; RV=right ventricular; RVFWLS=RV free wall longitudinal strain; RVGLS=RV global longitudinal strain; SAP=systolic artery pressure; sPAP=systolic pulmonary artery pressure; TAPSE=tricuspid annulus plane systolic excursion; TD=transversal displacement; WU=Wood Unit.

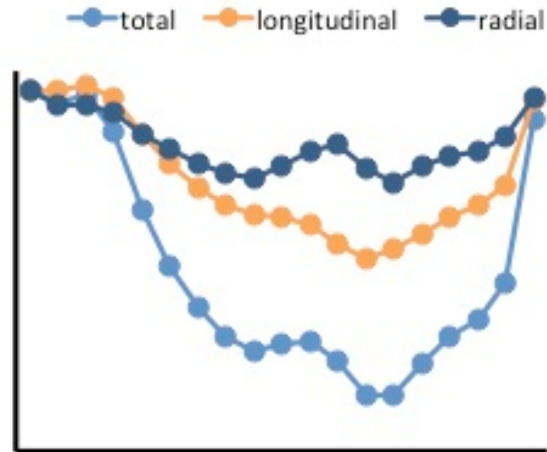


Figure 20. Time-volume curves of right ventricular total (light blue dotted curve), longitudinal (orange dotted curve) and radial (dark blue dotted curve) deformation in a pulmonary hypertension patient, evaluated by a custom-made software, showing a reduced radial component contribution to the global right ventricular pump function. Courtesy of Dr A Kovacs, Semmelweis University Heart and Vascular Center, Budapest.

Characterization of Right Ventricular function and mechanics in Healthy Subjects – Pulmonary Hypertension at risk of RV dysfunction – Pulmonary Hypertension with RV dysfunction

Comparative data among healthy subjects, PH patients at risk of and with RV dysfunction are reported in Table 14.

Patients with and without RV dysfunction were similar in age, gender distribution and anthropometric characteristics. PH patients with RV dysfunction showed a higher heart rate, compared with the other two groups, with similar arterial pressure values. Right atrial size was progressively larger in PH patients; and systolic PAP and PVR progressively higher in the two PH groups.

Patients with PH at risk of RV dysfunction demonstrated enlarged RV volumes with reduced RV pump function, although without reaching pathological values. Conversely PH

patients with RV dysfunction showed the largest RV volumes with a significantly impaired RV global pump function. The analysis of RV mechanics showed that in PH patients with preserved RVEF, both longitudinal and radial functions were reduced compared to healthy subjects, but still within the normal range, with normal values of longitudinal and radial relative contribution (Figure 21-A). Conversely, absolute values of longitudinal and radial components of RVEF were consistently reduced in presence of a reduced RVEF. Nevertheless, the relative contribution of the longitudinal component still remains preserved in PH population despite the reduced RV pump function, whereas the radial component was significantly reduced (Figure 21-B). TAPSE and S' were pathological only in the PH group with RV dysfunction. Deformation analysis showed that RVGLS and RVFWLS were slightly decreased in PH population with preserved RVEF but significantly reduced in presence of RV dysfunction. RVFW TD appeared preserved in the first population and slightly decrease in the latter. IVS TD demonstrated that the leftward septal motion progressively decrease with reducing RVEF. Then, the global TD is mildly reduced in presence of preserved RVEF and significantly impaired in presence of RV dysfunction.

Table 14. Comparative analysis between healthy subjects, patients with PH at risk of right ventricular dysfunction and patients with PH with right ventricular dysfunction.

	Healthy (57)	PH with RVEF \geq 45% (33)	PH with RVEF<45% (47)	p
<i>Anthropometric variables</i>				
Age, ys	56 \pm 10	60 \pm 13	59 \pm 15	0.23
Female, %	81	82	77	0.82
Height, cm	165 \pm 8	164 \pm 10	162 \pm 8	0.23
Weight, Kg	66 \pm 10	66 \pm 12	65 \pm 10	0.85
BSA, m ²	1.72 \pm 0.15	1.74 \pm 0.2	1.71 \pm 0.15	0.72
Heart rate, bpm	66 \pm 7	68 \pm 14	76 \pm 15	<0.0001
SAP, mmHg	126 \pm 17	129 \pm 20	125 \pm 17	0.12
DAP, mmHg	74 \pm 8	74 \pm 11	72 \pm 11	0.81
<i>Echocardiographic characteristics</i>				
2D RA MaxVol, ml/m ²	22 (18-26)	33 (27-43)	64 (42-82)	<0.0001
sPAP, mmHg	23 \pm 5	48 \pm 17	67 \pm 22	<0.0001
PVR, WU	1.4 (1.3-1.6)	2.7 (2.1-3)	3.9 (2.9-4.7)	<0.0001
RV EDA, cm ² /m ²	10 \pm 2*	14 \pm 3*	21 \pm 5*	<0.0001
RV FAC, %	52 \pm 5*	39 \pm 7*	25 \pm 7*	<0.0001
3D RV EDV, ml/m ²	67 \pm 14*	80 \pm 21*	126 \pm 38*	<0.0001
3D RV ESV, ml/m ²	28 \pm 7*	39 \pm 12*	83 \pm 31*	<0.0001
3D RVEF, %	58 \pm 4*	52 \pm 4*	34 \pm 7*	<0.0001
3D LongEF, %	27 \pm 4*	23 \pm 4*	15 \pm 5*	<0.0001
3D RadEF, %	27 \pm 5*	22 \pm 5*	10 \pm 4*	<0.0001
3D LongEF/EF	47 \pm 6	46 \pm 8	47 \pm 10	0.10
3D RadEF/EF	47 \pm 6	42 \pm 9	32 \pm 10*	<0.0001
TAPSE, mm	26 \pm 2	22 \pm 5	16 \pm 4	<0.0001
S', cm/sec	15 \pm 2	13 \pm 3	10 \pm 3	<0.0001
RV Global LS, %	-25 \pm 3*	-21 \pm 3*	-13 \pm 4*	<0.0001
RVFW LS, %	-31 \pm 4*	-26 \pm 4*	-17 \pm 6*	<0.0001
FW RV TD, mm	5.3 \pm 2	4.8 \pm 2	3.5 \pm 2*	0.011
IVS RV TD, mm	-4.8 \pm 1.3*	-2.9 \pm 2.5*	-1.1 \pm 3.2*	<0.0001
Global RV TD, mm	5 \pm 1.4*	3.8 \pm 1.9*	2.3 \pm 2.4*	<0.0001

*p=significant. BSA=body surface area; DAP=diastolic artery pressure; EDA=end-diastolic area; EDV=end-diastolic volume; EF=ejection fraction; ESA=end-systolic area; ESV=end-systolic volume; FAC=fractional area change; IVS=interventricular septum; LongEF=longitudinal ejection fraction; LV=left ventricular; PVR=pulmonary vascular resistance; RA=right atrial; Rad/EF=radial ejection fraction; RV=right ventricular; RVFWLS=RV free wall longitudinal strain; RVGLS=RV global longitudinal strain; SAP=systolic artery pressure; sPAP=systolic pulmonary artery pressure; TAPSE=tricuspid annulus plane systolic excursion; TD=transversal displacement; WU=Wood Unit.

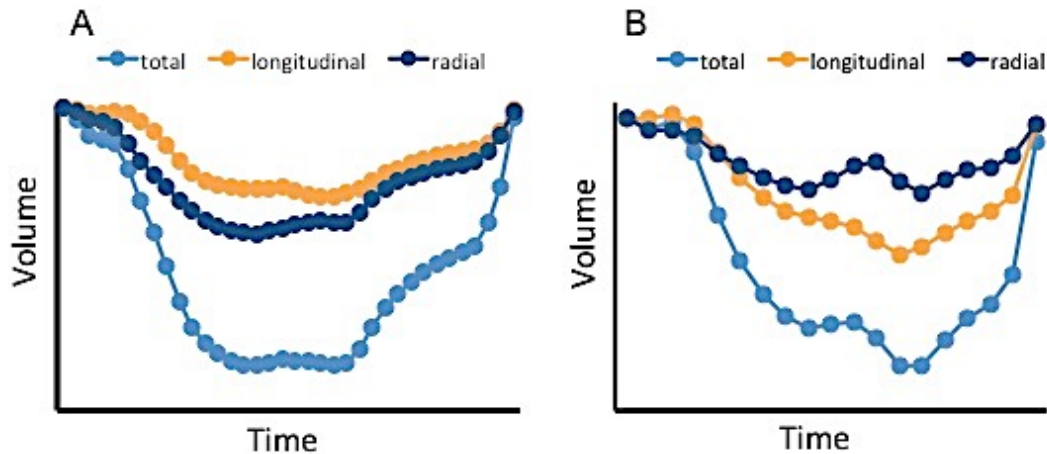


Figure 21. A - Pulmonary Hypertension patient with preserved right ventricular ejection fraction, showing preserved and similar values of longitudinal (orange dotted curve) and radial (dark blue dotted curve) contribution to global systolic function (light blue dotted curve). B - Pulmonary Hypertension patient with impaired right ventricular ejection fraction, showing preserved longitudinal (orange dotted curve) contribution and reduced radial (dark blue dotted curve) contribution to global systolic function (light blue dotted curve). Courtesy of Dr A Kovacs, Semmelweis University Heart and Vascular Center, Budapest.

Different patterns of interventricular septum transversal displacement in Pulmonary Hypertension patients

Data reported above showed a pathological involvement of the IVS TD even in presence of preserved RV global pump function, suggesting its early involvement within the pathological changes of RV motion due to a pressure overload. By the evaluation of the IVS TD of each PH patient, we demonstrated the presence of four different patterns, with different distribution according to the presence or absence of reduced RVEF. Particularly, the four patterns are: type 0, normal motion with a single negative curve at TD analysis (Figure 22-A); type 1, characterized by a preliminary negative curve followed by a positive deflection (Figure 22-B); type 2, characterized by a positive deflection followed by a negative one (Figure 22-C); type 3, characterized by a single positive curve (Figure 22-D).

PH patients with normal RV pump function showed type 0 in 64% of cases, type 1 in 11% and type 2 in the remaining cases. Otherwise, PH population with reduced RVEF showed type 0 in 37% of cases, no type 1, type 2 in 56% of patients and type 3 in 7% of cases ($p=0.005$). Indeed, type 0 and 1 showed normal 3DE RVEF (44 ± 9 and $53\pm 4\%$, respectively), while type 2 and type 3 showed lower 3DE RVEF (38 ± 10 and 34 ± 9 , respectively) with $p=NS$ among type 0 and 1 and among type 2 and 3 but with $p=0.009$ among type 1 and 2. Instead of it, no significant differences among systolic PAP values among the different IVS TD patterns have been found. Particularly, type 0 showed systolic PAP 58 ± 20 mmHg, while it was 78 ± 34 , 74 ± 22 and 84 ± 5 in the remaining three groups with statistical significance only among type 0-type 2 ($p=0.005$) and type 0-type 3 ($p=0.04$).

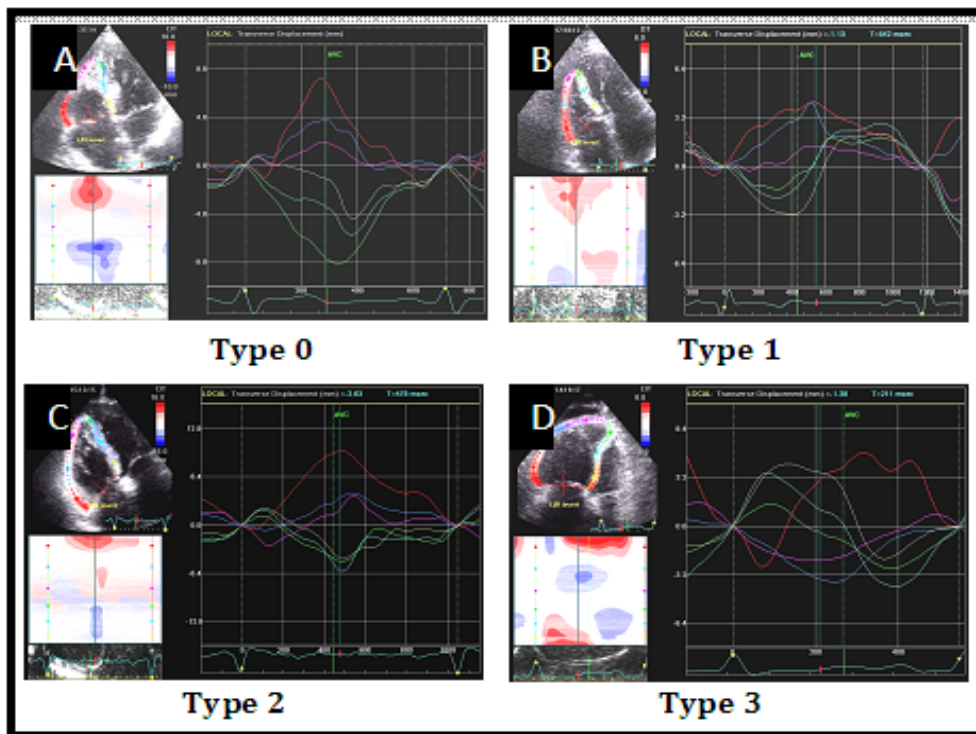


Figure 22. Different patterns of interventricular septum transversal displacement in pulmonary hypertension patients. A: Type 0, normal motion with a single negative curve. B: Type 1, a negative deflection followed by a positive one. C: Type 2, a positive deflection followed by a negative one. D: type 3, a single positive deflection.

Determinants of right ventricular global pump function in Pulmonary Hypertension patients

Univariate analysis showed strong linear correlations among 3D RVEF and longitudinal function, radial function, PVR and systolic PAP. Particularly, it showed that the reduction of RVEF is correlated with a reduction of longitudinal and radial function (Figure 23 A-B), and with higher PVR and systolic PAP values (Figure 23 C-D).

The multivariate analysis demonstrated that only longitudinal and radial motion are independent predictors of reduced 3DE RV EF, but not PVR and systolic PAP (Table 15).

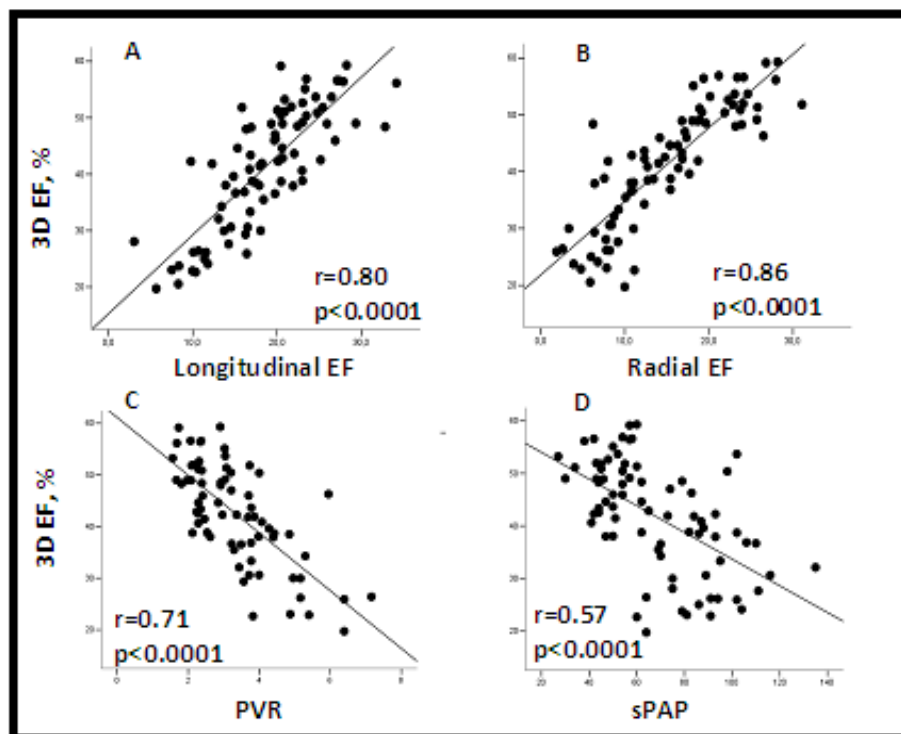


Figure 23. Linear correlations among 3DE right ventricular ejection fraction (EF) and longitudinal EF (A), radial EF (B), pulmonary vascular resistance (PVR) (C) and systolic pulmonary artery pressure (sPAP) (D).

Table 15. Multivariate analysis. Independent predictors of impaired right ventricular pump function

	OR	IC	p
LongEF	2.2	1.2 - 3.9	0.009
RadEF	2.5	1.3 - 4.6	0.005
PVR	--	--	NS
sPAP	--	--	NS

LongEF=longitudinal ejection fraction; PVR=pulmonary vascular resistance; RadEF=radial ejection fraction; sPAP=systolic pulmonary artery pressure

Discussion

This is the first echocardiographic study investigating the RV mechanical components, such as longitudinal and radial displacement, in healthy subjects and their changes occurring in presence of various degrees of PH, a pathological condition characterized by pressure overload. The results of our study can be summarized as follows: i) in healthy subjects the radial and longitudinal components of RV mechanics appear to participate equally to the global RV pump function; ii) in healthy subjects the IVS shows a leftward septal motion; iii) SSc patients without PH, classified as a population at high risk of PH, show normal RV size and function with unchanged longitudinal and radial contribution and unchanged deformation parameters compared to healthy subjects; iv) in PH patients with preserved RV pump function the relative contribution of longitudinal and radial displacement is unchanged compared to healthy subjects. Conversely, in PH patients with reduced RVEF there is a prevalent reduction of the relative contribution of radial displacement, although a progressive decrease of both longitudinal and radial motion occurs; v) in PH patients, the IVS changes progressively its motion pattern, showing a correlation with a progressive RVEF impairment but not with the RV loading conditions, defined by systolic PAP values.

RV mechanics in healthy subjects

Anatomical evidences demonstrated that the RV is characterized by a two-layered structure with the subepicardial myofibres arranged more or less circumferentially in a direction that is parallel to the atrioventricular groove and encircle the subpulmonary infundibulum, and the deep myofibres aligned longitudinally, apex to base. [192]. Differently, the LV has a three-layered structure with the epicardial cells oriented

obliquely, the mid-myocardial cells more circumferentially, and the endocardial cells again obliquely, with a well-developed midwall circumferential layer responsible for the predominance of circumferential shortening and radial thickening of the LV [275-276]. The RV myocardial structure explains why RVEF seems to be determined mainly by longitudinal shortening [193]. Nevertheless, this statement does not have clear demonstrations. To the best of our knowledge, there is only one echocardiographic study in which RV longitudinal and circumferential shortening have been investigated [194] which showed that compared with the left ventricle, in the RV the longitudinal shortening is dominant over short-axis function [194]. Nevertheless, no study investigating the relative contribution of the two components are available.

The single observation of the presence of a well-developed longitudinal layer does not exclude automatically the possible consistent contribution of other motion components in the genesis of RV global pump function. Haber et al reported that RV contributes by itself mainly to its long-axis deformation, whereas the tangential component of its displacement was larger due to LV coupling [195]. Our study is the first investigating the relative contribution of the two components, over their absolute values, highlighting for the first time that both longitudinal and radial motion contribute equally to the RV global pump function.

Deformation analysis allowed us to demonstrate that in normal conditions the interventricular septum shows a leftward systolic motion. Indeed, the evaluation of the RV radial motion by 2D-STE showed that the IVS moves away from the RV cavity during systole, describing a negative curve. This finding is in agreement with previous observations showing that, under normal conditions, the IVS has a right convexity, and this configuration is maintained during the cardiac cycle [277].

RV mechanics in Systemic Sclerosis patients without Pulmonary Hypertension

Our results demonstrated that the RV of SSc patients, in absence of PH, maintains normal size and pump function. Moreover, they showed normal RV mechanics, both in term of relative contribution of longitudinal and radial displacement as in term of RV myocardial deformation.

Previous observations demonstrated that the RV impairment in SSc patients is mainly related to the appearance of PH [278]. Nevertheless, primary RV myocardial involvement has been described [279-281] and thought to be the consequence of a general vasospastic mechanism [282]. The suspicion of an intrinsic RV myocardial involvement derives from the observation that patients with SSc related-PH have a worse prognosis respect to patients with idiopathic PH [2]. Few and discordant data about the RV function in SSc patients have been reported in studies which used 2D-STE to assess RV myocardial function. In a previous study reported by Matias et al [283], the RV basal free wall strain of SSc patients without PH was not different from controls. Conversely, Schattke et al. [284] reported that the RV basal and mid-free wall strain values of SSc patients without PH was lower than controls. Recently, Durmus et al [285] reported that patients with SSc in absence of PH showed lower values of RV LS respect to a healthy control group. The only data about RV size and function using 3DE come from a previous paper from our research group [286]. It showed that PH free-SSc patients have slightly larger RV with lower RV pump function (despite still within normal values) in presence of a normal myocardial deformation by 2D-STE. The differences between the results of the previous study and the actual one may be due to the different sample size (larger in the latter analysis) and the

application of a new and more powerful version of the software for the 3DE RV analysis [287].

RV mechanics in Pulmonary Hypertension patients

The main findings of our study are the changes of the RV mechanics in presence of PH. Our results suggested that despite the fact that RV pump function impairment in PH patients is correlated to a progressive reduction of both longitudinal and radial displacement, the radial component was more affected than the longitudinal one. Our conclusion are in contrast with the data by Mauritz et al [210]. They studied the longitudinal and radial function of PAH patients by cardiac CMR and stated that the progressive RV failure in PAH is associated with a parallel decline in longitudinal and transverse shortening until a floor effect is reached for longitudinal shortening, with a further reduction of RV function is due to progressive leftward IVS displacement. However, the two studies are not comparable and many aspects have to be taken into account. Particularly, they compared CMR studies obtained at baseline and at 1 year, while we consider single echocardiographic exams without a follow-up control. They divided patients according to a clinical parameter, survival rate, while we classified patients according to an instrumental parameter, the 3DE RVEF. Finally, they studied the longitudinal and transversal motion, but not their relative contribution to the global RV function.

In agreement with the findings of Mauritz et al, Simon et al [238] demonstrated a reduction of RVFW longitudinal shortening in compensated PH patients, that worsens in decompensated ones, stating that RV FWLS reduction may be an earlier step in the development of RVF. Accordingly, our compensated PH patients showed lower values of RVGLS and RVFWLS compared to normal subjects, but without reaching abnormal values. It has to be underlined that strain analysis have been done with different methods, not

comparable to each other, and that the study from Simon et al merely evaluated the longitudinal shortening. Indeed, deformation analysis by 2D-STE obtained in our PH population showed that the first parameter consistently impaired in presence of preserved RVEF is the IVS TD but not the longitudinal RV motion. Our conclusion is that maybe the first modification in presence of PH condition is the change of the IVS deformation.

Moreover, our results demonstrated that the IVS progressively changes its transversal motion showing several patterns, differently distributed according to the presence or absence of RV pump dysfunction, without significant correlations with systolic PAP values. It is well known that abnormal IVS curvature has been associated to the presence of PH [113, 276]. However, the novel finding regards the dynamic behaviour of the IVS, and not its static appearance. Mori S et al [288], applying M-mode echocardiography, demonstrated that patients with PH show two different peculiar transversal motion patterns of the IVS, with different clinical and haemodynamic significance. They distinguished an “early systolic anterior motion” (Type A) and an “early diastolic posterior motion” (Type B) with the first showing a low cardiac index despite similar systolic PAP. These data are in agreement with our findings. Type A septal motion from Mori et al can be assimilated to our type 2 and type 3 septal motion patterns, which were not associated to increased systolic PAP values but to significantly lower 3DE RVEF values. Conversely, type B can be assimilated to our Type 1 pattern. Similarly Sato et al [289] developed a “paradoxical IVS motion index”, evaluating the IVS motion by 2D-STE in short-axis views. They demonstrated that higher values of this index correlated with the amount of the late gadolinium enhancement at ventricular insertion points. The concept coming from their results is that, greater is the paradoxical septal motion, with a progressively more pronounced early systolic motion toward the RV cavity, and more pronounced is the amount of the late gadolinium enhancement at CMR. Late gadolinium enhancement

junctional pattern has been reported to be related to worse outcome in terms of death, need of lung transplantation, initiation of prostacyclin therapy, and decompensated RVF, stratifying prognosis [290]. All these results are in agreement and suggest that more pronounced is the rightward IVS TD in PH patients and worse is the clinical presentation of the patients. Larger studies are needed to confirm this observation and to demonstrate its clinical relevance.

Limitations

Some limitations of our study have to be taken into account. This is a single center study with a limited sample size of PH patients. No data about follow-up of the patients are available; then the prognostic predictivity of the echocardiographic parameters, in term of clinical outcome, has not been evaluated.

Conclusions

In healthy subjects, RV pump function seems to be determined by an equally contribution of longitudinal and radial deformation. In presence of SSc, without PH, the RV appeared to be preserved, both in term of global function and of relative longitudinal and radial displacement. In presence of PH, a pathological condition characterized by pressure overload, both these two components appeared to be reduced. However, the progressive lowering of global RV pump function appeared to be mainly driven by the impairment of the radial function, with the IVS firstly involved.

References

1. Hoeper MM, Bogaard HJ, Condliffe R et al. Definitions and diagnosis of pulmonary hypertension. *J Am Coll Cardiol* 2013;62(25 Suppl):D42–D50.
2. Galiè N, Humbert M, Vachiery JL et al. 2015 ESC/ERS Guidelines for the diagnosis and treatment of pulmonary hypertension: The Joint Task Force for the Diagnosis and Treatment of Pulmonary Hypertension of the European Society of Cardiology (ESC) and the European Respiratory Society (ERS): Endorsed by: Association for European Paediatric and Congenital Cardiology (AEPC), International Society for Heart and Lung Transplantation (ISHLT). *Eur Heart J* 2016;37(1):67-119.
3. Simonneau G, Galie` N, Rubin LJ et al. Clinical classification of pulmonary hypertension. *J Am Coll Cardiol* 2004;43(Suppl 1):S5–S12.
4. Hatano S, Strasser T. World Health Organization 1975. Primary pulmonary hypertension. Geneva: WHO; 1975.
5. Humbert M, Maitre S, Capron F, Rain B, Musset D, Simonneau G. Pulmonary edema complicating continuous intravenous prostacyclin in pulmonary capillary hemangiomatosis. *Am J Crit Care Med* 1998;157:1681–5.
6. Resten A, Maitre S, Musset D, et al. Pulmonary arterial hypertension; thin-section CT predictors of epoprostenol failure. *Radiology* 2002; 222:782–8.
7. Dorfmu¨ller P, Humbert M, Sanchez O, et al. Significant occlusive lesions of pulmonary veins are in common with pulmonary hypertension (PH) associated to connective tissue (CTD) (abstr). *Am J Crit Care Med* 2003;167:A694.
8. Ruchelli ED, Nojadera G, Rutstein RM, Rudy B. Pulmonary veno-occlusive disease: another vascular disorder associated with human immunodeficiency virus infection? *Arch*

Pathol Lab Med 1994;118: 664 –6.

9. Escamilla R, Hermant C, Berjaud KL, Mazerolles C, Daussy X. Pulmonary veno-occlusive disease in a HIV-infected intravenous drug abuser. *Eur Respir J* 1995;8:1982–4.

10. Woordes CG, Kuipers JRG, Elema J. Familial pulmonary venoocclusive disease: a case report. *Thorax* 1977;32:763–6.

11. Langleben D, Heneghan JM, Batten AP, et al. Familial pulmonary capillary hemangiomatosis resulting in primary pulmonary hypertension. *Ann Intern Med* 1988;109 (2):106 –9.

12. Galiè N, Hoeper MM, Humbert M et al; ESC Committee for Practice Guidelines (CPG). Guidelines for the diagnosis and treatment of pulmonary hypertension: the Task Force for the Diagnosis and Treatment of Pulmonary Hypertension of the European Society of Cardiology (ESC) and the European Respiratory Society (ERS), endorsed by the International Society of Heart and Lung Transplantation (ISHLT). *Eur Heart J* 2009;30(20):2493-2537.

13. Machado RD, Aldred MA, James V et al. Mutations of the TGF-beta type II receptor BMPR2 in pulmonary arterial hypertension. *Hum Mutat* 2006;27:121–132.

14. Machado R, Eickelberg O, Elliott CG et al. Genetics and genomics of pulmonary arterial hypertension. *J Am Coll Cardiol* 2009;54:S32–S42.

15. Galie` N, Manes A, Palazzini M et al. Management of pulmonary arterial hypertension associated with congenital systemic-to-pulmonary shunts and Eisenmenger's syndrome. *Drugs* 2008;68:1049–1066

16. Lapa MS, Ferreira EV, Jardim C, Martins BC, Arakaki JS, Souza R. Clinical characteristics of pulmonary hypertension patients in two reference centers in the city of Sao Paulo. *Rev Assoc Med Bras* 2006;52:139–143

17. Dhillon R. The management of neonatal pulmonary hypertension. *Arch Dis Child Fetal Neonatal Ed* 2012;97:F223–F228.
18. Porta NF, Steinhorn RH. Pulmonary vasodilator therapy in the NICU: inhaled nitric oxide, sildenafil, and other pulmonary vasodilating agents. *Clin Perinatol* 2012; 39:149 – 164.
19. Ivy DD, Abman SH, Barst RJ et al. Pediatric pulmonary hypertension. *J Am Coll Cardiol* 2013;62:D117–D126.
20. Hoeper MM, Humbert M, Souza R et al. A global view of pulmonary hypertension. *Lancet* 2016; 4: 306-322.
21. Peacock AJ, Murphy NF, McMurray JJ, Caballero L, Stewart S. An epidemiological study of pulmonary arterial hypertension. *Eur Respir J* 2007;30:104-109
22. Humbert M, Sitbon O, Chaouat A et al. Pulmonary arterial hypertension in France: results from a national registry. *Am J Respir Crit Care Med* 2006;173:1023–1030
23. Spagnolo P, Cordier JF, Cottin V. Connective tissue diseases, multimorbidity and the ageing lung. *Eur Resp J* 2016; 47(5):1535-58.
24. McLaughlin VV, Archer SL, Badesch DB et al; American College of Cardiology Foundation Task Force on Expert Consensus Documents; American Heart Association; American College of Chest Physicians; American Thoracic Society, Inc; Pulmonary Hypertension Association. ACCF/AHA 2009 expert consensus document on pulmonary hypertension a report of the American College of Cardiology Foundation Task Force on Expert Consensus Documents and the American Heart Association developed in collaboration with the American College of Chest Physicians; American Thoracic Society, Inc.; and the Pulmonary Hypertension Association. *J Am Coll Cardiol*. 2009;53(17):1573-1619.

25. Rich S, Dantzker DR, Ayres SM et al. Primary pulmonary hypertension. A national prospective study. *Ann Intern Med.* 1987;107:216-223
26. Simonneau G, Robbins IM, Beghetti M et al. Updated clinical classification of pulmonary hypertension. *JACC* 2009;54(Suppl):S43-54
27. Vachiéry JL, Adir Y, Barberà JA et al. Pulmonary hypertension due to left heart diseases. *JACC* 2013;62(25 Suppl):D100-108.
28. Fang JC, DeMarco T, Givertz MM et al. World Health Organization Pulmonary Hypertension group 2: pulmonary hypertension due to left heart disease in the adult--a summary statement from the Pulmonary Hypertension Council of the International Society for Heart and Lung Transplantation. *J Heart Lung Transplant* 2012;31:913-933.
29. Ghio S, Gavazzi A, Campana C et al. Independent and additive prognostic value of right ventricular systolic function and pulmonary artery pressure in patients with chronic heart failure. *JACC* 2001;37(1):183-188
30. Thenappan T, Shah SJ, Gomberg-Maitland M et al. Clinical characteristics of pulmonary hypertension in patients with heart failure and preserved ejection fraction. *Circ Heart Fail* 2011;4(3):257-265.
31. Seeger W, Adir Y, Barberà JA et al. Pulmonary hypertension in chronic lung diseases. *J Am Coll Cardiol* 2013;62(Suppl 25):D109 – D116
32. Hurdman J, Condliffe R, Elliot CA et al. Pulmonary hypertension in COPD: results from the ASPIRE registry. *Eur Respir J* 2013;41(6):1292–1301
33. Cottin V, Nunes H, Brillet PY et al; Groupe d'Etude et de Recherche sur les Maladies Orphelines Pulmonaires (GERM O P). Combined pulmonary fibrosis and emphysema: a distinct underrecognised entity. *Eur Respir J* 2005;26(4):586 –593

34. Thabut G, Dauriat G, Stern JB et al. Pulmonary hemodynamics in advanced COPD candidates for lung volume reduction surgery or lung transplantation. *Chest* 2005;127(5):1531-1536.
35. Chaouat A, Bugnet AS, Kadaoui N et al. Severe pulmonary hypertension and chronic obstructive pulmonary disease. *Am J Respir Crit Care Med* 2005;172(2):189-194.
36. Oswald-Mammosser M, Weitzenblum E, Quoix E et al. Prognostic factors in COPD patients receiving long-term oxygen therapy. Importance of pulmonary artery pressure. *Chest* 1995;107:1193-98.
37. Lettieri CJ, Nathan SD, Barnett SD, Ahmad S, Shorr AF. Prevalence and outcomes of pulmonary arterial hypertension in advanced idiopathic pulmonary fibrosis. *Chest* 2006;129(3):746-752.
38. Escribano-Subias P, Blanco I, López-Meseguer M et al; REHAP investigators. Survival in pulmonary hypertension in Spain: insights from the Spanish registry. *Eur Respir J* 2012;40(3):596-603
39. Pengo V, Lensing AW, Prins MH et al; Thromboembolic Pulmonary Hypertension Study Group. Incidence of chronic thromboembolic pulmonary hypertension after pulmonary embolism. *N Engl J Med*. 2004;350(22):2257-2264
40. Pepke-Zaba J, Delcroix M, Lang I et al. Chronic thromboembolic pulmonary hypertension (CTEPH): results from an international prospective registry. *Circulation* 2011;124(18):1973-1981
41. Pietra GG, Capron F, Stewart S et al. Pathologic assessment of vasculopathies in pulmonary hypertension. *J Am Coll Cardiol* 2004;43(12 Suppl S):25S-32S.
42. Tuder RM, Abman SH, Braun T et al. Pulmonary circulation: development and pathology.

J Am Coll Cardiol 2009;54(1 Suppl):S3-S9.

43. Tuder RM, Archer SL, Dorfmueller P et al. Relevant issues in the pathology and pathobiology of pulmonary hypertension. JACC 2013;62(25 Suppl):D4-12.

44. Heath D, Edwards JE. The pathology of hypertensive pulmonary vascular disease; a description of six grades of structural changes in the pulmonary arteries with special reference to congenital cardiac septal defects. Circulation 1958;18(4 Part 1):533-547.

45. Heath D, Helmholz HF Jr, Burchell HB, Dushane JW, Edwards JE. Graded pulmonary vascular changes and hemodynamic findings in cases of atrial and ventricular septal defect and patent ductus arteriosus. Circulation 1958;18(6):1155-1166.

46. Smith, P, Heath D. Electron microscopy of the plexiform lesion. Thorax 1979;34(2):177-186.

47. de Jesus Perez VA. Molecular pathogenesis and current pathology of pulmonary hypertension. Heart Fail Rev 2016; 21(3): 239-57.

48. Stacher E, Graham BB, Hunt JM et al. Modern age pathology of pulmonary arterial hypertension. Am J Respir Crit Care Med 2012;186(3):261-272.

49. Fedullo PF, Auger WR, Kerr KM, Rubin LJ. Chronic thromboembolic pulmonary hypertension. N Engl J Med 2001;345(20):1465-1472.

50. Galie N, Kim NHS. Pulmonary microvascular disease in chronic thromboembolic pulmonary hypertension. Proc Am Thorac Soc 2006;3(7):571-576.

51. Humbert M, Morrell NW, Archer SL et al. Cellular and molecular pathobiology of pulmonary arterial hypertension. Am Coll Cardiol 2004;43(12 Suppl S):13S-24S.

52. Hassoun PM, Mouthon L, Barberà JA et al. Inflammation, growth factors, and pulmonary

vascular remodeling. *J Am Coll Cardiol* 2009;54(1 Suppl):S10–S19.

53. Morrell NW, Adnot S, Archer SL et al. Cellular and molecular basis of pulmonary arterial hypertension. *J Am Coll Cardiol* 2009;54(1 Suppl):S20–S31

54. Tuder RM, Voelkel NF. Pulmonary hypertension and inflammation. *J Lab Clin Med* 1998;132:16–24

55. Dib H, Tamby MC, Bussone G et al. Targets of anti-endothelial cell antibodies in pulmonary hypertension and scleroderma. *Eur Respir J* 2012;39(6):1405–1414.

56. Nicolls MR, Taraseviciene-Stewart L, Rai PR, Badesch DB, Voelkel NF. Autoimmunity and pulmonary hypertension: a perspective. *Eur Respir J* 2005;26(6):1110–1118

57. Delgado JF, Conde E, Sánchez V et al. Pulmonary vascular remodeling in pulmonary hypertension due to chronic heart failure. *Eur J Heart Fail* 2005;7(6):1011–1016.

58. Lang IM. Chronic thromboembolic pulmonary hypertension—not so rare after all. *N Engl J Med* 2004;350(22):2236–2238

59. Deng Z, Morse JH, Slager SL et al. Familial primary pulmonary hypertension (gene PPH1) is caused by mutations in the bone morphogenetic protein receptor-II gene. *Am J Hum Genet* 2000;67(3):737–744.

60. Machado RD, Pauciulo MW, Thomson JR et al. BMPR2 haploinsufficiency as the inherited molecular mechanism for primary pulmonary hypertension. *Am J Hum Genet* 2001;68(1):92–102.

61. Thomson JR1, Machado RD, Pauciulo MW et al. Sporadic primary pulmonary hypertension is associated with germline mutations of the gene encoding BMPR-II, a receptor member of the TGF-beta family. *J Med Genet* 2000;37(10):741–745.

62. Soubrier F, Chung WK, Machado R et al. Genetics and genomics of pulmonary arterial hypertension. *JACC* 2013;62(25 Suppl):D13-D21.
63. Lane KB, Machado RD, Pauciulo MW et al. Heterozygous germline mutations in *BMP2*, encoding a TGF-beta receptor, cause familial primary pulmonary hypertension. *Nat Genet* 2000;26(1):81-84.
64. Machado RD, Aldred MA, James V et al. Mutations of the TGF-beta type II receptor *BMP2* in pulmonary arterial hypertension. *Hum Mutat* 2006;27(2):121-132
65. Trembath RC, Thomson JR, Machado RD et al. Clinical and molecular genetic features of pulmonary hypertension in patients with hereditary hemorrhagic telangiectasia. *N Engl J Med* 2001;345(5):325-334.
66. Chaouat A, Coulet F, Favre C et al. Endoglin germline mutation in a patient with hereditary haemorrhagic telangiectasia and dexfenfluramine associated pulmonary arterial hypertension. *Thorax* 2004;59(5):446-448.
67. Shintani M, Yagi H, Nakayama T, Saji T, Matsuoka R. A new nonsense mutation of *SMAD8* associated with pulmonary arterial hypertension. *J Med Genet* 2009;46(5):331-337.
68. Austin ED, Ma L, LeDuc C et al. Whole exome sequencing to identify a novel gene (*caveolin-1*) associated with human pulmonary arterial hypertension. *Circ Cardiovasc Genet* 2012;5(3):336-343.
69. Ma L, Roman-Campos D, Austin ED, et al. A novel channelopathy in pulmonary arterial hypertension. *N Engl J Med* 2013;369(4):351-361.
70. Girerd B, Montani D, Coulet F et al. Clinical outcomes of pulmonary arterial hypertension in patients carrying an *ACVRL1* (*ALK1*) mutation. *Am J Respir Crit Care Med* 2010;181(8):851-861.

71. Sankelo M, Flanagan JA, Machado R et al. BMPR2 mutations have short lifetime expectancy in primary pulmonary hypertension. *Hum Mutat* 2005;26(2):119–124.
72. Elliott CG, Glissmeyer EW, Havlena GT et al. Relationship of BMPR2 mutations to vasoreactivity in pulmonary arterial hypertension. *Circulation* 2006;113(21):2509–2515.
73. Merklinger SL, Jones PL, Martinez EC, Rabinovitch M. Epidermal growth factor receptor blockade mediates smooth muscle cell apoptosis and improves survival in rats with pulmonary hypertension. *Circulation* 2005;112(3):423–431.
74. Cruz JC, Reeves JT, Russell BE, Alexander AF, Will DH. Embryo transplanted calves: the pulmonary hypertensive trait is genetically transmitted. *Proc Soc Exp Biol Med* 1980;164(2):142–5.
75. Newman JH, Holt TN, Hedges LK et al. High-altitude pulmonary hypertension in cattle (brisket disease): Candidate genes and gene expression profiling of peripheral blood mononuclear cells. *Pulm Circ* 2011;1(4):462–469.
76. Eyries M, Montani D, Girerd B et al. EIF2AK4 mutations cause pulmonary veno-occlusive disease, a recessive form of pulmonary hypertension. *Nat Genet* 2014;46(1):65–69.
77. Oudiz RJ. Pulmonary hypertension associated with left-sided heart disease. *Clin Chest Med* 2007;28(1):233–241.
78. Eddahibi S, Chaouat A, Morrell N et al. Polymorphism of the serotonin transporter gene and pulmonary hypertension in chronic obstructive pulmonary disease. *Circulation* 2003;108(15):1839–1844.
79. Humbert M, Hoeper MM. Severe pulmonary arterial hypertension: a forme fruste of cancer? *Am J Respir Crit Care Med* 2008;178(6):551–552.

80. Lee SD, Shroyer KR, Markham NE, Cool CD, Voelkel NF, Tuder RM. Monoclonal endothelial cell proliferation is present in primary but not secondary pulmonary hypertension. *J Clin Invest* 1998;101(5):927–934.
81. Rai PR, Cool CD, King JA, et al. The cancer paradigm of severe pulmonary arterial hypertension. *Am J Respir Crit Care Med* 2008; 178(6):558–564
82. Tuder RM, Radisavljevic Z, Shroyer KR, Polak JM, Voelkel NF. Monoclonal endothelial cells in appetite suppressant-associated pulmonary hypertension. *Am J Respir Crit Care Med* 1998;158(6):1999–2001
83. Archer SL, Gomberg-Maitland M, Maitland ML, Rich S, Garcia JG, Weir EK. Mitochondrial metabolism, redox signaling, and fusion: a mitochondria-ROS-HIF-1 α -Kv1.5 O₂-sensing pathway at the intersection of pulmonary hypertension and cancer. *Am J Physiol Heart Circ Physiol* 2008;294(2):H570-578.
84. Bonnet S, Michelakis ED, Porter CJ et al. An abnormal mitochondrial-hypoxia inducible factor-1 α -Kv channel pathway disrupts oxygen sensing and triggers pulmonary arterial hypertension in fawn hooded rats: similarities to human pulmonary arterial hypertension. *Circulation* 2006;113(22):2630-2641.
85. Fijalkowska I, Xu W, Comhair SA et al. Hypoxia inducible-factor1 α regulates the metabolic shift of pulmonary hypertensive endothelial cells. *Am J Pathol* 2010;176(3):1130-1138.
86. Masri FA, Xu W, Comhair SA et al. Hyperproliferative apoptosis-resistant endothelial cells in idiopathic pulmonary arterial hypertension. *Am J Physiol Lung Cell Mol Physiol* 2007;293(3):L548-554.
87. Semenza GL. Involvement of hypoxia-inducible factor 1 in pulmonary pathophysiology.

CHest 2005; 128(6 Suppl):592S-594S.

88. Tudor RM, Chacon M, Alger L et al. Expression of angiogenesis-related molecules in plexiform lesions in severe pulmonary hypertension: evidence for a process of disordered angiogenesis. *J Pathol* 2001;195(3):367-374.

89. Xu W, Koeck T, Lara AR et al. Alterations of cellular bioenergetics in pulmonary artery endothelial cells. *Proc Natl Acad Sci USA* 2007;104(4):1342-1347.

90. Yuan K, Orcholski M, Tian X, Liao X, de Jesus Perez VA, Orcholski M. MicroRNAs: promising therapeutic targets for the treatment of pulmonary arterial hypertension. *Expert Opin Ther Targets* 2013 17(5):557–564.

91. Bienertova-Vasku J, Novak J, Vasku A. MicroRNAs in pulmonary arterial hypertension: pathogenesis, diagnosis and treatment. *J Am Soc Hypertens* 2015;(3):221–234.

92. Kim GH, Ryan JJ, Marsboom G, Archer SL. Epigenetic mechanisms of pulmonary hypertension. *Pulm Circ* 2011;1(3):347–356.

93. Bruneau BG. Epigenetic regulation of the cardiovascular system: introduction to a review series. *Circ Res* 2010;107(3):324–326.

94. Rajkumar R, Konishi K, Richards TJ et al. Genomewide RNA expression profiling in lung identifies distinct signatures in idiopathic pulmonary arterial hypertension and secondary pulmonary hypertension. *Am J Physiol Heart Circ Physiol* 2010;298(4):H1235–1248.

95. Atkinson C, Stewart S, Upton PD et al. Primary pulmonary hypertension is associated with reduced pulmonary vascular expression of type II bone morphogenetic protein receptor. *Circulation* 2002;105(14):1672–1678.

96. Voelkel NF, Bogaard HJ, Gomez-Arroyo J. The need to recognize the pulmonary

circulation and the right ventricle as an integrated functional unit: facts and hypotheses (2013 Grover Conference series). *Pulm Circ* 2015; 5(1):81-89.

97. Bristow MR1, Zisman LS, Lowes BD et al. The pressure-overloaded right ventricle in pulmonary hypertension. *Chest* 1998;114(1 Suppl):101S-106S.

98. Vonk-Noordegraaf A, Haddad F, Chin KM et al. Right heart adaptation to pulmonary arterial hypertension: physiology and pathobiology. *J Am Coll Cardiol* 2013;62(25 Suppl):D22-33.

99. Urashima T, Zhao M, Wagner R et al. Molecular and physiological characterization of RV remodeling in a murine model of pulmonary stenosis. *Am J Physiol Heart Circ Physiol* 2008;295(3):H1351-H1368.

100. Gomez-Arroyo J, Mizuno S, Szczepanek K et al. Metabolic gene remodeling and mitochondrial dysfunction in failing right ventricular hypertrophy secondary to pulmonary arterial hypertension. *Circ Heart Fail* 2013;6(1):136-144.

101. Bogaard HJ, Natarajan R, Henderson SC et al. Chronic pulmonary artery pressure elevation is insufficient to explain right heart failure. *Circulation* 2009;120(20):1951-1960.

102. May D, Gilon D, Djonov V et al. Transgenic system for conditional induction and rescue of chronic myocardial hibernation provides insights into genomic programs of hibernation. *Proc Natl Acad Sci USA* 2008;105(1):282-287.

103. Rain S, Handoko ML, Trip P et al. Right ventricular diastolic impairment in patients with pulmonary arterial hypertension. *Circulation* 2013;128(18):2016-2025.

104. Bogaard HJ, Abe K, Vonk Noordegraaf A, Voelkel NF. The right ventricle under pressure: cellular and molecular mechanisms of right-heart failure in pulmonary hypertension. *Chest* 2009; 135(3):794-804.

105. Kay JM, Waymire JC, Grover RF. Lung mast cell hyperplasia and pulmonary histamine-forming capacity in hypoxic rats. *Am J Physiol* 1974;226(1):178–184.
106. Zhang Q, Raouf M, Chen Y et al. Circulating mitochondrial DAMPs cause inflammatory responses to injury. *Nature* 2010;464(7285):104–107.
107. Bonderman D, Wexberg P, Martischnig AM et al. A noninvasive algorithm to exclude pre-capillary pulmonary hypertension. *Eur Respir J* 2011;37(5):1096–1103.
108. Berger M, Haimowitz A, Van Tosh A, Berdoff RL, Goldberg E. Quantitative assessment of pulmonary hypertension in patients with tricuspid regurgitation using continuous wave Doppler ultrasound. *J Am Coll Cardiol* 1985;6(2):359-365.
109. Currie PJ, Seward JB, Chan KL et al. Continuous wave Doppler determination of right ventricular pressure: a simultaneous Doppler-catheterization study in 127 patients. *J Am Coll Cardiol* 1985;6(4):750-756.
110. Bossone E, D'Andrea A, D'Alto M et al. Echocardiography in pulmonary arterial hypertension: from diagnosis to prognosis. *J Am Soc Echocardiogr.* 2013;26(1):1-14.
111. Armstrong WF, Ryan T. Feigenbaum's Echocardiography. 7th ed. Philadelphia, PA: Lippincott Williams & Wilkins; 2009.
112. Oh JK, Seward JB, Tajik AJ. The Echo Manual. 2nd ed. Philadelphia: Lippincott Williams & Wilkins; 1999. 222
113. Rudski LG, Lai WW, Afilalo J et al. Guidelines for the echocardiographic assessment of the right heart in adults: a report from the American Society of Echocardiography endorsed by the European Association of Echocardiography, a registered branch of the European Society of Cardiology, and the Canadian Society of Echocardiography. *J Am Soc Echocardiogr* 2010;23(7):685–713.

114. Lang RM, Badano LP, Mor-Avi V et al. Recommendations for cardiac chamber quantification by echocardiography in adults: an up- date from the American Society of Echocardiography and the European Association of Cardiovascular Imaging. *Eur Heart J Cardiovasc Imaging* 2015;16(3):233–271.
115. Foale R, Nihoyannopoulos P, McKenna W et al. Echocardiographic measurement of the normal adult right ventricle. *Br Heart J* 1986;56(1):33–44.
116. Trip P, Nossent EJ, de Man FS et al. Severely reduced diffusion capacity in idiopathic pulmonary arterial hypertension: patient characteristics and treatment responses. *Eur Respir J* 2013;42(6):1575-1585.
117. Sun XG, Hansen JE, Oudiz RJ, Wasserman K. Pulmonary function in primary pulmonary hypertension. *J Am Coll Cardiol* 2003;41(6):1028–1035.
118. Pellegrino R, Viegi G, Brusasco V et al. Interpretative strategies for lung function tests. *Eur Respir J* 2005;26(5):948–968.
119. Holverda S, Bogaard HJ, Groepenhoff H, Postmus PE, Boonstra A, Vonk-Noordegraaf A. Cardiopulmonary exercise test characteristics in patients with chronic obstructive pulmonary disease and associated pulmonary hypertension. *Respiration* 2008;76(2):160–167.
120. Jilwan FN, Escourrou P, Garcia G, Jaïs X, Humbert M, Roisman G. High occurrence of hypoxemic sleep respiratory disorders in precapillary pulmonary hypertension and mechanisms. *Chest* 2013;143(1):47–55.
121. Rafanan AL, Golish JA, Dinner DS, Hague LK, Arroliga AC. Nocturnal hypoxemia is common in primary pulmonary hypertension. *Chest* 2001;120(3):894–899.
122. Rajaram S, Swift AJ, Condliffe R et al. CT features of pulmonary arterial hypertension

and its major subtypes: a systematic CT evaluation of 292 patients from the ASPIRE Registry. *Thorax* 2015;70(4):382–387.

123. Resten A, Maitre S, Humbert M et al. Pulmonary hypertension: CT of the chest in pulmonary venoocclusive disease. *Am J Roentgenol* 2004;183(1):65–70.

124. Tunariu N, Gibbs SJ, Win Z et al. Ventilation-perfusion scintigraphy is more sensitive than multidetector CTPA in detecting chronic thromboembolic pulmonary disease as a treatable cause of pulmonary hypertension. *J Nucl Med* 2007;48(5):680–684.

125. Kim NH, Delcroix M, Jenkins DP et al. Chronic thromboembolic pulmonary hypertension. *J Am Coll Cardiol* 2013;62(25 Suppl):D92–D99.

126. Dartevelle P, Fadel E, Mussot S et al. Chronic thromboembolic pulmonary hypertension. *Eur Respir J* 2004;23(4):637–648.

127. Reichelt A, Hoeper MM, Galanski M, Keberle M. Chronic thromboembolic pulmonary hypertension: evaluation with 64-detector row CT versus digital subtraction angiography. *Eur J Radiol* 2008;71(1):49–54.

128. He J, Fang W, Lv B et al. Diagnosis of chronic thromboembolic pulmonary hypertension: comparison of ventilation/perfusion scanning and multidetector computed tomography pulmonary angiography with pulmonary angiography. *Nucl Med Commun* 2012;33(5):459–463.

129. Tunariu N, Gibbs SJ, Win Z et al. Ventilation-perfusion scintigraphy is more sensitive than multidetector CTPA in detecting chronic thromboembolic pulmonary disease as a treatable cause of pulmonary hypertension. *J Nucl Med* 2007;48(5):680 – 684.

130. Fedullo PF, Auger WR, Kerr KM, Rubin LJ. Chronic thromboembolic pulmonary hypertension. *N Engl J Med* 2001;345(20):1465–1472.

131. Fukui S, Ogo T, Morita Y et al. Right ventricular reverse remodelling after balloon pulmonary angioplasty. *Eur Respir J* 2014;43(5):1394–1402.
132. Hoepfer MM, Lee SH, Voswinckel R et al. Complications of right heart catheterization procedures in patients with pulmonary hypertension in experienced centers. *JACC* 2006;48(12):2546-2552.
133. Frost AE, Farber HW, Barst RJ, Miller DP, Elliott CG, McGoon MD. Demographics and outcomes of patients diagnosed with pulmonary hypertension with pulmonary capillary wedge pressures 16 to 18 mm Hg: insights from the REVEAL Registry. *Chest* 2013;143(1):185–195.
134. Abraham WT, Adamson PB, Bourge RC et al; CHAMPION Trial Study Group. Wireless pulmonary artery haemodynamic monitoring in chronic heart failure: a randomised controlled trial. *Lancet* 2011;377(9766):658–666.
135. Prasad A, Hastings JL, Shibata S et al. Characterization of static and dynamic left ventricular diastolic function in patients with heart failure with a preserved ejection fraction. *Circ Heart Fail* 2010;3(5):617–626.
136. Fujimoto N, Borlaug BA, Lewis GD et al. Hemodynamic responses to rapid saline loading: the impact of age, sex, and heart failure. *Circulation* 2013;127(1):55-62.
137. Peacock AJ, Vonk Noordegraaf A. Cardiac magnetic resonance imaging in pulmonary arterial hypertension. *Eur Respir Rev* 2013;22(130):526–534.
138. Swift AJ, Rajaram S, Condliffe R et al. Diagnostic accuracy of cardiovascular magnetic resonance imaging of right ventricular morphology and function in the assessment of suspected pulmonary hypertension results from the ASPIRE registry. *J Cardiovasc Magn Reson* 2012;14:40.

139. Swift AJ, Rajaram S, Hurdman J et al. Noninvasive estimation of PA pressure, flow, and resistance with CMR imaging: derivation and prospective validation study from the ASPIRE registry. *JACC Cardiovasc Imaging* 2013;6(10):1036–1047.
140. van Wolferen SA, Marcus JT, Boonstra A et al. Prognostic value of right ventricular mass, volume, and function in idiopathic pulmonary arterial hypertension. *Eur Heart J* 2007;28(10):1250–1257.
141. Peacock AJ, Crawley S, McLure L et al. Changes in right ventricular function measured by cardiac magnetic resonance imaging in patients receiving pulmonary arterial hypertension-targeted therapy: the EURO-MR Study. *Circ Cardiovasc Imaging* 2014;7(1):107–114.
142. van de Veerdonk MC, Kind T, Marcus JT et al. Progressive right ventricular dysfunction in patients with pulmonary arterial hypertension responding to therapy. *J Am Coll Cardiol* 2011;58(24):251–259.
143. Sitbon O, Humbert M, Nunes H et al. Long-term intravenous epoprostenol infusion in primary pulmonary hypertension: prognostic factors and survival. *J Am Coll Cardiol* 2002;40(4):780–788.
144. Nickel N, Golpon H, Greer M et al. The prognostic impact of follow-up assessments in patients with idiopathic pulmonary arterial hypertension. *Eur Respir J* 2012;39(3):589–596.
145. Barst RJ, Chung L, Zamanian RT, Turner M, McGoon MD. Functional class improvement and 3-year survival outcomes in patients with pulmonary arterial hypertension in the REVEAL Registry. *Chest* 2013;144(1):160–168.
146. Benza RL, Miller DP, Gomberg-Maitland M et al. Predicting survival in pulmonary

arterial hypertension: insights from the Registry to Evaluate Early and Long-Term Pulmonary Arterial Hypertension Disease Management (REVEAL). *Circulation* 2010;122(2):164-172.

147. Savarese G, Paolillo S, Costanzo P et al. Do changes of 6-minute walk distance predict clinical events in patients with pulmonary arterial hypertension? A meta-analysis of 22 randomized trials. *J Am Coll Cardiol* 2012;60(13):1192-1201.

148. Fritz JS, Blair C, Oudiz RJ et al. Baseline and follow-up 6-min walk distance and brain natriuretic peptide predict 2-year mortality in pulmonary arterial hypertension. *Chest* 2013;143(2):315-323.

149. Paciocco G, Martinez FJ, Bossone E, Pielsticker E, Gillespie B, Rubenfire M. Oxygen desaturation on the six-minute walk test and mortality in untreated primary pulmonary hypertension. *Eur Resp J* 2001;17(4):647-652.

150. Provencher S, Chemla D, Hervé P, Sitbon O, Humbert M, Simonneau G. Heart rate responses during the 6-minute walk test in pulmonary arterial hypertension. *Eur Resp J* 2006;27(1):114-120.

151. Wensel R, Opitz CF, Anker SD et al. Assessment of survival in patients with primary pulmonary hypertension: importance of cardiopulmonary exercise testing. *Circulation* 2002;106(3):319-324.

152. Arena R, Lavie CJ, Milani RV, Myers J, Guazzi M. Cardiopulmonary exercise testing in patients with pulmonary arterial hypertension: an evidence-based review. *J Heart Lung Transplant* 2010;29(2):159-173.

153. Warwick G, Thomas PS, Yates DH. Biomarkers in pulmonary hypertension. *Eur Resp J* 2008;32(2):503-512.

154. Zafrir N, Zingerman B, Solodky A et al. Use of noninvasive tools in primary pulmonary hypertension to assess the correlation of right ventricular function with functional capacity and to predict outcome. *Int J Cardiovasc Imaging* 2007;23(2):209–215.
155. Kawut SM, Horn EM, Berekashvili KK et al. New predictors of outcome in idiopathic pulmonary arterial hypertension. *Am J Cardiol* 2005;95(2):199-203.
156. Voelkel NF, Quaife RA, Leinwand LA et al; National Heart, Lung, and Blood Institute Working Group on Cellular and Molecular Mechanisms of Right Heart Failure. Right ventricular function and failure: report of a National Heart, Lung, and Blood Institute working group on cellular and molecular mechanisms of right heart failure. *Circulation* 2006;114(17):1883-1891.
157. Raymond RJ, Hinderliter AL, Willis PW et al. Echocardiographic predictors of adverse outcomes in primary pulmonary hypertension. *J Am Coll Cardiol* 2002;39(7):1214–1219.
158. Ghio S, Klersy C, Magrini G et al. Prognostic relevance of the echocardiographic assessment of right ventricular function in patients with idiopathic pulmonary arterial hypertension. *Int J Cardiol* 2010;140(3):272-278.
159. Badesch DB, Champion HC, Sanchez MA et al. Diagnosis and assessment of pulmonary arterial hypertension. *J Am Coll Cardiol* 2009;54(1 Suppl):S55-S66.
160. Thenappan T, Shah SJ, Rich S, Tian L, Archer SL, Gomberg-Maitland M. Survival in pulmonary arterial hypertension: a reappraisal of the NIH risk stratification equation. *Eur Respir J* 2010;35(5):1079-1087.
161. Peluso D, Tona F, Muraru D et al. Right ventricular geometry and function in pulmonary hypertension: non-invasive evaluation. *Diseases* 2014;2:274-295

162. Swift AJ, Rajaram S, Marshall H et al. Black blood MRI has diagnostic and prognostic value in the assessment of patients with pulmonary hypertension. *Eur Radiol* 2012;22(3):695-702.
163. Swift AJ, Rajaram S, Campbell MJ et al. Prognostic value of cardiovascular magnetic resonance imaging measurements corrected for age and sex in idiopathic pulmonary arterial hypertension. *Circ Cardiovasc Imag* 2014;7(1):100-106.
164. Galiè N, Corris PA, Frost A et al. Updated treatment algorithm of pulmonary arterial hypertension. *J Am Coll Cardiol* 2013;62(25 Suppl):D60-D72.
165. Jaïs X, Olsson KM, Barbera JA et al. Pregnancy outcomes in pulmonary arterial hypertension in the modern management era. *Eur Resp J* 2012;40(4):881-885.
166. Guillevin L, Armstrong I, Aldrighetti R et al. Understanding the impact of pulmonary arterial hypertension on patients' and carers' lives. *Eur Respir Rev* 2013;22(130):535-542.
167. Mereles D, Ehlken N, Kreuzer S et al. Exercise and respiratory training improve exercise capacity and quality of life in patients with severe chronic pulmonary hypertension. *Circulation* 2006;114(14):1482-1489.
168. de Man FS, Handoko ML, Groepenhoff H et al. Effects of exercise training in patients with idiopathic pulmonary arterial hypertension. *Eur Respir J* 2009;34(3):669-675.
169. Grünig E, Ehlken N, Ghofrani A et al. Effect of exercise and respiratory training on clinical progression and survival in patients with severe chronic pulmonary hypertension. *Respiration* 2011;81(5):394-401.
170. Becker-Grünig T, Klose H, Ehlken N et al. Efficacy of exercise training in pulmonary arterial hypertension associated with congenital heart disease. *Int J Cardiol* 2013;168(1):375-381.

171. Grünig E, Lichtblau M, Ehlken N et al. Safety and efficacy of exercise training in various forms of pulmonary hypertension. *Eur Respir J* 2012;40(1):84-92.
172. Meyer S, McLaughlin VV, Seyfarth HJ et al. Outcomes of noncardiac, nonobstetric surgery in patients with PAH: an international prospective survey. *Eur Respir J* 2013;41(6):1302–1307.
173. Olofsson C1, Bremme K, Forssell G, Ohqvist G. Cesarean section under epidural ropivacaine 0.75% in a parturient with severe pulmonary hypertension. *Acta Anaesthesiol Scand* 2001;45(2):258–260.
174. Raines DE, Liberthson RR, Murray JR. Anesthetic management and outcome following noncardiac surgery in nonparturients with Eisenmenger's physiology. *J Clin Anesth* 1996;8(5):341–347
175. Olsson KM, Delcroix M, Ghofrani HA et al. Anticoagulation and survival in pulmonary arterial hypertension: results from the Comparative, Prospective Registry of Newly Initiated Therapies for Pulmonary Hypertension (COMPERA). *Circulation* 2014;129(1):57-65.
176. Galie` N, Delcroix M, Ghofrani A et al. Anticoagulant therapy does not influence long-term outcomes in patients with pulmonary arterial hypertension (PAH): insights from the randomised controlled SERAPHIN trial of macitentan. *Eur Heart J* 2014;35:10.
177. Preston RJ, Roberts KE, Miller DP, Hill NS, Farber HW. Effect of warfarin treatment on survival of patients with pulmonary arterial hypertension (PAH) in the Registry to Evaluate Early and Long-Term PAH Disease Management (REVEAL). *Am J Respir Crit Care Med* 2014;189:A2464
178. Rich S, Kaufmann E, Levy PS. The effect of high doses of calcium-channel blockers on survival in primary pulmonary hypertension. *N Engl J Med* 1992;327(2):76–81.

179. Sitbon O, Humbert M, Jaïs X et al. Long-term response to calcium channel blockers in idiopathic pulmonary arterial hypertension. *Circulation* 2005;111(23):3105–3111.
180. Mukerjee D, St George D, Coleiro B et al. Prevalence and outcome in systemic sclerosis associated pulmonary arterial hypertension: application of a registry approach. *Ann Rheum Dis* 2003;62(11): 1088 –1093.
181. Montani D, Savale L, Natali D et al. Long-term response to calcium-channel blockers in non-idiopathic pulmonary arterial hypertension. *Eur Heart J* 2010;31(15):1898–1907.
182. Giaid A, Yanagisawa M, Langleben D et al. Expression of endothelin-1 in the lungs of patients with pulmonary hypertension. *N Engl J Med* 1993;328(24):1732–1739.
183. Galie´ N, Manes A, Branzi A. The endothelin system in pulmonary arterial hypertension. *Cardiovasc Res* 2004;61(2):227–237.
184. Wharton J, Strange JW, Møller GM et al. Antiproliferative effects of phosphodiesterase type 5 inhibition in human pulmonary artery cells. *Am J Respir Crit Care Med* 2005;172(1):105–113.
185. Tantini B, Manes A, Fiumana E et al. Antiproliferative effect of sildenafil on human pulmonary artery smooth muscle cells. *Basic Res Cardiol* 2005;100(2):131–138
186. Jones DA, Benjamin CW, Linseman DA. Activation of thromboxane and prostacyclin receptors elicits opposing effects on vascular smooth muscle cell growth and mitogen-activated protein kinase signaling cascades. *Mol Pharmacol* 1995;48(5):890–896.
187. Galiè N, Manes A, Branzi A. Prostanoids for pulmonary arterial hypertension. *Am J Respir Med* 2003;2(2):123-137
188. Mayer E, Jenkins D, Lindner J et al. Surgical management and outcome of patients

with chronic thromboembolic pulmonary hypertension: results from an international prospective registry. *J Thorac Cardiovasc Surg* 2011;141(3):702–710.

189. Madani MM, Auger WR, Pretorius V et al. Pulmonary endarterectomy: recent changes in a single institution's experience of more than 2,700 patients. *Ann Thorac Surg* 2012;94(1):97–103.

190. Jenkins D, Mayer E, Screatton N, Madani M. State-of-the-art chronic thromboembolic pulmonary hypertension diagnosis and management. *Eur Respir Rev* 2012;21(123):32–39.

191. Jiang L. Right ventricle. In: Weyman AE, ed. *Principle and Practice of Echocardiography*. Baltimore, Md: Lippincott Williams & Wilkins; 1994:901–921.

192. Ho SY, Nihoyannopoulos P. Anatomy, echocardiography, and normal right ventricular dimensions. *Heart* 2006;92(Suppl1):i2-13

193. Valsangiacomo Buechel ER, Mertens LL. Imaging the right heart: the use of integrated multimodality imaging. *Eur Heart J* 2012;33(8):949-960.

194. Kukulski T, Hübbert L, Arnold M, Wranne B, Hatle L, Sutherland GR. Normal regional right ventricular function and its change with age: a Doppler myocardial imaging study. *J Am Soc Echocardiogr* 2000;13(3):194-204

195. Haber I, Metaxas DN, Geva T, Axel L. Three-dimensional systolic kinematics of the right ventricle. *Am J Physiol Heart Circ Physiol* 2005;289(5):H1826-1826.

196. Selton-Suty C1, Juillière Y. Non-invasive investigations of the right heart: how and why? *Arch Cardiovasc Dis* 2009;102(3):219-232

197. Geva T, Powell AJ, Crawford EC, Chung T, Colan SD. Evaluation of regional differences in right ventricular systolic function by acoustic quantification echocardiography

and cine magnetic resonance imaging. *Circul* 1998;98(4):339-345.

198. McConnell MV, Solomon SD, Rayan ME, Come PC, Goldhaber SZ, Lee RT. Regional right ventricular dysfunction detected by echocardiography in acute pulmonary embolism. *Am J Cardiol* 1996;78(4):469-473.

199. Sanchez-Quintana D, Anderson RH, Ho SY. Ventricular myoarchitecture in tetralogy of Fallot. *Heart* 1996;76(3):280-286.

200. Pettersen E, Helle-Valle T, Edvardsen T et al. Contraction pattern of the systemic right ventricle shift from longitudinal to circumferential shortening and absent global ventricular torsion. *JACC* 2007;49(25):2450-2456.

201. Davidson C, Bonow R. Cardiac catheterization. In: Zipes D, Libby P, Bonow R, Braunwald E, eds. *Braunwald's Heart Disease: A Textbook of Cardiovascular Medicine*. 7th ed. Philadelphia, Pa: Elsevier; 2005: chap 11

202. MacNee W. Pathophysiology of cor pulmonale in chronic obstructive pulmonary disease. Part One. *Am J Respir Crit Care Med* 1994;150(4):833-852.

203. Chin KM, Kim NH, Rubin LJ. The right ventricle in pulmonary hypertension. *Coron Artery Dis* 2005;16(1):13-18.

204. Santamore WP, Dell'Italia LJ. Ventricular interdependence: significant left ventricular contributions to right ventricular systolic function. *Prog Cardiovasc Dis* 1998;40(4):289-308.

205. Hoffman D, Sisto D, Frater RW, Nikolic SD. Left-to-right ventricular interaction with a noncontracting right ventricle. *J Thorac Cardiovasc Surg* 1994;107(6):1496-1502.

206. Haddad F, Doyle R, Murphy DJ, Hunt SA. Right ventricular function in Cardiovascular

disease. Part II. Pathophysiology, clinical importance, and management of right ventricular failure. *Circulation* 2008; 117: 1717-31

207. Hoeper MM, Barberà JA, Channick RN et al. Diagnosis, assessment, and treatment of non-pulmonary arterial hypertension pulmonary hypertension. *JACC* 2009;54(1 Suppl):S85-S96.

208. Hopkins WE, Ochoa LL, Richardson GW, Trulock EP. Comparison of the hemodynamics and survival of adults with severe primary pulmonary hypertension or Eisenmenger syndrome. *J Heart Lung Transplant* 1996;15(1 Pt 1):100-105.

209. Ruiter G, van de Veerdonk MC, Bogaard HJ et al. The interventricular septum in pulmonary hypertension does not show features of right ventricular failure. *Int J Cardiol* 2014;173(3):509-512.

210. Mauritz GJ, Kind T, Marcus JT et al. Progressive changes in right ventricular geometric shortening and long-term survival in pulmonary arterial hypertension. *Chest* 2012; 141(4):935:943.

211. Vitarelli A, Mangieri E, Terzano C et al. Three-dimensional echocardiography and 2D-3D speckle-tracking imaging in chronic pulmonary hypertension: diagnostic accuracy in detecting hemodynamic signs of right ventricular (RV) failure. *JAHA* 2015;4(3):1584.

212. Vitarelli A, Barillà F, Capotosto L et al. Right ventricular function in acute pulmonary embolism: a combined assessment by three-dimensional and speckle-tracking echocardiography. *J Am Soc Echocardiogr* 2014;27(3):329–338.

213. Ichikawa K, Dohi K, Sugiura E et al. Ventricular function and dyssynchrony quantified by speckle-tracking echocardiography in patients with acute and chronic right ventricular pressure overload. *J Am Soc Echocardiogr* 2013;26(5):483–492.

214. Unlu S, Farsalinos K, Ameloot K et al. Apical traction: a novel visual echocardiographic parameter to predict survival in patients with pulmonary hypertension. *Eur Heart J CV Imag* 2016;17(2):177-183.
215. Forfia PR, Fisher MR, Mathai SC et al. Tricuspid annular displacement predicts survival in pulmonary hypertension. *Am J Respir Crit Care Med* 2006;174(9):1034-1041.
216. Giusca S, Dambrauskaite V, Scheurwegs C et al. Deformation imaging describes right ventricular function better than longitudinal displacement of the tricuspid ring. *Heart* 2010;96(4):281-288.
217. Teske AJ, De Boeck BW, Olimulder M, Prakken NH, Doevendans PA, Cramer MJ. Echocardiographic assessment of regional right ventricular function: A head-to-head comparison between 2-dimensional and tissue Doppler-derived strain analysis. *J Am Soc Echocardiogr* 2008;21(3):275-283.
218. Scherptong RW, Mollema SA, Blom NA et al. Right ventricular peak systolic longitudinal strain is a sensitive marker for right ventricular deterioration in adult patients with tetralogy of Fallot. *Int J Cardiovasc Imaging* 2009;25(7):669-676.
219. Dragulescu A, Mertens LL. Developments in echocardiographic techniques for the evaluation of ventricular function in children. *Arch Cardiovasc Dis* 2010;103(11-12):603-614.
220. Mertens LL, Friedberg MK. Imaging the right ventricle-Current state of the art. *Nat Rev Cardiol* 2010;7(10), 551-563.
221. Pirat B, McCulloch ML, Zoghbi WA. Evaluation of global and regional right ventricular systolic function in patients with pulmonary hypertension using a novel speckle tracking method. *Am J Cardiol* 2006;98(5):699-704.

222. Fukuda Y, Tanaka H, Sugiyama D et al. Utility of right ventricular free wall speckle-tracking strain for evaluation of right ventricular performance in patients with pulmonary hypertension. *J Am Soc Echocardiogr* 2011;24(10):1101-1108.
223. Sachdev A, Villarraga HR, Frantz RP et al. Right ventricular strain for prediction of survival in patients with pulmonary arterial hypertension. *Chest* 2011;139(6):1299-309.
224. Haeck ML, Scherptong RW, Antoni ML et al. Right ventricular longitudinal peak systolic strain measurements from the subcostal view in patients with suspected pulmonary hypertension: A feasibility study. *J Am Soc Echocardiogr* 2012;25(6):674-681.
225. Haeck ML, Scherptong RW, Marsan NA et al. Prognostic value of right ventricular longitudinal peak systolic strain in patients with pulmonary hypertension. *Circ Cardiovasc Imaging* 2012;5(5):628-636.
226. Meris A, Faletra F, Conca C et al. Timing and magnitude of regional right ventricular function: a speckle tracking-derived strain study of normal subjects and patients with right ventricular dysfunction. *J Am Soc Echocardiogr* 2010;23(8):823-31.
227. Leong DP, Grover S, Molaei P et al. Nonvolumetric echocardiographic indices of right ventricular systolic function: validation with cardiovascular magnetic resonance and relationship with functional capacity. *Echocardiography* 2012;29(4):455-463.
228. Muraru D, Onciul S, Peluso D. Sex- and Method-specific reference values for right ventricular strain by 2-dimensional speckle-tracking echocardiography. *Circ CV Imag* 2016; 9(2):e003866.
229. Giusca S, Popa E, Amzulescu MS et al. Is Right Ventricular Remodeling in Pulmonary Hypertension Dependent on Etiology? An Echocardiographic Study. *Echocardiography* 2015;33(4):546-554.

230. Morris DA, Gailani M, Vaz Pérez A et al. Right ventricular myocardial systolic and diastolic dysfunction in heart failure with normal left ventricular ejection fraction. *J Am Soc Echocardiogr* 2011;24(8):886-897.
231. Focardi M, Cameli M, Carbone SF et al. Traditional and innovative echocardiographic parameters for the analysis of right ventricular performance in comparison with cardiac magnetic resonance. *Eur Heart J Cardiovasc Imaging* 2015;16(1):47-52.
232. Puwanant S1, Park M, Popović ZB et al. Ventricular geometry, strain, and rotational mechanics in pulmonary hypertension. *Circulation* 2010;121(2):259-266.
233. Dambrauskaite V, Delcroix M, Claus P et al. Regional right ventricular dysfunction in chronic pulmonary hypertension. *JASE* 2007;20(10):1172-1180.
234. Li Y, Wie M, Wang X, Lu Q, Fu M. Right ventricular regional and global systolic function is diminished in patients with pulmonary arterial hypertension: a 2-dimensional ultrasound speckle tracking echocardiography study. *Int J Cardiovasc Imag* 2013;29(3):545-51.
235. Freed BH, Tsang W, Bhave NM et al. Right ventricular strain in pulmonary arterial hypertension: a 2D echocardiography and cardiac magnetic resonance study. *Echocardiography* 2015;32(2):257-263.
236. Motoji Y, Tanaka H, Fukuda Y et al. Efficacy of right ventricular free-wall longitudinal speckle-tracking strain for predicting long-term outcome in patients with pulmonary hypertension. *Circ J* 2013;77(3):756-763.
237. Fine NM, Chen L, Bastiansen PM et al. Outcome prediction by quantitative right ventricular function assessment in 575 subjects evaluated for pulmonary hypertension. *Circ Cardiovasc Imag* 2013;6(5):711-721.

238. Simon MA, Rajagopalan N, Mathier MA, Shroff SG, Pinsky MR, López-Candales A. Tissue Doppler imaging of right ventricular decompensation in pulmonary hypertension. *Congest Heart Fail* 2009;15(6):271-276.
239. Reichek N. Right ventricular strain in pulmonary hypertension: flavor du jour or enduring prognostic index? *Circul CV Imag* 2013;6(5):609-611.
240. La Gerche A, Jurcut R, Voigt JU. Right ventricular function by strain echocardiography. *Curr Opin Cardiol* 2010;25(5):430-436.
241. Hardegree EL, Sachdev A, Villarraga HR et al. Role of serial quantitative assessment of right ventricular function by strain in pulmonary arterial hypertension. *Am J Cardiol* 2013;111(1):143-148.
242. López-Candales A, Dohi K, Bazaz R, Edelman K. Relation of right ventricular free wall mechanical delay to right ventricular dysfunction as determined by tissue Doppler imaging. *Am J Cardiol* 2005;96(4):602-606.
243. Kalogeropoulos AP, Georgiopoulou VV, Howell S et al. Evaluation of right intraventricular dyssynchrony by two-dimensional strain echocardiography in patients with pulmonary arterial hypertension. *J Am Soc Echocardiogr* 2008;21(9):1028-1034.
244. Marcus JT, Gan CT, Zwanenburg JJ et al. Interventricular mechanical asynchrony in pulmonary arterial hypertension: left-to-right delay in peak shortening is related to right ventricular overload and left ventricular underfilling. *J Am Coll Cardiol* 2008;51(7):750-757.
245. Hill AC, Maxey DM, Rosenthal DN et al. Electrical and mechanical dyssynchrony in pediatric pulmonary hypertension. *Heart Lung Transplant* 2012;31(8):825-30.
246. Badagliacca R, Reali M, Poscia R et al. Right Intraventricular Dyssynchrony in Idiopathic, Heritable, and Anorexigen-Induced Pulmonary Arterial Hypertension: Clinical

Impact and Reversibility. *JACC Cardiovasc Imaging* 2015;8(6):642-652.

247. Badagliacca R, Poscia R, Pezzuto B et al. Right ventricular dyssynchrony in idiopathic pulmonary arterial hypertension: determinants and impact on pump function. *J Heart Lung Transplant* 2015;34(3):381-389.

248. Schindera ST, Mehwald PS, Sahn DJ, Kececioglu D. Accuracy of real-time three-dimensional echocardiography for quantifying right ventricular volume: static and pulsatile flow studies in an anatomic in vitro model. *J. Ultrasound Med* 2002;21(10): 1069-1075.

249. Nesser HJ, Tkalec W, Patel AR et al. Quantitation of right ventricular volumes and ejection fraction by three-dimensional echocardiography in patients: comparison with magnetic resonance imaging and radionuclide ventriculography. *Echocardiography* 2006;23(8):666-680.

250. Chen G, Sun K, Huang G. In vitro validation of right ventricular volume and mass measurement by real-time three-dimensional echocardiography. *Echocardiography* 2006;23(5):395-399.

251. Angelini ED, Homma S, Pearson G, Holmes JW, Laine AF. Segmentation of real-time three-dimensional ultrasound for quantification of ventricular function: a clinical study on right and left ventricles. *Ultrasound Med Biol* 2005;31(9):1143-1158.

252. Jenkins C, Chan J, Bricknell K, Strudwick M, Marwick TH. Reproducibility of right ventricular volumes and ejection fraction using real-time three-dimensional echocardiography: comparison with cardiac MRI. *Chest* 2007;131(6):1844-51.

253. Maffessanti F, Muraru D, Esposito R et al. Age-, body size-, and sex-specific reference values for right ventricular volumes and ejection fraction by three-dimensional echocardiography: a multicenter echocardiographic study in 507 healthy volunteers. *Circ*

Cardiovasc Imag 2013;6(5):700–710.

254. Chua S, Levine RA, Yosefy C et al. Assessment of right ventricular function by real-time three-dimensional echocardiography improves accuracy and decreases interobserver variability compared with conventional two-dimensional views. *Eur J Echocardiogr* 2009;10(5):619-624.

255. Niemann PS, Pinho L, Balbach T et al. Anatomically oriented right ventricular volume measurements with dynamic three-dimensional echocardiography validated by 3-Tesla magnetic resonance imaging. *J Am Coll Cardiol*. 2007;50(17):1668-1676

256. Badano LP, Bocalini F, Muraru D et al. Current clinical applications of transthoracic three-dimensional echocardiography. *J Cardiovasc Ultrasound* 2012;20(1):1-22.

257. Lu X, Nadvoretzkiy V, Bu L et al. Accuracy and reproducibility of real-time three-dimensional echocardiography for assessment of right ventricular volumes and ejection fraction in children. *J Am Soc Echocardiogr* 2008;21(1):84-89.

258. Grison A, Maschietto N, Reffo E et al. Three-dimensional echocardiographic evaluation of right ventricular volume and function in pediatric patients: validation of the technique. *J Am Soc Echocardiogr* 2007;20(8):921-9.

259. Grewal J, Majdalany D, Syed I, Pellikka P, Warnes CA. Three-dimensional echocardiographic assessment of right ventricular volume and function in adult patients with congenital heart disease: comparison with magnetic resonance imaging. *J Am Soc Echocardiogr* 2010;23(2):127-133.

260. Leibundgut G, Rohner A, Grize L et al. Dynamic assessment of right ventricular volumes and function by real-time three-dimensional echocardiography: a comparison study with magnetic resonance imaging in 100 adult patients. *J Am Soc Echocardiogr*

2010;23(2):116-126.

261. Shimada YJ, Shiota M, Siegel RJ, Shiota T. Accuracy of right ventricular volumes and function determined by three-dimensional echocardiography in comparison with magnetic resonance imaging: a meta-analysis study. *JASE* 2010;23(9):943-953.

262. Li Y, Wang Y, Zhai Z, Guo X, Yang Y, Lu X. Real-time three-dimensional echocardiography to assess right ventricle function in patients with pulmonary arterial hypertension. *PLOS ONE* | DOI:10.1371/journal.pone.0129557

263. Tamborini G, Marsan NA, Gripari P et al. Reference values for right ventricular volumes and ejection fraction with real-time three-dimensional echocardiography: evaluation in a large series of normal subjects. *JASE* 2010;23(2):109-115.

264. Kawut SM, Lima JA, Barr RG et al. Sex and race differences in right ventricular structure and function: the multi-ethnic study of atherosclerosis-right ventricle study. *Circulation* 2011;123(22):2542-2551.

265. Calcuttea A, Chung R, Lindqvist P, Hodson M, Henein MY. Differential right ventricular regional function and the effect of pulmonary hypertension: three-dimensional echo study. *Heart* 2011;97(12):1004-1011.

266. Kong D, Shu X, Pan C et al. Evaluation of right ventricular regional volume and systolic function in patients with pulmonary arterial hypertension using three-dimensional echocardiography. *Echocardiography* 2012;29(6):706-712.

267. Addetia K, Maffesanti F, Yamat M et al. Three-dimensional echocardiography-based analysis of right ventricular shape in pulmonary arterial hypertension. *Eur Heart J Cardiovasc Imaging* 2016;17(5):564-75.

268. Zhang QB, Sun JP, Gao RF et al. Feasibility of single-beat full-volume capture real-

time three-dimensional echocardiography for quantification of right ventricular volume: validation by cardiac magnetic resonance imaging. *Int J Cardiol* 2013;168(4):3991-5.

269. Sugeng L, Mor-Avi V, Weinert L et al. Multimodality comparison of quantitative volumetric analysis of the right ventricle. *JACC Cardiovasc Imag* 2010;3(1):10-18.

270. Pickett CA, Cheezum MK, Kassop D, Villines TC, Hulten EA. Accuracy of cardiac CT, radionuclide and invasive ventriculography, two- and three-dimensional echocardiography, and SPECT for left and right ventricular ejection fraction compared with cardiac MRI: a meta-analysis. *Eur Heart J CV Imaging* 2015;16(8):848-852.

271. Di Bello V, Conte L, Delle Donne MG et al. Advantages of real time three-dimensional echocardiography in the assessment of right ventricular volumes and function in patients with pulmonary hypertension compared with conventional two-dimensional echocardiography. *Echocardiography* 2013;30(7):820-828.

272. van den Hoogen F, Khanna D, Fransen J, Johnson SR, Baron M, Tyndall A et al. 2013 classification criteria for systemic sclerosis: an American college of rheumatology/European league against rheumatism collaborative initiative. *Ann Rheum Dis* 2013;72:1747–1755

273. Abbas AE, Franey LM, Marwick T et al. Noninvasive assessment of pulmonary vascular resistance by Doppler echocardiography. *JASE* 2013;26(10):1170-7

274. Du Bois D and Du Bois EF. A formula to estimate the approximate surface area if height and weight be known. *Arch Intern Med* 1916; 17: 863-871

275. Sengupta PP, Korinek J, Belohlavek M et al. Left ventricular structure and function: basic science for cardiac imaging. *J Am Coll Cardiol* 2006;48:1988–2001.

276. Sengupta PP, Krishnamoorthy VK, Korinek J et al. Left ventricular form and function revisited: applied translational science to cardiovascular ultrasound imaging. *J Am Soc*

277. Mendez C, Soler R, Rodriguez E et al. Magnetic resonance imaging of abnormal ventricular septal motion in heart disease: a pictorial review. *Insig Imag* 2011;2:483-492
278. De Azevedo AB, Sampaio-Barros PD, Torres RM, Moreira C. Prevalence of pulmonary hypertension in systemic sclerosis. *Clin Exp Rheumatol* 2005; 23: 447-54
279. Bewley AP, Cooper JP, Levell NJ, Walker JM, Dowd PM: Systemic sclerosis associated with right ventricular cardiomyopathy. *Br J Dermatol* 1996; 134: 1141-3.
280. Meune C, Allanore Y, Devaux JY et al. High prevalence of right ventricular systolic dysfunction in early systemic sclerosis. *J Rheumatol* 2004; 31: 1941-5.
281. Meune C, Allanore Y, Vignaux O, Merceron O, Assous N, Legmann P, Kahan A. Predominant primitive right ventricular involvement in systemic sclerosis. *Cin Exp Rheumatol* 2007; 25 (4): 658
282. Allanore Y, Meune C. Primary myocardial involvement in systemic sclerosis: evidence for a microvascular origin. *Clin Exp Rheumatol* 2010;28(Suppl 61):S48-53
283. Matias C, Perez de Isla L, Vasconcelos M et al. Speckle-tracking-derived strain and strain-rate analysis: a technique for the evaluation of early alterations in right ventricle systolic function in patients with systemic sclerosis and normal pulmonary artery pressure. *J Cardiovasc Med* 2009;10:129-34
284. Schattke S, Knebel F, Grohmann A et al. Early right ventricular systolic dysfunction in patients with systemic sclerosis without pulmonary hypertension: a Doppler Tissue and speckle tracking echocardiography study. *Cardiovasc Ultras* 2010;8:3
285. Durmus E, Sunbul M, Tigen K et al. Right ventricular and atrial functions in systemic

sclerosis patients without pulmonary hypertension. Speckle-tracking echocardiographic study. *Heart* 2015;40:709-15

286. Pigatto E, Peluso D, Zanatta E et al. Evaluation of right ventricular function performed by 3D-echocardiography in scleroderma patients. *Reumatismo* 2014;66(4):259-263.

287. Muraru D, Spadotto V, Cecchetto A et al. New speckle-tracking algorithm for right ventricular volume analysis from three-dimensional echocardiographic data sets: validation with cardiac magnetic resonance and comparison with the previous analysis tool. *Eur Heart J Cardiovasc Imaging*. 2015 Dec 8. pii: jev309. [Epub ahead of print].

288. Mori S, Nakatani S, Kanzaki H et al. Patterns of the interventricular septal motion can predict conditions of patients with pulmonary hypertension. *JASE* 2008;21(4):386-393

289. Sato T, Tsujino I, Ohira H et al. Paradoxical interventricular septal motion as a major determinant of late gadolinium enhancement in ventricular insertion points in pulmonary hypertension. *PLOS ONE* 2013;8(6):e66724

290. Freed BH, Gomberg-Maitland M, Chandra, S et al. Late gadolinium enhancement cardiovascular magnetic resonance predicts clinical worsening in patients with pulmonary hypertension. *J Cardiovasc Magn Res*. 2012, 14, doi:10.1186/1532-429X-14-11

Acknowledgments

Al termine di questo percorso ringrazio con affetto:

- Il Dr. Luigi P Badano per avermi guidato in questo cammino di crescita professionale, sia clinica che scientifica;
- Il Prof. Gaetano Thiene per avermi dato la possibilità di realizzare questa bellissima e unica esperienza;
- Il mio tutor, Prof Sabino Iliceto, per avermi dato la possibilità di svolgere questa bellissima esperienza nella Clinica Cardiologica di Padova;
- La Dr.ssa Martina Perazzolo Marra per avermi coinvolto nelle attività dell'Ambulatorio dell'Ipertensione Polmonare;
- Tutto il gruppo del Laboratorio di Ecocardiografia di Padova con cui ho trascorso 3 bellissimi anni, intensi ed indimenticabili;
- La clinica Reumatologica di Padova, ed in particolare il Prof F. Cozzi, la Dr.ssa E. Pigatto ed il Prof L. Punzi per la loro preziosa collaborazione;
- La mia famiglia per essermi stata vicina ed avermi supportato.

**FORMATO EUROPEO
PER IL CURRICULUM
VITAE**



INFORMAZIONI PERSONALI

Nome	PELUSO DILETTA
Indirizzo	VIA SOGRAFI 33 35128 PADOVA
Telefono	340-2878259
E-mail	dile_pls@yahoo.it
Nazionalità	italiana
Data di nascita	06/11/1982

**ESPERIENZA
LAVORATIVA**

Da aprile 2016 a oggi

Ospedale dell'Angelo. Mestre

Contratto a tempo Determinato per Dirigente Medico di
Cardiologia

Da marzo a Dicembre 2015

Istituto Oncologico Veneto IRCCS, servizio di Cardiologia

Contratto libero-professionale

Ambulatorio di Cardiologia

Dal 02/05/2012 a marzo 2015

Cittadella Socio Sanitaria di Cavarzere S.r.l., Cavarzere (VE)

Contratto di Prestazione d'Opera Intellettuale con attività libero
professionale

Ambulatorio di Cardiologia con esecuzione di esami strumentali
(ecocardiografia)

Dal 17/09/2012 al 31/12/2012

Casa di Cura Dott. Pederzoli, Peschiera del Garda (Vr)

Contratto di libero professionista

Turni di guardia in reparto di Cardiologia

**ISTRUZIONE E
FORMAZIONE**

Da Gennaio 2013 a giugno 2016

Università degli Studi di Padova

Scuola di **Dottorato di Ricerca** in Scienze Mediche, Cliniche e
Sperimentali, indirizzo Scienze Cardiovascolari

Da Marzo 2008 a Marzo 2012

Università degli Studi di Padova

Scuola di specializzazione in Cardiologia, ai sensi del DLg 368/1999.

Specializzazione in Cardiologia, voto 70/70 e Lode

Da Novembre 2007 a Gennaio 2008

Università degli Studi di Padova

Tirocinio professionalizzante

Abilitazione alla Professione Medica

Da Settembre 2001 a Luglio 2007

Università degli Studi di Padova

Facoltà di Medicina e Chirurgia

**Laurea Specialistica in Medicina e Chirurgia, voto 110/110 e
Lode**

Da Settembre 1991 a Ottobre 2003

Pianoforte; solfeggio; storia della musica; armonia.

Diploma di Pianoforte

**CAPACITÀ E COMPETENZE
PERSONALI**

MADRELINGUA

ITALIANA

ALTRE LINGUE

INGLESE

Capacità di scrittura: buona

Capacità di lettura: buona

Capacità di espressione orale: discreta

ATTIVITÀ
SCIENTIFICHE

- Corsi/congressi:

- presentazione di comunicazioni orali a 4 congressi nazionali;
- presentazione di poster a 7 congressi, di cui 2 nazionali e 5 internazionali;
- relatrice ad un congresso nazionale;
- partecipazione come uditore a 19 congressi/seminari/corsi;
- corso ACLS Provider 2011;
- corso intensivo di Risonanza Magnetica Cardiaca presso il Dipartimento di Scienze Cardiache, Toraciche e Vascolari dell'Università di Padova.

- Pubblicazioni:

Paper

- Napodano M, Ramondo A, Tarantini G, **Peluso D**, Compagno S, Fraccaro C, Frigo AC, Razzolini R, Iliceto S. "Predictors and time-related impact of distal embolization during primary angioplasty" *Eur Heart J*. 2009 Feb;30(3):305-13.
- Napodano M, Tarantini G, Ramondo A, Cacciavillani L, Corbetti F, Marra MP, Fraccaro C, **Peluso D**, Razzolini R, Iliceto S. Myocardial abnormalities underlying persistent ST-segment elevation after anterior myocardial infarction. *J Cardiovasc Med* 2009 Jan;10(1):44-50
- Pepe M, Napodano M, Tarantini G, Fraccaro C, Cutolo A, **Peluso D**, Isabella G, Ramondo A, Iliceto S. "Percutaneous coronary intervention for unprotected left main disease in very high risk patients: safety of drug-eluting stents" *Heart Vessel* 2011; 26: 17-24.
- Cresce GD, **Peluso D**, Panfili M, Favaro A, Cannarella A, Picichè M, Salvador L. Left Atrial Wall Hematoma as a Consequence of Percutaneous Coronary Angioplasty. *Ann Thorac Surg* 2012; 93:

e57-9.

- Badano LP, Boccalini F, Muraru D, Dal Bianco L, **Peluso D**, Bellu R, Zoppellaro G, Iliceto S. Current Clinical Applications of Transthoracic Three-Dimensional Echocardiography. *J Cardiovasc Ultras* 2012; 20(1): 1-22
- Muraru D, Cattarina M, Boccalini F, Dal Lin C, **Peluso D**, Zoppellaro G, Bellu R, Sarais C, Xhyheri B, Iliceto S, Badano LP. Mitral Valve anatomy and function-new insights from three dimensional echocardiography. *J Cardiovasc Med* 2013 Feb; 14 (2): 91-9
- Kocabay G, **Peluso D**, Badano LP, Iliceto S. Diastolic Mitral Regurgitation in 2:1 Atrioventricular Block: Insight of the Diastolic Pressure. *Echocardiography* 2012; 0: 1-3
- Kocabay G, Muraru D, **Peluso D**, Iliceto S, Badano LP. Three-Dimensional Transesophageal Echocardiography of Aortic Atherosclerosis. *Echocardiography* 2012;0:1-3
- Napodano M, **Peluso D**, Perazzolo Marra M, Frigo AC, Tarantini G, Buja P, Gasparetto V, Fraccaro C, Isabella G, Razzolini R, Iliceto S. Time-dependent Detrimental Effects of Distal Embolization on Myocardium and Microvasculature during Primary Percutaneous Coronary Intervention. *JACC Cardio Interv* 2012; 5 (11): 1170-77
- Muraru D, Boccalini F, Cattarina M, **Peluso D**, Dal Bianco L, Zoppellaro G, Segafredo B, Nour A, Sarais C, Badano LP. Quantitation of cardiac chamber geometry and function using transthoracic three-dimensional echocardiography. *J Cardio Echogr* 2012; 22 (4): 146-158
- **Peluso D**, Badano L, Denisa M, Dal Bianco L, Cucchini U, Kocabay G, Kòvacs A, Casablanca S, Iliceto S. Right atrial size and function assessed with three-dimensional and speckle tracking echocardiography in 200 healthy volunteers. *Eur Heart J Cardio Imag* 2013; 14 (11): 1106-14.
- Muraru D, Badano LP, **Peluso D**, Dal Bianco L, Casablanca S,

- Kocabay G, Zoppellaro G, Iliceto S. Comprehensive analysis of left ventricular geometry and function by three-dimensional echocardiography in healthy adults. *JASE* 2013; 26 (6): 618-28
- Muraru D, Maffesanti F, Kocabay G, **Peluso D**, Bianco LD, Piasentini E, Jose SP, Iliceto S, Badano LP. Ascending Aorta Diameters Measured by Echocardiography Using Both Leading Edge-to-Leading Edge and Inner Edge-to-Inner Edge Conventions in Healthy Volunteers. *Eur Heart J CV Imag* 2013; 15 (4): 415-22.
 - Kocabay G, Muraru D, **Peluso D**, Cucchini U, Mihaila S, Padayattil-Josè S, Gentian D, Iliceto S, Vinereanu D, Badano LP. Normal Left Ventricular Mechanics by Two-dimensional Speckle-tracking Echocardiography. Reference Values in Healthy Adults. *Rev Esp Cardiol* 2014; 67 (8) 651-8.
 - Mihăilă S, Muraru D, Piasentini E, Miglioranza MH, **Peluso D**, Cucchini U, Iliceto S, Vinereanu D, Badano LP. Quantitative Analysis of Mitral Annular Geometry and Function in Healthy Volunteers Using Transthoracic Three-Dimensional Echocardiography. *JASE* 2014; 27 (8): 846-57
 - Muraru D, Cucchini U, Mihăilă S, Miglioranza MH, Aruta P, Cavalli G, Cecchetto A, Padayattil-Josè S, **Peluso D**, Iliceto S, Badano LP. Left Ventricular Myocardial Strain by Three-Dimensional Speckle-Tracking Echocardiography in Healthy Subjects: Reference Values and Analysis of Their Physiologic and Technical Determinants. *JASE* 2014; 27 (8): 858-871.
 - Pigatto E, **Peluso D**, Zanatta E, Polito P, Miatton P, Bourji K, Badano LP, Punzi L, Cozzi F. Evaluation of right ventricular function performed by 3d-echocardiography in scleroderma patients. *Reumatismo* 2014; 66 (4): 259-63
 - **Peluso D**, Tona F, Muraru D, Romeo G, Cucchini U, PerazzoloMarra M, Iliceto S and Badano LP. Right Ventricular Geometry and Function in Pulmonary Hypertension: Non-Invasive Evaluation. *Diseases* 2014, 2, 274-295

- Mihaila S, Muraru D, Haertel Miglioranza M, Piasentini E, **Peluso D**, Cucchini U, Iliceto S, Vinereanu D, Badano LP. Normal mitral annulus dynamics and its relationship with left ventricular and left atrial function. *Int J Cardiovasc Imag* 2015 ; 31 (2): 279-290
- The EchoNoRMAL (Echocardiographic Normal Ranges Meta-Analysis of the Left Heart) Collaboration. Ethnic-Specific Normative Reference Values for Echocardiographic LA and LV Size, LV Mass, and Systolic Function The EchoNoRMAL Study. *JACC Cardiovasc Imag* 2015; 8 (6): 656-665
- **Peluso D**, Bianchi A, Bonanno L, Banzato A. Unusual echocardiographic appearance of a cardiac metastasis from lung carcinoma. *J Cardiovasc Ultras* 2015 Dec 17. doi: 10.1002/jcu.22325. [Epub ahead of print]
- Muraru D, Onciul S, **Peluso D**, Soriani N, Cucchini U, Aruta P, Romeo G, Cavalli G, Iliceto S, and Badano LP. Sex- and Method-Specific Reference Values for Right Ventricular Strain by Two-Dimensional Speckle-Tracking Echocardiography. *Circulation Cardiovasc Imag* 2016; 9: e003866
- Surkova E, Peluso D, Kasprzak JD, Badano LP. Use of novel echocardiographic techniques to assess right ventricular geometry and function. *Kardiol Pol* 2016 Apr 4. doi: 10.5603/KP.a2016.0041. [Epub ahead of print.]

Book chapter: The Right Atrium chapter of the II edition of the “Textbook of Real - Time Three Dimensional Echocardiography”, edited by Dr. Badano, Dr. Lang, Dr. Mor-Avi and Dr. Muraru. In press.

Abstracts: pubblicazione di 103 abstracts dal 2008 ad oggi di cui: 20 come primo nome; 62 a congressi internazionali e 41 a congressi nazionali;

- Docente del Master di “Ecocardiografia di base ed avanzata” del Dipartimento di Scienze Cardiache, Toraciche e Vascolari dell’Università di Padova.
- Peer reviewer per le riviste: Journal of the American Heart Association; Journal of Advances in Medical and Pharmaceutical Sciences
- Frequenza presso il Laboratorio di Ecocardiografia della Cl. Cardiologica di Padova, responsabile Dr. L.P. Badano (aprile 2011 ad oggi), dove ho sviluppato esperienza nell’ambito di: ecocardiografia standard mono- e bidimensionale; ecocardiografia tridimensionale transtoracica e transesofagea utilizzando le macchine GE Vivid E9 e Philips IE33, entrambe dotate delle rispettive sonde 3D transtoracica e transesofagea; ecostress farmacologico con dipiridamolo e dobutamina; esame della riserva coronarica; gestione digitale delle immagini e loro post-processing, acquisendo esperienza con i software EchoPac (GE Healthcare, Horten, N), TomTec 4D LV, TomTec 4D LA e TomTec 4D RV (TomTec Imaging Systems GmbH, Unterschleissheim-D), Philips QLAB (Koninklijke Philips Electronics).

Activities during PhD period

Durante il periodo di dottorato è stata svolta la seguente **attività formativa**:

- Cicli di conferenze clinico-patologiche del Dipartimento di Scienze Cardiache, Toraciche e Vascolari. AA 2012/2013, 2013/2014, 2014/2015.
- Summer School. 23-27 settembre 2013 c/o IOV IRCCS, Padova
- Corso Scientific Writing. 3-6 giugno 2014 Padova
- Autumn School. 20 ottobre 2014 c/o Palazzo del Bo, Padova
- Spring School. 29-30 maggio 2015, Bressanone (BZ).

L'attività di ricerca è esitata nella pubblicazione dei seguenti **lavori scientifici**:

1. Muraru D, Cattarina M, Boccalini F, Dal Lin C, **Peluso D**, Zoppellaro G, Bellu R, Sarais C, Xhyheri B, Iliceto S, Badano LP. Mitral Valve anatomy and function-new insights from three dimensional echocardiography. *J Cardiovasc Med* 2013 Feb; 14 (2): 91-9
2. Kocabay G, **Peluso D**, Muraru D, Iliceto S, Badano LP. Diastolic Mitral Regurgitation in 2:1 Atrioventricular Block: Insight of the Diastolic Pressure. *Echocardiography* 2013; 30 (2): E51-2.
3. **Peluso D**, Badano L, Denisa M, Dal Bianco L, Cucchini U, Kocabay G, Kòvacs A, Casablanca S, Iliceto S. Right atrial size and functional assessed with three-dimensional and speckle tracking echocardiography in 200 healthy volunteers. *Eur Heart J Cardiovasc Imag* 2013; 14 (11): 1106-14
4. Muraru D, Badano LP, **Peluso D**, Dal Bianco L, Casablanca S, Kocabay G, Zoppellaro G, Iliceto S. Comprehensive analysis of left ventricular geometry and function by three-dimensional echocardiography in healthy adults. *JASE* 2013; 26 (6): 618-28
5. Muraru D, Maffesanti F, Kocabay G, **Peluso D**, Bianco LD, Piasentini E, Jose SP, Iliceto S, Badano LP. Ascending Aorta Diameters Measured by Echocardiography Using Both Leading Edge-to-Leading Edge and Inner Edge-to-Inner Edge Conventions in Healthy Volunteers. *Eur Heart J CV Imag* 2013; 15 (4): 415-22.
6. Kocabay G, Muraru D, **Peluso D**, Cucchini U, Mihaila S, Padayattil-Josè S, Gentian D, Iliceto S, Vinereanu D, Badano LP. Normal Left Ventricular Mechanics by Two-dimensional Speckle-tracking Echocardiography. Reference Values in Healthy Adults. *Rev Esp Cardiol* 2014; 67 (8): 651-8

7. Mihăilă S, Muraru D, Piasentini E, Miglioranza MH, **Peluso D**, Cucchini U, Iliceto S, Vinereanu D, Badano LP. Quantitative Analysis of Mitral Annular Geometry and Function in Healthy Volunteers Using Transthoracic Three-Dimensional Echocardiography. *JASE* 2014; 27(8): 846-57.
8. Muraru D, Cucchini U, Mihăilă S, Miglioranza MH, Aruta P, Cavalli G, Cecchetto A, Padayattil-Josè S, **Peluso D**, Iliceto S, Badano LP. Left Ventricular Myocardial Strain by Three-Dimensional Speckle-Tracking Echocardiography in Healthy Subjects: Reference Values and Analysis of Their Physiologic and Technical Determinants. *JASE* 2014; 27(8): 858-871.
9. Pigatto E, **Peluso D**, Zanatta E, Polito P, Miatton P, Bourji K, Badano LP, Punzi L, Cozzi F. Valutazione della funzione ventricolare destra mediante ecocardiografia tridimensionale nei pazienti con sclerosi sistemica". *Reumatismo* 2014; 66 (4): 259-263
10. **Peluso D**, Tona F, Muraru D, Romeo G, Cucchini U, Perazzolo Marra M, Iliceto S and Badano LP. Right Ventricular Geometry and Function in Pulmonary Hypertension: Non-Invasive Evaluation. *Diseases* 2014; 2: 274-295
11. Mihaila S, Muraru D, Haertel Miglioranza M, Piasentini E, **Peluso D**, Cucchini U, Iliceto S, Vinereanu D, Badano LP. Normal mitral annulus dynamics and its relationship with left ventricular and left atrial function. *Int J Cardiovasc Imag* 2014 Oct 16 DOI 10.1007/s10554-014-0547-0
12. The EchoNoRMAL (Echocardiographic Normal Ranges Meta-Analysis of the Left Heart) Collaboration. Ethnic-Specific Normative Reference Values for Echocardiographic LA and LV Size, LV Mass, and Systolic Function The EchoNoRMAL Study. *JACC Cardiovasc Imag* 2015; 8 (6): 656-665.
13. **Peluso D**, Bianchi A, Bonanno L, Banzato A. Unusual echocardiographic appearance of a cardiac metastasis from lung carcinoma. *J Cardiovasc Ultras* 2015 Dec 17. doi: 10.1002/jcu.22325. [Epub ahead of print]
14. Muraru D, Onciul S, **Peluso D**, Soriani N, Cucchini U, Aruta P, Romeo G, Cavalli G, Iliceto S, and Badano LP. Gender- and Method-Specific Reference Values for Right Ventricular Strain by Two- Dimensional Speckle-Tracking Echocardiography. *Circulation Cardiovasc Imag* 2016 Feb;9(2):e003866. doi: 10.1161/CIRCIMAGING.115.003866.

15. Surkova E, **Peluso D**, Kasprzak JD, Badano LP. Use of novel echocardiographic techniques to assess right ventricular geometry and function. *Kardiologia Polonica* 2016 Apr 4. doi: 10.5603/KP.a2016.0041. [Epub ahead of print]

L'attività di ricerca è esitata nella stesura dei seguenti abstracts:

2013

• 5th World Symposium of Pulmonary Hypertension

1. **Peluso D**, Kovács A, Dal Bianco L, Muraru D, Perazzolo Marra M, Sarais C, Badano LP, Iliceto S. "Impairment of right atrial mechanics and function in pulmonary hypertension patients assessed by 2D speckle tracking and three-dimensional echocardiography". Poster.
2. **Peluso D**, Kovács A, Dal Bianco L, Muraru D, Cucchini U, Badano LP, Iliceto S. "Characterization of right atrial mechanics by 2D-speckle tracking echocardiography in healthy subjects". Poster
3. **Peluso D**, Kovács A, Dal Bianco L, Muraru D, Padayattil S, Badano LP, Iliceto S. "RA volumes and phasic function by 3-dimensional echocardiography in healthy subjects". Poster
4. Kovács A, **Peluso D**, Muraru D, Perazzolo Marra M, Badano LP, Dal Bianco L, De Lazzari M, Iliceto S. "Paradoxical septal motion index strongly correlates with invasive hemodynamic parameters". Poster
5. Kovács A, **Peluso D**, Muraru D, Ermacora D, Badano LP, Dal Bianco L, Zoppellaro G, Iliceto S. Characterization of a novel parameter of right ventricular function by speckle tracking echocardiography in healthy subjects". Poster
6. Kovács A, **Peluso D**, Muraru D, Perazzolo Marra M, Badano LP, Dal Bianco L, Segafredo B, Iliceto S. "Transverse displacement: a novel echocardiographic parameter describing right ventricular function in pulmonary hypertension". Poster

• European Congress of Rheumatology

7. Pigatto E, **Peluso D**, Rizzo M, Zanatta E, Muraru D, Favaro M, Badano L, Punzi L, Cozzi F. Right ventricular function by 3D-echocardiography and 2D-speckle tracking

in scleroderma patients without pulmonary hypertension. *Ann Rheum Dis* 2013; 72 (suppl 3): 509

- **American College of Cardiology**

8. Badano LP, Muraru D, Zoppellaro G, Cucchini U, Ermacora D, De Lazzari M, **Peluso D**, Perazzolo-Marra M, Iliceto S. "Predictive value of 2D and 3D deformation parameters and wall motion score to identify transmural myocardial necrosis in stemi patients: a comparative study against CMR". *JACC* 2013; 61 (10 S)doi:10.1016/S0735-1097(13)61013
9. Badano LP, **Peluso D**, Muraru D, Dal Bianco L, Kovacs A, Iliceto S. "Right atrial volumes and phasic functions by 3D echocardiography in healthy subjects" *JACC* 2013; 61 (10S) doi:10.1016/S0735-1097(13)61101-8

- **European Congress of Cardiology**

10. **Peluso D**, Muraru D, Cucchini U, Dal Bianco L, Pigatto E, Zanatta E, Punzi L, Cozzi F, Badano LP, Iliceto S. "Right ventricular function by 3D-echocardiography and 2D-speckle tracking in scleroderma patients in absence of pulmonary hypertension". 34 (suppl 1): doi:10.1093/eurheartj/eh308.P1181
11. Ermacora D, Badano LP, Muraru D, Denas G, Dal Bianco L, Casablanca S, **Peluso D**, Zoppellaro G, Cucchini U, Iliceto S. Reference values of right ventricular longitudinal strain by speckle tracking echocardiography in 219 healthy volunteers. 34 (suppl 1): doi:10.1093/eurheartj/eh309.P3848
12. Mihaila S, Muraru D, Badano LP, Casablanca S, **Peluso D**, Cucchini U, Zoppellaro G, Vinereanu D, Iliceto S. Changes in mitral annulus and leaflets size are related to regurgitation severity in organic mitral regurgitation: a three-dimensional transthoracic study. 34 (suppl 1): doi:10.1093/eurheartj/eh310.P4750
13. Mihaila S, Muraru D, Casablanca S, **Peluso D**, Cucchini U, Dal Bianco L, Vinereanu D, Iliceto S, Badano LP. Three-dimensional changes in mitral valve annulus geometry in organic and functional mitral regurgitation: insights for mitral valve repair. 34 (suppl 1): doi:10.1093/eurheartj/eh310.P4751
14. Badano LP, Muraru D, Mihaila S, Haertel-Miglioranza M, Padayattil-Jose S, Ucci L, Dal Bianco L, **Peluso D**, Cucchini U, Iliceto S. Quantitative analysis of mitral valve

geometry by transthoracic three-dimensional echocardiography: accuracy, feasibility, reproducibility and reference values. 34 (suppl 1): doi:10.1093/eurheartj/eh311.5863

15. Kovacs A, **Peluso D**, Muraru D, Badano LP, Casablanca S, Dal Bianco L, Zoppellaro G, Iliceto S. Shift in relative contribution of radial and longitudinal mechanics to right ventricular ejection fraction between normal subjects and patients with pulmonary hypertension. 34 (suppl 1): doi:10.1093/eurheartj/eh307.P231

- **Società Italiana di Ecografia Cardiovascolare**

16. Casablanca S, Kocabay G, Badano LP, Muraru D, **Peluso D**, Ucci L, Padayattil-Josè S, Mihaila S, Haertel-Miglioranza M, Iliceto S. Valori di riferimento per i diametri ecocardiografici dell'aorta ascendente ottenuti sia con metodo leading edge-to-leading edge che con metodo inner edge-to-inner edge in 220 volontari sani. Poster
17. Piasentini E, Muraru D, Mihaila S, Dal Bianco L, **Peluso D**, Kocabay G, Casablanca S, Sarais C, Iliceto S, Badano LP. Accuratezza e riproducibilità dell'ecocardiografia transtoracica tridimensionale per l'analisi quantitativa della valvola mitrale: confronto con l'approccio ecocardiografici transesofageo 3D. Poster
18. Mihaila S, Muraru D, Casablanca S, **Peluso D**, Zoppellaro G, Denas G, Calore C, Cucchini U, Iliceto S, Badano LP. Analisi quantitativa della geometria della valvola mitrale tramite ecocardiografia transtoracica tridimensionale: valori di riferimento, fattibilità e riproducibilità. Poster
19. Ermacora D, **Peluso D**, Muraru D, Badano LP, De Lazzari M, Perazzolo Marra M, Zoppellaro G, Casablanca S, Cucchini U, Iliceto S. Lo strain longitudinale 2D e lo strain circonferenziale 3D risultano predittori accurati di necrosi transmurale alla risonanza magnetica dopo uno STEMI. Poster
20. Zoppellaro G, **Peluso D**, Muraru D, Badano LP, Ermacora D, Piasentini E, Casablanca S, Ucci L, De Lazzari M, Cucchini U, Kocabay G, Iliceto S. Accuratezza diagnostica dello strain nell'identificazione della necrosi transmurale nei pazienti con STEMI: superiorità del 2D rispetto al 3D. Poster
21. Padayattil-Josè S, **Peluso D**, Muraru D, Cucchini U, Piasentini E, Casablanca S, Badano LP, Razzolini R, Iliceto S. Impact of aortic valve area indexation in aortic valve stenosis evaluation in adult patients. Poster

- **Società Italiana di Reumatologia**

22. Pigatto E, Peluso D, Zanatta E, Polito P, Miatton P, Bourji K, Badano L, Punzi L, Cozzi F. Valutazione della funzione ventricolare destra mediante ecocardiografia tridimensionale nei pazienti con sclerosi sistemica. Poster .

- **Società Italiana di Cardiologia**

23. **Peluso D**, Padayattil S, Pigatto E, Cozzi F, Punzi L, Puma L, Cucchini U, Muraru D, Badano LP, Iliceto S. Subclinical left ventricular myocardial impairment in scleroderma patients. Comunicazione orale

24. **Peluso D**, Ucci L, Muraru D, Mihaila S, Cucchini U, Casablanca S, Pigatto E, Cozzi F, Punzi L, Badano LP, Iliceto S. Right heart function by 3D-echocardiography and 2D-speckle tracking in scleroderma patients in absence of pulmonary hypertension. Comunicazione orale

- **EuroEcho-Imaging**

25. **Peluso D**, Muraru D, Mihaila S, Cucchini U, Casablanca S, Pigatto E, Punzi L, Cozzi F, Badano LP, Iliceto S. Right heart function by 3D-echocardiography and 2D-speckle tracking in scleroderma patients in absence of pulmonary hypertension. Eur Heart J Cardiovasc Imag 2013; 14 (suppl 2):doi:10.1093/ehjci/jet202

26. Mihaila S, Piasentini S, Muraru D, **Peluso D**, Casablanca S, Puma L, Naso P, Iliceto S, Vinereanu D, Badano LP. Dynamic changes of mitral annular geometry during the cardiac cycle - a three-dimensional echo study in healthy volunteers. Eur Heart J Cardiovasc Imag 2013; 14 (suppl 2): doi:10.1093/ehjci/jet204

27. Mihaila S, Muraru D, Piasentini E, **Peluso D**, Cucchini U, Casablanca S, Naso P, Iliceto S, Vinereanu D, Badano LP. Static and dynamic analysis of the mitral valve annulus in normal subjects: a three-dimensional transthoracic echocardiography study. Eur Heart J Cardiovasc Imag 2013; 14 (Suppl 2): doi:10.1093/ehjci/jet203

28. Mihaila S, Muraru D, Piasentini E, **Peluso D**, Casablanca S, Naso P, Puma L, Iliceto S, Vinereanu D, Badano LP. Validation of a new, semiautomated software for quantitative assessment of the mitral annulus by three-dimensional echocardiography. Eur Heart J Cardiovasc Imag 2013; 14 (suppl 2): doi:10.1093/ehjci/jet207

29. Miglioranza MH, Muraru D, **Peluso D**, Cucchini U, Mihaila S, Naso P, Puma L, Kocabay G, Iliceto S, Badano LP. Two-dimensional assessment of tricuspid annulus dynamics and diameters: study for new reference values. *Eur Heart J Cardiovasc Imag* 2013; 14 (suppl 2): doi:10.1093/ehjci/jet216
30. Muraru D, Piasentini, Mihaila S, Naso P, Casablanca S, **Peluso D**, Denas G, Ucci L, Iliceto S, Badano LP. Reference values for 3D echo parameters describing left ventricular mechanics obtained by vendor- independent software. *Eur Heart J Cardiovasc Imag* 2013; 14 (suppl 2): doi:10.1093/ehjci/jet212
31. Muraru D, Piasentini E, Mihaila S, Padayattil Jose' S, **Peluso D**, Ucci L, Naso P, Puma L, Casablanca S, Iliceto S. Reference ranges for left ventricular geometry and function by 3D echocardiography using a vendor- independent software for quantitative analysis. *Eur Heart J Cardiovasc Imag* 2013; 14 (Suppl 2):doi:10.1093/ehjci/jet203
32. Muraru D, Calore C, Badano LP, Melacini P, Mihaila S, **Peluso D**, Puma L, Kocabay G, Rizzon G, Iliceto S. Left ventricular outflow tract planimetry by 3D echocardiography predicts obstruction and heart failure symptoms in hypertrophic cardiomyopathy. *Eur Heart J Cardiovasc Imag* 2013; 14 (Suppl 2): doi:10.1093/ehjci/jet205
33. Calore C, Muraru D, Melacini P, Badano LP, Mihaila S, Puma L, **Peluso D**, Casablanca S, Ortile A, Iliceto S. Left atrial longitudinal strain correlates better than its emptying fraction with left ventricular impairment in hypertrophic cardiomyopathy. *Eur Heart J Cardiovasc Imag* 2013; 14 (Suppl 2): doi:10.1093/ehjci/jet204

2014

- **Congresso Nazionale Brasileiro de Cardiologia**

1. Mihaila S, Muraru D, Miglioranza M, **Peluso D**, Casablanca S, Puma L, Naso P, Iliceto S, Vinereanu D, Badano L. Alterações Dinâmicas na Geometria Anular Mitral Durante o Ciclo Cardíaco: Estudo Ecocardiográfico 3D em Voluntários Normais. *Arq Bras Cardiol: imagemcardiovasc* 2014; 28(2): 109-116. Poster 030
2. **Peluso D**, Miglioranza M, Pigatto E, Cozzi F, Puma L, Piasentini E, Cucchini U, Muraru D, Badano L, Iliceto S. Comprometimento Miocárdico Ventricular Esquerdo Subclínico na Esclerose Sistêmica. *Arq Bras Cardiol: imagemcardiovasc* 2014; 28(2): 109-116. Poster 028

3. Muraru D, Badano L, Miglioranza M, Calore C, Melacini C, Mihaila S, **Peluso D**, Puma L, Rizzon G, Iliceto S. Planimetria do Trato de Saída Ventricular Esquerdo por Ecocardiograma 3D Prediz Obstrução e Sintomas de Insuficiência Cardíaca na Cardiomiopatia Hipertrófica. *Arq Bras Cardiol: imagemcardiovasc* 2014; 28(2): 109-116. Poster 003

- **American College of Cardiology**

4. Haertel Miglioranza M, Muraru D, Mihaila S, **Peluso D**, Cucchini U, Casablanca S, Iliceto S, Badano L. Reference Values of Tricuspid Annulus Size and Dynamics by Two-Dimensional Transthoracic Echocardiography in 220 Healthy Volunteers. *JACC* 2014; 63 (12_S2)
5. Muraru D, Cucchini U, Padayattil José S, Mihaila S, Miglioranza M, **Peluso D**, Cecchetto A, Casablanca S, Iliceto S, Badano L. Left Ventricular Myocardial Strain by ThreeDimensionalSpeckleTrackingEchocardiography in Healthy Volunteers: a Normative Study. *JACC* 2014; 63 (12_S2)
6. Muraru D, Calore C, Melacini P, Cucchini U, Mihaila S, **Peluso D**, Ucci L, Miglioranza M, Iliceto S, Badano L. Mitral Valve Leaflet Abnormalities Correlate With Left Ventricular Remodelling and Obstruction in Hypertrophic Cardiomyopathy: a Quantitative 3D Transthoracic Echocardiographic Study. *JACC* 2014; 63 (12_S2)
7. Mihaila S, Muraru D, HaertelMiglioranza M, **Peluso D**, Piasentini E, Iliceto S, Vinereanu D, Badano LP. Quantitative analysis of the mitral annulus geometry and function in healthy volunteers: a transthoracic three-dimensional echocardiography study. *JACC* 2014; 63 (12_S2)

- **European Congress of Cardiology**

8. Muraru D, Valente F, Aruta P, Cavalli G, Calore C, Mihaila S, **Peluso D**, Melacini P, Iliceto S, Badano LP. Characterisation of transmural longitudinal and circumferential mechanics by multi-layer strain analysis in hypertrophic cardiomyopathy. *Eur Heart J* 2014; 35 (Suppl 1): P596
9. Cecchetto A, Muraru D, PerazzoloMarra M, Cucchini U, **Peluso D**, Vannan M, S. Mihaila, Iliceto S, Lang RM, Badano LP. Accuracy and reproducibility of three-dimensional echo left ventricular volumes obtained using fully automatedand

manually edited endocardial border tracing algorithms. Eur Heart J 2014; 35 (Suppl 1): P1559

10. Mihaila S, Muraru D, Piasentini E, Aruta P, Cavalli G, Casablanca S, **Peluso D**, Iliceto S, Vinereanu D, Badano LP. Three-dimensional changes of the mitral annulus geometry and dynamics in patients with functional mitral regurgitation: insights for mitral valve repair. Eur Heart J 2014; 35 (Suppl 1): P1390

- **EuroEcho-Imaging**

11. S. Mihaila; D. Muraru; P. Aruta; E. Piasentini; G. Cavalli; L. Ucci; **D. Peluso**; D. Vinereanu; S. Iliceto; LP. Badano. The extent of mitral annulus dysfunction is related to regurgitation severity and Left Atrial size and function in patients with Organic Mitral Regurgitation. Eur Heart J CV Imag 2014; 15 (Suppl 2): ii 154-160

12. S. Mihaila, D. Muraru, E. Piasentini, P. Aruta, S. Casablanca, **D. Peluso**, M. Haertel Miglioranza, U. Cucchini, S. Iliceto, D. Vinereanu, LP. Badano. In Patients With Organic Mitral Regurgitation And Normal Left Ventricular Systolic Function, Mitral Valve Leaflet Flail Is Associated With Reduced Shortening Of The Mitral Annulus area.

13. S. Mihaila, D. Muraru, E. Piasentini, P. Aruta, S. Casablanca, **D. Peluso**, M. Haertel Miglioranza, U. Cucchini, S. Iliceto, D. Vinereanu, LP. Badano. In Patients With Organic Mitral Regurgitation, The Extent Of The Mitral Annulus Dysfunction Is Related To Regurgitation Severity And Left Atrial Size And Function. Eur Heart J CV Imag 2014; 15 (Suppl 2)

2015

- **European Congress of Cardiology**

1. V Spadotto, D. Muraru, A. Cecchetto, G. Romeo, P. Aruta, A Maddalozzo, MH Miglioranza, **D. Peluso**, S. Iliceto, LP. Badano. Novel vendor independent software for right ventricular quantification by 3D echocardiography shows good reproducibility and improved accuracy in comparison with cardiac magnetic resonance. Eur Heart J 2015; 36 (Suppl 1): 509-847

2. **D. Peluso**, E. Pigatto, G. Romeo, U. Cucchini, D. Muraru, P. Aruta, F. Cozzi, L. Punzi, S. Iliceto, LP Badano. Left atrial remodeling and dysfunction occur early in patients with systemic sclerosis and normal left ventricular function. *Eur Heart J* 2015; 36 (Suppl 1): 1-161
 3. MH. Miglioranza , D. Muraru , S. Mihaila , U. Cucchini , **D. Peluso** , D. Ermacora , A. Maddalozzo , C. Palermo, S. Iliceto , LP. Badano. Normative study of left atrium phasic volumetric changes by 3D echocardiography in 225 healthy volunteers. *Eur Heart J* 2015; 36 (Suppl 1): 163-508
 4. D. Muraru , MH. Miglioranza , D. Ermacora , S. Mihaila , U. Cucchini , **D. Peluso** , P. Aruta , G. Romeo , S. Iliceto , LP. Badano. Left atrial volumes are larger when measured with 3D than 2D echocardiography: implications for the definition of normality. *Eur Heart J* 2015; 36 (Suppl 1): 163-508
- **3D-Echo 360**
5. **D. Peluso**, D. Muraru, U. Cucchini, E. Pigatto, E. Zanatta, L. Punzi, F. Cozzi, S. Iliceto, LP Badano. Right ventricular function by 3D-echocardiography and 2D-speckle tracking in scleroderma patients in absence of pulmonary hypertension. Poster
- **EuroEcho-Imaging**
6. **D. Peluso**, E. Pigatto, G. Romeo, D. Muraru, F. Cozzi, S. Iliceto, LP Badano. Left atrial remodeling and dysfunction occur early in patients with systemic sclerosis and normal left ventricular function. Accepted at EuroEcho 2015 Poster
 7. **D. Peluso**, E. Pigatto, G. Romeo, U. Cucchini, D. Muraru, P. Aruta, F. Cozzi, L. Punzi, S. Iliceto, LP. Badano. Left ventricular subclinical dysfunction by 2D-speckle tracking in systemic sclerosis patients according to autoantibody pattern. Accepted at EuroEcho 2015 Poster
 8. **D. Peluso**, E. Pigatto, G. Romeo, D. Muraru, F. Cozzi, L. Punzi, S. Iliceto, LP. Badano. Incidence of subclinical myocardial dysfunction in patients with systemic sclerosis and normal left ventricular systolic and diastolic function. Accepted at EuroEcho 2015 Poster
 9. **D. Peluso**, G. Romeo, M. Perazzolo Marra, F. Tona, G. Famoso, E. Pigatto, F. Cozzi, S. Iliceto, LP. Badano. Right ventricular mechanics changes according to pressure

overload increasing, a 2D-speckle tracking echocardiographic evaluation. Accepted at Euroecho 2015 Poster

Altre attività svolte durante il corso di dottorato:

- Book chapter: The Right Atrium chapter of the II edition of the “Textbook of Real - Time Three Dimensional Echocardiography”, edited by Dr. Badano, Dr. Lang, Dr. Mor-Avi and Dr. Muraru. In press.
- Docente del Master in “Ecocardiografia di base ed avanzata” del Dipartimento di Scienze Cardiache, Toraciche e Vascolari dell’Università di Padova.
- Peer-reviewer degli articoli:
 - “Evaluation of Right Ventricular Diastolic Function in Patients with Chronic Obstructive Pulmonary Disease Using Pulsed Doppler Tissue Imaging” for the *Journal of Advances in Medical and Pharmaceutical Sciences* (2014)
 - “Right atrial myocardial deformation by speckle tracking echocardiography predicts recurrence in paroxysmal atrial fibrillation” for the *Journal of the American Heart Association* (2015)